Traceability of electrolytic conductivity measurements for ultra pure water

POLITECNICO DI TORINO

Dottorato in METROLOGY: MEASURING SCIENCE AND TECHNIQUE

Tesi di Dottorato

Traceability of electrolytic conductivity measurements for ultra pure water

Elena Orrù

Tutore
Dr. Francesca Durbiano
Ing. Massimo Ortolano

Coordinatore del corso di dottorato

Prof. Ing. Franco Ferraris

Giugno 2014

Contents

List of Tables

List of Figures

Chapter 1

Metrology

1.1 Introduction to metrology

Metrology is the science of measurement. It studies theoretical and practical aspects of measurements and related legal requirements. Its primary task is to define, implement and disseminate at the highest degree of accuracy a system of measurement units for all quantities of interest in science, technology, trade and human activities in general. Metrology is involved in defining properties of measurements, instruments and standards, and in developing methods that allow their assessment. In this framework, the development of methods for the evaluation of measurement uncertainty, a parameter that quantifies the spread of the values of a measurement and that is part of the measurement result is of particular importance.

The need to have a measurement system accepted all over the world, whose units were understandable and accurately realisable, already emerged in the ancient times. In the modern globalised world, trade, industrial production, evaluation of biological effects and verification of physical theories are all activities that require reliable and universally recognisable measurement results. All countries therefore need to share the same system of units. The measurements used to verify the conformity of products should be traceable to the units of that system, and countries should share a mutual recognition arrangement of the measurements.

1.1.1 The International System of Units

A measurement unit is a quantity conventionally chosen as a reference to estimate the value of other quantities of the same kind. A system of units is a set of units, together with multiples and submultiples, each of which corresponds to a quantity. A system of units, defined according to given rules, is built around a number of independent base quantities and around mathematical relations that connect other units, called derived units, to the base ones. A base unit can be defined either by a

material measure (i.e. a particular artefact that realises the unit) or by assigning a particular value to the result of an ideal experiment or to a fundamental constant of nature (a property of a phenomenon that is invariant in space and time and independent from external conditions). At the end of the nineteenth century, units were mostly defined by unstable material measures which were difficult to reproduce. With the progress of scientific research, however, the metrology community gradually replaced the former material measures with natural phenomena and experiments whose results were dependent only on fundamental constants. This enables them to obtain reliable, reproducible and stable units everywhere.

The current unit system, the SI (International System of Units), has been in force since 1960. It consists of seven base units: the metre (symbol m) for length, the kilogram (kg) for mass, the second (s) for time, the ampere (A) for electric current, the kelvin (K) for the thermodynamic temperature, the mole (mol) for the amount of substance and the candela (cd) for the luminous intensity. All the derived units are products of powers of the base units and are unlimited in number.

1.1.2 Organisation of metrology

The task to define, implement and disseminate the units of the SI not only requires the carrying out of scientific activities, but also of diplomatic ones.

Metrologists have therefore set up a branched organisation including cross-border research bodies and institutions. Metrology, as a structured science, came into being on the 20th of May 1875, when 17 states signed the Convention of the Metre. The number of signatory countries has grown with time and at the end of 2013 the Convention of the Metre included 55 states and 38 associated states and economies. The signing of this diplomatic treaty established the *Bureau International des Poids et Mesures* (BIPM), an inter-governmental body whose purpose is currently to ensure the equivalence between national measurement standards and the measurement traceability to the units of the SI. At national level, the uniformity of measurements and their traceability to the SI is guaranteed by the National Metrology Institutes (NMIs), bodies founded by the signatory states of the Convention. The BIPM is directed and supervised by the *Comité International des Poids et Mesures* (CIPM), a scientific committee consisting of 18 members from different countries. The CIPM, which meets annually, is in turn subject to the authority of the *Conférence Générale des Poids et Mesures* (CGPM), a conference formed by delegates of the countries signatories of the Convention of the Metre. The CGPM meets every four years to review the work of the BIPM, to discuss developments and to decide the updates to the SI on the basis of the recommendations issued by the CIPM. The CIPM, in its scientific work, is supported by 10 Consultative Committees (CCs) for different areas of metrology, chaired by CIPM members and constituted by experts of various NMIs. The CIPM also collaborates with a large number of international standard

organisations.

1.2 Metrology in chemistry

One of the tasks of a chemical measurement is the estimation of the concentration of a compound of interest, an analyte, in a more or less complex matrix. Many practical decisions are based on the results of quantitative chemical analysis which assume critical importance in quality control of manufacturing industries, in measurements for the compliance to regulation, in the determination of the economic value of traded goods, environmental monitoring and in clinical and basic research. As a consequence, chemists are increasingly asked to demonstrate the quality of the results of their analysis, in particular having to declare the level of confidence within which their measurements are in agreement with measurements made by others, in different times and places, generally regardless of the analytical method used. The realisation and the implementation of measurements traceable to SI becomes imperative for this kind of needs.

1.2.1 Organization of metrology in chemistry

Initially, the SI was developed in the field of physics, while in chemistry it has attracted the interest of the NMIs at an international level only recently. Since the last decade metrology in chemistry is growing progressively and trying to find an agreement on the development of chemical measurements comparable with what already exists in the field of metrology in physics. On the request of the International Union of Pure and Applied Chemistry (IUPAC) and the International Organization for Standardization (ISO), in 1971, the XIV CGPM decided to add the *mole* — the unit of amount of substance — to the SI. In 1991, the CIPM established a working group for metrology in chemistry, which in 1995 became the Consultative Committee for Amount of Substance (CCQM).

The CCs of the CIPM have the responsibility to choose and carry out key comparisons of measurements on national standards. The task of the CCQM is to investigate and identify measurement methods that have the potential to be considered as primary, to discuss the progress of the activities of the various institutions and to coordinate the activities and future developments of the measurements related to SI units in chemistry.

In 1995, the XX CGPM invited, with resolution n. 7, NMIs to start metrological activities in the field of chemical measurements. The CCQM has now identified pilot studies and key comparisons for the following areas: health, food, environment, legal metrology, general analytical applications. Now, other laboratory associations, such as CITAC (Cooperation on International Traceability in Analytical Chemistry) and

EURACHEM (Analytical Chemistry in Europe), have been set up around the world. EURACHEM, which is devoted to the issue of traceability in analytical chemistry, collaborates with the European Association of National Metrology Institutes (EURAMET). The Technical Committee of Metrology in Chemistry (TC-MC) operates to promote collaboration among the NMIs and to spread metrological activities in the chemical field.

Failing a direct and effective realisation of the mole, the CCQM identified the significant properties of a measurement method suitable to determine the amount of substance with traceability to the SI units.

1.2.2 Traceability in chemistry

The traceability of the result of a measurement in chemistry is established if one of the following techniques or standards is employed:

- a primary method or a comparison with it;
- standards for the calibration of the measuring equipment;
- a certified pure substance;
- an appropriate certified reference material in a matrix;
- a well-defined and accepted procedure.

Although there are measurement methods that are well-known and that provide repeatable results, most of them do not meet the criteria to ensure traceability to the SI units.

According to the definition of the CCQM, a primary method of measurement is: "a method having the highest metrological qualities, whose operations can be completely described and understood, for which a complete uncertainty statement can be written down in terms of SI units, and whose results are, therefore, accepted without reference to a standard of the quantity being measured" [2]. A primary method of measurement provides the means to transform the abstract definition of an SI unit into a practical measurement carried out with respect to that unit. The operations that constitute the method must be represented by a measurement model. The definition requires that this model includes only terms that can be expressed in SI units. If this model is complete and expressed only in SI units, then it is possible to get a complete definition of the uncertainty, following procedures accepted at an international level. The result of a primary method must have an uncertainty appropriate to the current state of technology. The uncertainty of the final result is a function of both the uncertainties of the input quantities and the effects resulting from an incomplete description of the various steps of

the measurement. The definition excludes those methods that meet the criteria listed above, but which require measurements that do not yield an appropriate level of accuracy. The primary methods must then provide long-term stable and accurate results. In some cases, the experimental confirmation that a method has the highest metrological qualities can be provided by comparisons with other methods or between different NMIs [3].

A measurement procedure for a primary method can be classified as direct or indirect. "A primary direct method measures the value of a unknown without reference to a standard of the same quantity, while the primary ratio method measures the value of a ratio of an unknown to a standard of the same quantity; its operation must be completely described by a measurement equation" [4]. Examples of methods with the potential to be considered primary and direct are: gravimetry, coulometry, titrimetry and the lowering of the freezing point; while a primary ratio method is the one based on isotope dilution mass spectrometry.

1.3 Primary electrochemical methods

The best feature of electrochemical methods is the direct conversion of chemical information into an electrical signal such as current, potential and charge. Due to their versatility, electroanalytical techniques are employed in environmental, food and health care monitoring, in industrial processes and production of advanced materials. Consequently, the reliability of the results is widely requested and also the traceability of the results to the units of SI. In this regard, the activity of CCQM EAWG (Electrochemical Analysis Working Group) is mainly focused on the improvement of the knowledge and the uncertainty of the primary methods in the field of electrochemical analysis and the development of new methods that have the characteristics to be considered primary. When EAWG started its activity in 1998, it was focused only on pH metrology, while afterwards, it included also electrolytic conductivity and coulometry.

1.3.1 pH

pH is one of the mostly applied electrochemical quantity in many areas of science and technology [5]. The traceability of its measurement values is required in many fields of economic and scientific importance. In 2002, IUPAC has defined particular rules for the traceability to the SI of pH values [6].

NMIs that develop primary measurement systems for pH have to refer for their measurements results to certain conventions that are not amenable to the requirements listed in the definition of a primay method.

Originally defined in terms of hydrogen ion (H^+) concentration, the pH value,

which express the acidity of the solution, is now based on the thermodynamic definition, the negative decadic logarithm of the relative activity of the solvated hydrogen ion, a_{H+} [6].

NMIs use the primary method recommended by IUPAC to perform pH measurement s whose values are at the top of the national traceability chains. This primary method is based on the measurement of the potential difference of a specific buffer solution included in a Harned cell [7]. From this measurement the quantity, known as the "acidity function" [6, 8], is obtained:

$$\mathrm{p}a = -\log(a_{\mathrm{H}^+}\gamma_{\mathrm{Cl}^-})\,, \tag{1.1}$$

where γ_{Cl^-} is the activity coefficient of the Cl^- ion corresponding to its molality m_{Cl^-}. The pH may then be calculated from Eq. 1.2:

$$\mathrm{pH} = \mathrm{p}a^0 + \log\gamma^0_{\mathrm{Cl}^-}\,, \tag{1.2}$$

where $\mathrm{p}a^0$ is the value of pa corresponding to zero chloride molality (linearly extrapolated to $m_{\mathrm{Cl}^-} \to 0\,\mathrm{mol\,kg^{-1}}$ and $\gamma^0_{\mathrm{Cl}^-}$ is the value of the limiting activity coefficient of Cl^- (at the ionic strength of the buffer with no added chloride).

Secondary pH reference solutions can be characterized by different measurement procedures derived from primary methods. It is possible, then to rank primary and secondary reference buffers on the basis of the methods used for the pH determination. The choice between the methods should be made according to the uncertainty required for the application [5].

1.3.2 Coulometry

Coulometry is a primary direct method for the amount of substance, because it is directly linked to the mole [3]. Since this method is based on the application of Faraday's law [9]), it does not require references of amount of substance. Faraday's law states that in a redox reaction the produced amount of substance of a specified species is proportional to the charge delivered by the driving circuit:

$$n = \frac{Q}{zF} = \frac{\int_{\Delta t} i(t)\,\mathrm{d}t}{zF}\,, \tag{1.3}$$

where n is the amount of substance produced in the time interval Δt, Q is electric charge, i is electric current, z is the charge number of the reaction and F is the Faraday constant.

Tipically the measurement is carried out either in *constant-voltage mode* or *constant-current mode*. In general, the constant-voltage mode is applied for precious metals, actinides, etc [10, 11, 12] because it provides high selectivity, while for other substances the constant-current mode is chosen because it yields a better uncertainty.

1.3.3 Electrolytic conductivity

Electrolytic conductivity is a non-specific parameter which yields an estimate of the total concentration of ionized substances in a liquid sample. It is a useful and accessible quantitative measure of water purity requested in pharmaceutical, drinking water and food industry, in health care and environmental monitoring.

Conductivity measurements are performed by means of resistance measurements of a solution in an electrolytic cell with defined geometry.

Theory of electrolytic conductivity, measurement method and procedures will be described in the next chapter.

Chapter 2

Electrolytic conductivity of aqueous solutions

Electrolytic conductivity measurements provide easily, quickly and accessible information about water quality and ion concentration. Therefore, conductivity measurement is applicable to impurity or trace detection; it is the main method for monitoring the performance of demineralization and other high-purity water treatment operations. It is also used to detect ionic contamination in boiler water, microelectronics rinse waters, pharmaceutical process waters, etc. [13, 14].

Increasing requests by industrial and medical sectors to have reliable results, have prompted many NMIs to extend the electrolytic conductivity range of metrological interest to low values ($\kappa < 1\,\mathrm{mS\,m^{-1}}$) where stable reference materials are not available due to contamination effects. NMIs are thus working in order to widen the traceability both to ultra-pure water values ($5.5 \times 10^{-3}\,\mathrm{mS\,m^{-1}}$).

Hence, during my Ph.D. activity, the aim has been to carried out measurements of low conductivity solutions (down to ultra pure water), avoiding contamination effects by means of the realization of a closed system. Moreover, I dealt also with the expansion of traceability to seawater samples (high conductivity values i.e. $5\,\mathrm{S\,m^{-1}}$).

2.1 Application: ultra pure water

Laboratories involved in chemical analysis use pure water as solvent and as reference material, for flow and density measurements, for heavy metals ultra-trace analysis and other chemicals and for steam to moisture tests. Pure water is also employed for the production of steam with a low corrosion rate in electrical energy generation plants, for the the cooling of wafer during the cutting process in integrated circuits and for temperature control systems in nuclear reactors . The production of solid state electronic devices, such as transistors, requires accurate impurity control and

involves final washes of the surfaces with ultra-pure water. Since the parameters involved in production processes have a direct effect on the quality of the accomplished product, it is necessary that water quality is guaranteed through values which indicate its purity by means of measurements traceable to the SI units.

One of the main difficulty in considering the ultra-pure water as a reference material is due to the dissolution, absorption and contamination from carbon dioxide (CO_2). CO_2 dissolves in water and reacts with it to form carbonic acid (H_2CO_3) which immediately dissociates into hydrogen (H^+) and carbonate (CO_3^{2-}) ions causing an increase in conductivity.

2.2 Electrochemical theory of electrolytic conductivity

In this chapter, basic information about electrochemical phenomena, impedance and electrolytic conductivity measurements are presented. This information is necessary for the choice of the instrumentation and for the settings of the parameters.

2.2.1 Electrolytic conductors

If a voltage is applied to the electrodes, current flow is allowed by the ions in solution. In general the electrical conductors can be distinguished in two categories:

- *First class conductors or metallic conductors* are metallic elements or alloy or semiconductor materials in which the current is related to electron motion (negative charge carriers) through the crystalline lattice without mass transfer. For these class of conductors, Ohm's law is applicable

$$V = RI\,, \tag{2.1}$$

  where V is the potential difference measured across the conductor, I is the current through the conductor and R is the resistance of the conductor. In this expression, R is a constant and it is independent of the current but, it depends on some physical and geometrical characteristics of the conductor, as the resistivity ρ, the length l and the section S. In the simplest case, in which the conductor is composed of a single material and it has uniform section and also the current flow is uniform, the resistivity is related to R by the relation

$$R = \rho\frac{l}{S}\,. \tag{2.2}$$

- *Second class conductors or electrolyte conductors* are aqueous solutions of electrolytes (salts, acids or bases and ionic solids in the melted/liquid state). The

current is carried in aqueous solutions by positive and negative ions, which derived from the dissociation and ionization of the electrolyte. They move towards the pole of opposite sign, with charge and mass transfer. Usually, for electrolytic conductors, the conductance is examined. It is defined as the reciprocal of resistance:

$$G = \frac{1}{R}\,. \tag{2.3}$$

G is related to the capability of dissolved ions to transport electric current depending on the volume of analysed solution and on geometrical characteristics of the measurement device.

Electrolytic conductivity κ, instead, is a specific property of the examined solution, which depends on the ions concentration, charge, mobility and temperature.

The aqueous solutions of acids, basis and salts are excellent ionic conductors because they provide charged ions which are responsible for electric conduction.

2.2.2 Fundamental relations

As a fundamental measure of the charge transport through an electrolyte, κ is the ratio between current density j and electric field strength E and it is the reciprocal of resistivity ρ:

$$\kappa\mathbf{E} = \mathbf{J} \qquad \kappa = \frac{|\mathbf{J}|}{|\mathbf{E}|} = \frac{1}{\rho}\,. \tag{2.4}$$

Since it is not possible to measure conductivity by itself, κ is obtained from the measurement of the solution resistance R of a homogeneous, isotropic electrolyte placed between metal electrodes in a conductivity cell under specified conditions. The relation between the solution bulk resistance R_b and the resistivity ρ is:

$$R_\mathrm{b} = \rho K_\mathrm{cell}\,, \tag{2.5}$$

where K_cell (m^{-1}) is the characteristic constant of each electrolytic cell, which is named geometric constant of the cell [15] and depends on the cell geometry.

From Eq. (2.4), substituting $1/\kappa = \rho$ in Eq. (2.5), the following relationship is obtained:

$$\kappa = \frac{K_\mathrm{cell}}{R_\mathrm{b}}\,. \tag{2.6}$$

In the simplest geometry, the electrolytic cell contains two parallel planar metal electrodes of area A, placed at a distance l, in which the electrical field between the electrodes is strictly homogeneous. Then, K_cell is obtained by:

$$K_\mathrm{cell} = \frac{l}{A}\,. \tag{2.7}$$

It is possible to develop cells that maximize homogeneity of the electric field and minimize fringe effects.

2.2.3 Dissociation and solvation processes

The charged species in an aqueous solution are variously solvated. When a ionic solid (as potassium chloride KCl) is dissolved in a polar solvent as water, it separates charged ions. Therefore, inside the solution an equilibrium between the concentration of positive and negative ions and the undissociated species is established. In the case of KCl when it is dissolved in water, it dissociates completely generating K^+ and Cl^- ions, as shown in the equilibrium equation (2.8) which is completely moved towards products equation right side:

$$KCl \longrightarrow K^+ + Cl^- . \tag{2.8}$$

This equilibrium is regulated by the dissociation constant

$$K_d = \frac{[K^+][Cl^-]}{[KCl]} \tag{2.9}$$

that indicates the solute dissociation degree in the solution. The square bracket represent the concentrations of different species ($mol\,L^{-1}$).

On the contrary, pure water is a very bad conductor, because, by definition, it contains only small quantities of hydronium H^+ and hydroxide OH^- ions as a consequence of the self dissociation reaction:

$$H_2O \rightleftharpoons H^+ + OH^- . \tag{2.10}$$

The equilibrium constant is expressed by

$$K_{eq} = \frac{[H^+][OH^-]}{[H_2O]} \tag{2.11}$$

The concentration of the undissociated form $[H_2O]$ is $55.6\,mol\,L^{-1}$. It is very large if it is compared to the concentration of $[H^+]$ and $[OH^-]$. As a consequence, $[H_2O]$ can be considered as a constant and therefore the dissociation constant of water, K_w can be expressed by

$$K_w = [H^+][OH^-] . \tag{2.12}$$

At 25 °C, $K_w = 1.00 \times 10^{-14}$ and the corresponding value for the electrolytic conductivity is $0.055\,\mu S\,cm^{-1}$.

Moreover, within the solution, water molecules (that are a strong dipole) orient themselves around each solute ion in a process called *solvation* shown in Fig. 2.1.

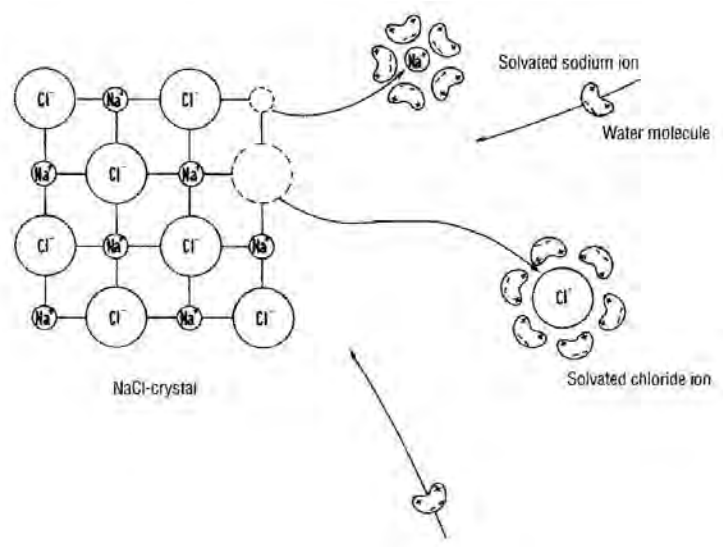

Figure 2.1: Dissolution process of a NaCl crystal in water and ionic solvation. The water molecule is positioned so as to have its hydrogen atoms, the electropositive portion, toward the anion and the oxygen, the electronegative part, towards the cation, in order to compensate the electric charge. [From: [1]]

Each positive and negative ion in solution is surrounded by a sheath of water molecules: the ion is in the central position and the water molecules are disposed all around and oriented so that the electric charge is compensated. On a macroscopic scale, the solvated ion is placed in the middle of several hydration layers. By increasing the distance from the ion, the water molecules organisation decreases.

The dissociation degree and the solvation degree of the solute depend on the electrolyte characteristics (as dimension and electric charge), and on the solvent polarity. Solvated ions move at different velocities, according to their size and charge.

Consequently, the solution is composed by charged species derived from the electrolyte dissociation, which will be variously solvated and from molecules of polar solvent.

2.2.4 Charge transport

As previously described, in electrolytic solutions, electric charge transport corresponds to the movement of ions. Several mechanisms of mass transport can be recognized.

Convection mechanism takes place when the ions transfer to or from an electrode is due to mechanical means such as stirring or agitation. Moreover, temperature and density gradients can cause convection which generate a flow of charges/ions.

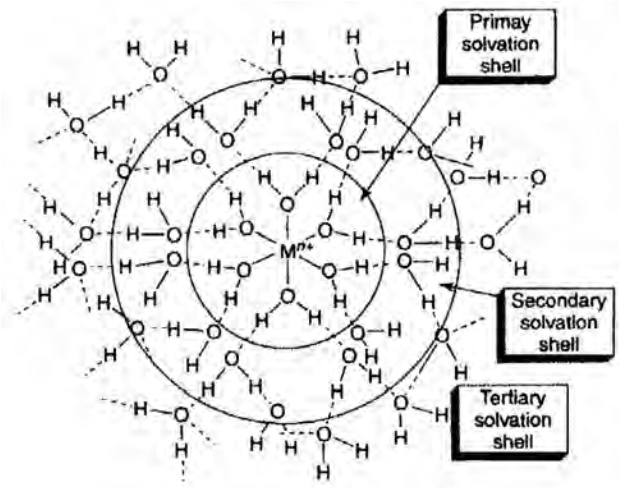

Figure 2.2: The localised structure of a hydrated metal cation in aqueous solution. In the middle, the metal cation (Mn^+), and around it, several layers of water molecules with the oxygen atoms oriented towards the cation. [From: [1]].

Diffusion occurs when in the solution, there are concentration gradients of ions. Ions move from the more concentrated region to the more dilute according to Fick's first law [16]:

$$J_\mathrm{i} = -D_\mathrm{i}\frac{\partial c_\mathrm{i}}{\partial x}\,, \tag{2.13}$$

where J_i is the flux of species i with concentration c_i in direction x, and $\partial c/\partial x$ is the concentration gradient. D_i is the proportionality factor between flux and concentration gradient, known as the diffusion coefficient. The negative sign arises because the flux of species tends to annul the concentration gradient.

Migration involves only charged species under the influence of an electric field. The displacement of anions (negatively charged particles) is towards the anode (positive pole) and the one of cations (positively charged ions) is towards the cathode (negative pole). So, when an electric field of strength $E = \partial\phi/\partial x$ is applied, Eq. (2.13) becomes:

$$J_\mathrm{i} = -D_\mathrm{i}\frac{\partial c_\mathrm{i}}{\partial x} - z_\mathrm{i}c_\mathrm{i}\frac{F}{RT}E\,, \tag{2.14}$$

where z_i is the charge number of species i, F is the Faraday constant, R the gas constant and T the temperature. The second term on the right-hand side represents migration.

2.2.5 Migration transport

Ion migration can occur by means of two different phenomenological descriptions, named *jump mechanism* and *viscous movement*, depending on the way ions move inside the electrolyte solution.

Jump mechanism Ion migration by jump mechanism can occur when real dimensions of solvated ions are small enough to allow their arrangement in the defected cavity of the crystal lattice, so they can move passing through free lattice positions (vacancies or interstitial positions). The jump mechanism is further promoted when the electronic structure of the ion and the solvent allow an ion arrangement in the jump positions, depending on both space arrangement and chemical bonds. In the case of migration of H^+ and OH^- ions in aqueous solutions, the process is different and it is favoured by the small size of these ions and by their affinity with the solvent water molecules. For the sake of simplicity, in Fig. 2.3, the jump mechanism for H^+ ions is represented. This mechanism can involve only water molecules which are favourably oriented. So, the hydrogen ion mobility depends on re-ordering velocity of water molecules and it is favourably influenced by temperature, which weakens the hydrogen bonds.

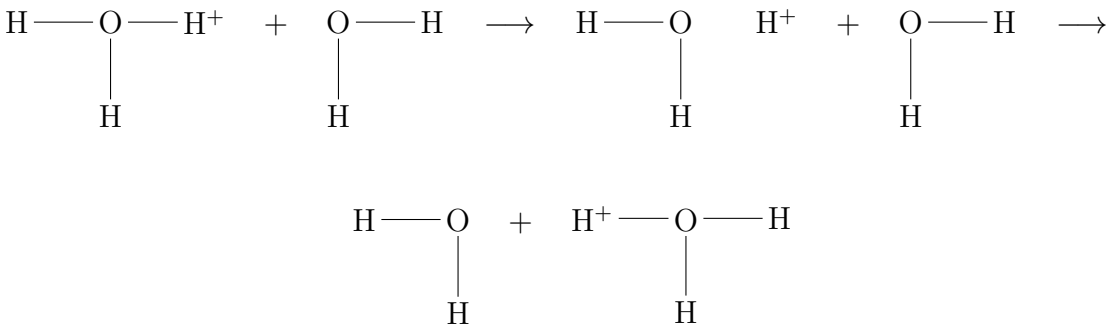

Figure 2.3: Schematic representation of the jump mechanism of a proton between two water molecules.

The proton H^+ has a jump time of $\approx 4\,\%$ of ion life, while in the remaining $96\,\%$ of its life, it is embodied into hydrogenion H_3O^+.

Viscous movement Considering the solution as a continuous viscous medium and the ion as a rigid sphere, the ion movement can be represented by a sphere motion proceeding into a medium (consisting of ions, atoms and/or molecules) in which it finds a resistance. This is a valid model when the ion radius is enough large with respect to the solvent molecular structure and its dimension is not negligible. Ion mobility can be increased by temperature (that additionally decreases solution

viscosity) and by solution concentration (that modifies the mean distance among ions, by varying the mutual interactions.) Only if the solution is diluted, we can assume that the ions are isolated entities, which can independently move, without mutual influences. During its motion, ion is retarded by three forces that oppose to the electric field force:

- a frictional force that depends on the size of the solvated ion;
- an asymmetric effect caused by the ion movement which distort the ionic atmosphere such that it is compressed in front of the ion and extended behind it;
- an electrophoretic effect due to the motion of ions with opposite charge associated to ion movement.

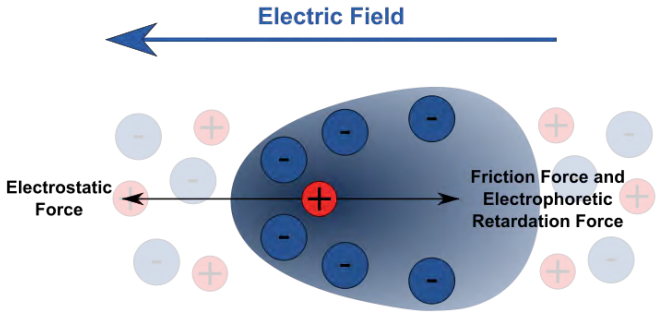

Figure 2.4: Representation of the ion transport in an electrolyte medium under the influence of an external electric field.

2.2.6 Faradaic and non-faradaic currents

At the electrode/solution interface two types of processes can occur.

Faradaic processes occur when the applied voltage is higher than the discharge voltage of the ions and involve charge exchange between the electrodes and the ions in solution, as a result of an electrochemical reaction (oxidation or reduction).

This type of process is governed by Faraday's law, which states that the amount of substance which takes part in a chemical reaction is proportional to the produced or supplied current.

If the applied voltage is lower than the discharge voltage, *nonfaradaic current* occurs which is only due to ion migration from bulk solution to the electrodes and which does not gives rise to electron exchange.

In this case, if the voltage is in continuous regime, there is an initial current flow that decreases rapidly to zero (Fig. 2.5): the current creates a progressive ions accumulation in the area close to electrodes surfaces resulting in a gradual decrease in ions concentration in the solution bulk. Then, in the solution immediately adjacent to each electrode, the molecules of the polar solvent and the ions are oriented to form an electric double layer, called *Helmholtz double layer*.

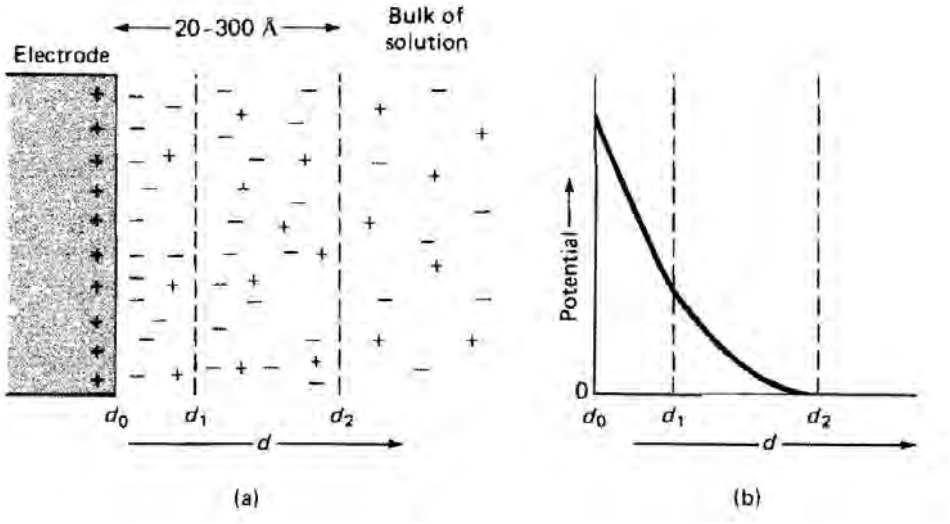

Figure 2.5: Electric double layer formed at electrode surface as a result of an applied potential.

As shown in Fig. 2.6, the *inner Helmholtz plane (IHP)* is closer to the electrode: the voltage decreases linearly by increasing the distance from the electrode surface. IHP is due to water molecules oriented with the positive ends toward the metal. In some points of the water double layer, an anion is in contact with the metal because of its so high adsorption energy that breaks the layer of water molecules and the primary hydration shell of the anion. The negative charge of the adsorbed ions is added to that existing in the metal and it is compensated by cations which can be adsorbed or cumulated in proximity of the interface. Generally, the adsorption of cations is weaker, in relation to their greater energy of hydration, whereby the adsorbed cations retain their primary hydration shell and they are arranged in a layer at a greater distance from the electrode surface called the *outer Helmholtz plane (OHP)* [17]. In this layer the voltage decreases exponentially by increasing the distance.

The alteration of the charge distribution at the electrodes is named *"polarization"* because there are a variation of potential difference between the electrodes.

Polarization phenomena decreases the efficiency of the electrolytic processes as it represents a deviation from the equilibrium conditions of the electrochemical cell.

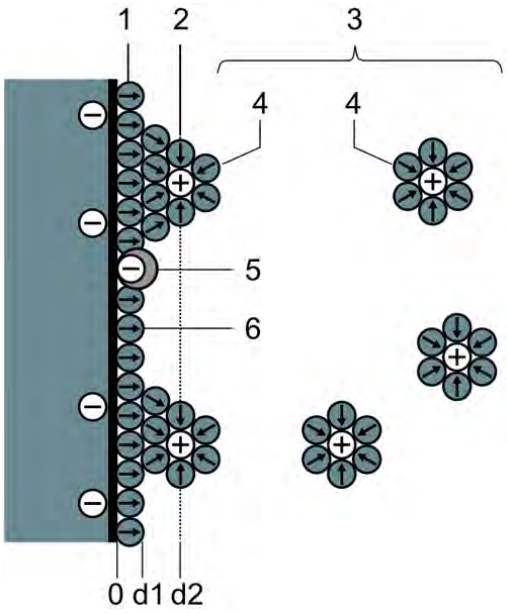

Figure 2.6: Scheme of the electrical double layer: 0 - metal surface plane (with potential ϕ_m), 1 - primary water layer, d1 - inner Helmholtz plane (IHP) with the specifically adsorbed anions, d2 - outer Helmholtz plane (OHP) with adsorbed solvated cations, 3 - diffuse double layer (solvated cations with oriented water molecules), 4 - solvated cations (adsorbed or not), 5 - adsorbed anions.

Even in this case, we can distinguish two types of polarization phenomena: *chemical polarization* and *concentration polarization*.

Chemical polarization involves a change in the chemical structure of the electrodes, as an oxide layer formation, different kind of metallic thin film deposition, etc. It occurs when the applied voltage is higher than the ion discharge voltage.

On the contrary, *concentration polarization* is due to concentration gradients in the solution induced by the current flow. The displacement of anions and cations towards opposite directions, just partially compensates local ionic deficiencies or discharge processes to the electrodes. From that, local variations in concentration occur usually close to the electrodes.

To avoid the polarization effects indeed, the AC voltage is utilised, so, by inverting the phase of the electric field, the positive and the negative ions are alternatively attracted on the surface of each electrode. By acting on the frequency, it is possible establish the conditions to reduce the polarization phenomena [16].

The double layer formed by an external potential involves a momentary non-faradaic current and the electrode becomes *polarized* if *faradaic processes* do not occur to cause *depolarization*.

Supplying a defined voltage value, if there are not chemical reactions including

a charge exchange between electrode and solution, the behaviour at the interface is analogous to a capacitor. This capacitance value is intrinsically connected to chemical-physical characteristics of the metal which constitutes the electrode, to ion attitude to be adsorbed from electrode, to solvent polarity, but also to the solution concentration and to the applied voltage.

When a voltage v is applied to a capacitor, a charge q is stored on its armatures:

$$C_{\mathrm{dl}} = \frac{q}{v}\,, \tag{2.15}$$

where C_{dl} is the double layer capacitance.

During the charge accumulation process, the cell is crossed by an electric current. In correspondence with a fixed voltage, there will be a charge on the metallic electrode, depending on the voltage at the interface and on the solution composition. Both the electrodes give rise to polarization phenomena, but with an opposite polarity.

The charge accumulation of the double layer on the electrode surface (thickness less than 0.1 Å [18]) determines of an v_{p}. The value of v_{p} can reach v at most, and in that case, the current becomes null. The v_{p} varies as a function of time and it is represented by the equation

$$v_{\mathrm{p}} = \frac{1}{C_{\mathrm{dl}}} \int_0^t i dt\,, \tag{2.16}$$

where C_{dl} is the interface capacitance, i is the electric current and t is the considered time interval.

The capacitive behaviour of the electrode-solution system differs from that of pure capacitor because there is a passage of non-faradaic current, only due to ion migration from bulk solution to the electrodes, as a function of the applied voltage, also if this voltage is lower than the one of discharge voltage. Since the electromotive force of polarization prevents an accurate measurement of the solution resistance, it is required to minimize the polarization phenomena. The most common technique is to perform the conductivity measurement in AC; on the other hand, applying alternating current requires to consider the reactive characteristics of the circuit. The modulus of the impedance Z of a system without any inductance is expressed by the equation:

$$Z = \sqrt{R^2 + \frac{1}{\omega^2 C^2}}\,, \tag{2.17}$$

where R is the resistance, $\omega = 2\pi f$ is the applied frequency and C is the system capacitance. For an accurate measurement, the value of Z should be as close as possible to R: that is possible if the second term under the square root tend to zero. Experimentally, it is obtained by high frequencies or high capacities.

2.2.7 Chemical-physical parameters for the electrolytic conductivity measurement

Different parameters can modify the electrolytic conductivity value of solutions. It is necessary to control these parameters, reported in the following.

Temperature In the electrolyte conductors, the electrolytic conductivity increases with temperature (but the variation is lower than the one of metallic conductors). In this case, the viscous medium friction, which acts in opposition to ion movement, decreases with the temperature rise and so the ions increase their kinetic energy and move more rapidly [19].

The conductivity dependence from the temperature can be expressed by:

$$\kappa(T) = \kappa(T_{\text{ref}}) \left[1 + \alpha_T(T - T_{\text{ref}}) + \beta_T(T - T_{\text{ref}})^2 + \dots\right] , \tag{2.18}$$

where α_T and β_T are the temperature coefficients, $\kappa(T)$ is the electrolytic conductivity at the measurement temperature T and $\kappa(T_{\text{ref}})$ is the conductivity at the reference temperature T_{ref} (the chemical reference temperature is typically 25 °C)

Considering only the first-degree term, at the temperature T, we obtain:

$$\frac{\mathrm{d}\kappa}{\mathrm{d}T} = \kappa_{T_0}\alpha_T \quad \text{and so} \quad \alpha_T = \frac{1}{\kappa_{T_0}}\frac{\mathrm{d}\kappa}{\mathrm{d}T} = \frac{\mathrm{dln}\kappa_{T_0}}{\mathrm{d}T} , \tag{2.19}$$

For the salt solutions, the conductivity temperature coefficient α_T depends on the concentration and on the chemical species.

Pressure Because of incompressibility property of liquids, an increasing in pressure shows a negligible effect on the ion movement. An important effect occurs on the chemical composition of the solution, since the increase in environmental pressure causes an increase in CO_2 solubility in the solution, with changes of the chemical species in it.

Ion concentration Due to the strong connection between electrolytic conductivity and electrolyte dissociation degree, dilution process influences the electrolyte conductance with two opposite effects:

- dilution causes the reduction of the number of ions contained in a unitary volume of solution, therefore it gives rise to an electrolytic conductivity decrease;
- the availability of a large number of solvent molecules gives rise to an increase of the dissociation degree of electrolytes, as a consequence, conductivity rises.

In a dilute solutions of strong electrolytes, in which they are completely dissociated (dissociation coefficient $a = 1$, e.g. KCl solution), the electrolytic conductivity decreases proportionally to the dilution. Instead, for weak electrolyte solutions (as acetic acid CH_3COOH), in which they are not completely dissociated (dissociation coefficient $a < 1$), the dilution initially gives rise to an increase of electrolyte dissociation degree in consequence of a weak increase of conductivity; subsequently, with the rise dilution, the effect of the decrease of ion number per unit volume prevails, caused by the solvent addition, and so the conductivity decreases.

With solutions of molar concentration higher than $1 \times 10^{-3}\,\mathrm{mol\,L^{-1}}$, it is required to employ the activity a (active concentration), instead of the concentration C, by the following relation:

$$a = \gamma C\,, \tag{2.20}$$

where γ is the activity coefficient and it depends on dilution level [20, 15].

For high concentrated solutions, the number of active ions does not correspond to the electrolyte concentration, due to the strong interaction among ions, so $\gamma < 1$. In fact, the ion capability to take part in charge transport is partially nullified, as a consequence of inter-ionic attractions, and so the active concentration results lower than the effective concentration. In this case, the solution conductivity is not exactly proportional to solution concentration, but rather to its activity. With a progressive reduction of concentration, $a \to C$, and so $\gamma \to 1$. Simple electrolytes solutions, e.g. KCl solutions, have equivalent conductance Λ defined as:

$$\Lambda = \frac{\kappa}{C_{\mathrm{eq}}}\,, \tag{2.21}$$

where C_{eq} is the concentration of positive (or negative) charges and Λ represents the conductivity per unit of charge concentration.

The Kohlrausch law (2.22) empirically describes the conductivity value as a function of the concentration of a dissolved species:

$$\Lambda = \Lambda^0 - Ac^{1/2}\,, \tag{2.22}$$

where A is a constant, c is the solute concentration and Λ^0 is the equivalent conductivity at infinite dilution condition.

Ion charge Comparing two solutions, at the same conditions, containing the same ionic species, but having a different oxidation state, solution with ions having a higher electric charge results be more conductive.

Ion mobility and migration velocity Between two ionic species with the same electric charge (considered at the same conditions), the species more conductive is the one with lower ion dimensions and mass. The mobility of ions with small dimension is easier, because the migration is due to jump mechanism [20, 15].

Solvent viscosity Solvent viscosity (η) reliance on temperature can modify the ion mobility and, consequently, the solution conductivity. If different effects do not occur in the viscous motion model, ion velocity results inversely proportional to viscosity. Rising temperature, viscosity decreases and the solution conductivity increases [15]. The Walden law ($\eta\lambda = constant$) defines that the product of viscosity η and ionic equivalent conductivity λ is constant by varying on external parameters (such as temperature). The Walden law is employed to distinguish ions moving by viscous motion (Walden law is verified) and ions moving by jump mechanism [15].

Solvent polarity The solvent can affects the solution conductivity in a different way. Considering the jump mechanism, increasing the solvent polarity, the electric interaction force between the ion and the solvent molecule and the ion jump velocity (from a molecule to another) increase, therefore the solution conductivity increases. Nevertheless, if the solvent polarity rises, also the ion solvation degree increases, therefore their motion possibility is hindered and then a decreasing in conductivity occurs [15]. Due to the dimensional characteristics of solute, there is a prevalence of the ion movement velocity or the solvation effect.

Intensity and frequency of the applied electric field If the applied voltage is higher than the one of ion discharge, the cell is crossed by a faradaic current. This phenomenon modifies the surface of the electrodes and it changes the solute concentration inside the solution. Therefore, it is necessary to hold a voltage value which gives rise to a non-faradaic current. In order to avoid faradaic process, for aqueous solutions of K^+ and Cl^- ions electrolytes, the voltage must be kept lower than 1 V [20]. The applied voltage in DC regime gives rise to polarization phenomena in solution, local variations of concentration close to the electrodes, which can modify the conductivity behaviour during the time. The result is a decreasing in electrolytic conductivity. To minimize polarization effects, it is required to apply an electric field in AC regime.

2.3 Electrolytic conductivity measurements

Electrolytic conductivity determination consists of a resistance measurement of the examined solution and it is performed using alternating current AC of suitable frequency ω and low-intensity, whose passage through the solution does not alter

any characteristic. The use of AC eliminates net electrolysis of the sample and reduces polarization at the electrodes, but it complicates the electrical technique required for high-accuracy measurements, owing to the need for compensation of capacitive and inductive effects in the circuit [15].

Therefore, electrochemical systems are described by means of methods based on impedance measurement, called electrochemical impedance spectroscopy (IES).

2.3.1 Impedance

The measured impedance of an electrolytic cell is the sum of the bulk impedance Z_b and the electrode/solution interface Z_e:

$$Z(f) = R(f) + jX(f) = Z_\mathrm{b} + Z_\mathrm{e} \tag{2.23}$$

It is therefore necessary to identify Z_b as the sum of resistance R_b and reactance X_b of the bulk solution:

$$Z_\mathrm{b}(f) = R_\mathrm{b} + jX_\mathrm{b} \tag{2.24}$$

The behaviour of Z_e is dependent on the liquid under study and on the electrode composition and surface structure. In particular, the double layer occurring at the electrode/liquid interface gives impedance increasing for lower frequencies.

With proper modelling of Z_e [21, 22, 23, 24, 25], it can be shown that $R_\mathrm{b} = R(f^*)$ at the particular frequency f^* for which $X(f^*) = 0$ (or, more precisely, a minimum of $|X(f)|$) occurs. The particular f^* value is dependent on the sample and on the measurement cell, and has to be experimentally identified.

Hence, measurements of $Z(f)$ over a wide frequency bandwidth are needed.

Typically, commercial LCR bridges are the impedance meters employed for the measurement, programmed to perform repeated frequency sweeps.

A useful graphical representation to find f^* is the Cole–Cole (or Nyquist) $R(f) - X(f)$ graph.

2.3.2 Experimental apparatus and measurement procedure

Accurate and precise electrolytic conductivity measurements are performed by using an Agilent Technologies E4980A LCR bridge [26].

The LCR bridge is connected to the electrolytic cell by coaxial cables with BNC connectors, using a four terminal configuration. The shielded cables were made of insulated Teflon® AXON cable. At present the coaxial cables join the cell by two terminal connections, because of at INRIM entirely shielded cells have been not yet developed. The transition from four terminals to two terminals was performed in proximity of the electrodes. The applied excitation is a sine wave with an rms value of 0.5 V to avoid ion discharge at the electrodes.

To check the electrical performance for compensating parasitic circuit elements and to correct the impedance of the cables, LCR bridge OPEN/SHORT procedure is carried out before impedance measurements. Periodically, a check is carried out on the measurement system: a calibrated impedance standard, having a nominal value close to resistance of analysed solution, is connected to the bridge, and the measured value is compared to the value reported in the calibration certificate [27], [28].

During the resistance measurements, temperature is determined simultaneously. The reference temperature is maintained by an air thermostatic bath, Branca Idealair Measure Box, model 3715 [29]. This air bath guarantees a sufficient temperature stability (at 25 °C the stated stability is within ±0.005 °C and at 15 °C it is within ±0.01 °C), by using a Peltier cell system and moreover it performs a temperature spatial uniformity, by a low noise ventilation system. The air-bath reaches the temperature stability more slowly in comparison to an oil-bath (about 5 hours versus 2), but it avoids sample contaminations, due to oil vapour, which represent a significant improvement in order to measure low electrolytic conductivity solutions.

Temperature was acquired by using an Agilent Technologies 3458A digital multimeter [30], connected to a calibrated platinum thermoresistance Pt100, named Termics02, which was placed adhering to the cell wall, for the solution temperature monitoring. The Pt100 resistance thermometer was calibrated at INRIM Thermodynamic Division.

The LCR meter and the multimeter are connected to the computer via controller National Instruments GIPB 488. Acquisition data procedures are automatically performed by using a software developed at INRIM in LabWindows/CVI.

To perform electrolytic conductivity measurement, cells must be perfectly clean before use. If no evident residual impurities are present (that can be removed by mechanical means), the cleaning procedure consists in several washing steps with ultra-pure water.

A Millipore® system was employed for ultra-pure water production, to obtain KCl aqueous solutions and also as pure water sample for low conductivity measurements.

To check leakage and to clean residual impurities from glass surfaces and interstices, all the systems are filled with ultra-pure water and left to rest for at least 1 h. When water conductivity results lower than 1 µS cm^{-1} (estimated with a commercial conductivity meter, WTW inoLab® TetraCon 325 [31]), the devices are considered clean and ready to be primed.

Priming consists in filling and emptying the cell with shares of the measurement solution, in order to wet the glass walls of the cell and to avoid the solution dilution during the effective measurement.

After priming, the cell is ready to be used and it is filled with the measurement solution, it is positioned inside the thermostatic air bath and connected to LCR bridge and multimeter. Measurement parameters are set and experiment begins.

Measurements are performed during the night in order to achieve the best thermal stability conditions.

2.3.3 Data processing

As a result of experimental procedure described in the previous paragraph, sets of data $[f,\ R(f),\ X(f),\ T]$ are organized in successive sweeps. The extrapolation of R_b from the AC behaviour is critical, since the total impedance includes also a reactance contribution and parasitic terms.

In order to evaluate R_b, only sequences of impedance sweeps corresponding to stable temperature values were considered. To identify anomalous behaviours, resistance and temperature data are plotted with respect to time (Fig. 2.7).

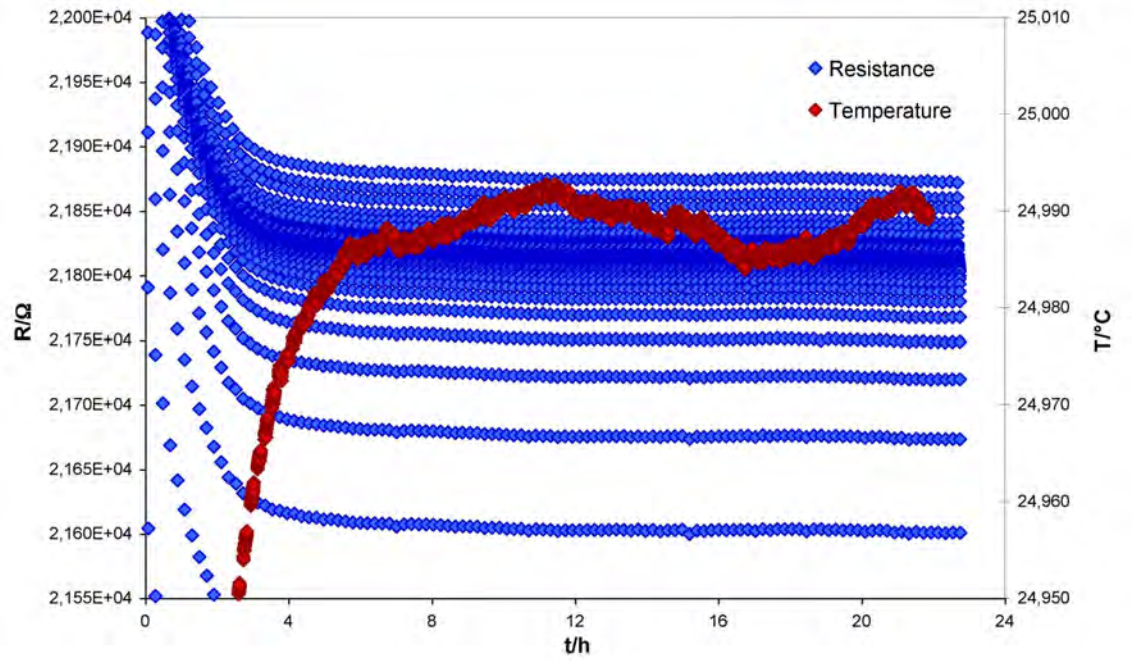

Figure 2.7: Resistance and temperature behaviours versus time for a solution of nominal conductivity $\kappa = 15\,\mathrm{mS\,m^{-1}}$ at 25 °C measured by primary cell.

After identifying suitable sweeps, resistance R and reactance X values are plotted with respect to frequency f (logarithmic frequency scale) to visualize the behaviour of the sample impedance versus frequency (Fig. 2.8).

Fig. 2.8 shows that at low frequencies, polarization effects occur and they give rise to an increase of the measured resistance while at high frequencies, circuital effects (usually capacitive) are responsible for the decreasing of measured resistance. But, for intermediate frequencies, a plateau region exists in which the resistance of the

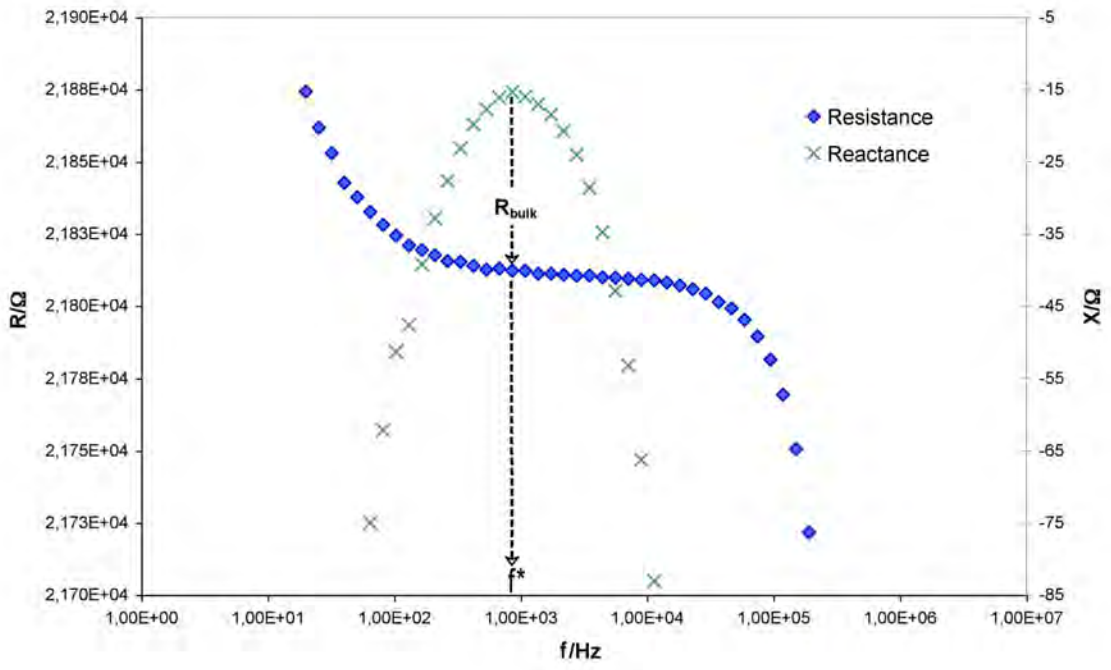

Figure 2.8: Impedance behaviour versus frequency (resistance R and reactance X) for a solution of nominal conductivity $\kappa = 15\,\mathrm{mS\,m^{-1}}$ at 25 °C measured by primary cell.

solution bulk R_b is the corresponding resistance value at f^* where the modulus of the reactance, i.e. the imaginary part of the impedance, has a minimum value. R_b is then used to calculate κ according to primary or secondary measurement procedure (see Sec. 2.4, 2.5).

Moreover, when the measurement temperature does not correspond to the reference one, the measured resistance value $R(T)$ has to be corrected using the following equation:

$$R(T_\mathrm{ref}) = R(T)\left[1 + \alpha_\mathrm{T}(T - T_\mathrm{ref})\right] , \tag{2.25}$$

where $R(T_\mathrm{ref})$ is the resistance value corrected to reference temperature T_ref, T is the temperature measured during the experiment and α_T is the temperature coefficient.

Finally, the electrolytic conductivity value at the reference temperature T_ref is obtained by Eq. (2.6), where $R_\mathrm{b} = R(T_\mathrm{ref})$.

2.4 Primary method of electrolytic conductivity measurement

Absolute conductivity determination is performed by resistance measurement of an electrolytic solution in a cell with a defined geometric constant K_{cell}.

Given that the cell constant K_{cell} is affected by the imperfect definition of the cell geometry (e.g. roughness of electrode surfaces, non-parallelism of the electrodes, non-ideal cell shape) and by the inhomogeneity of the electric field between the electrodes (e.g. edge effects), conductivity measurements were performed using a cell with variable geometry, composed by two parallel electrodes and a cylindrical removable central section.

During the time, NMIs developed different geometries for primary cells [32]. This type of cells is known as Jones-type cell [33, 34, 35] and it was firstly developed at NIST. The cell design is schematically shown in Fig. 2.9.

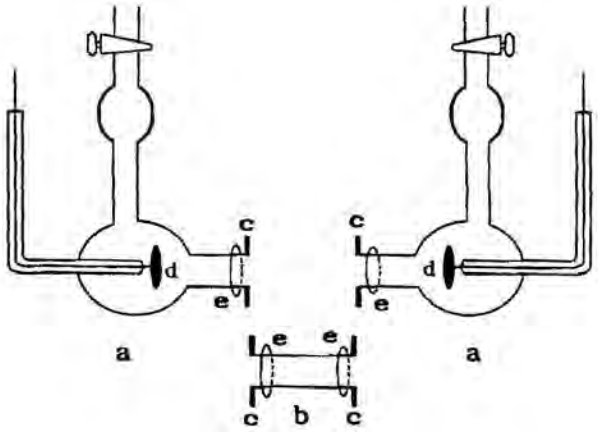

Figure 2.9: Jones-type conductivity cell: a – electrode chambers (half-cells); b – removable center tube; c – flanges; d – platinum disk electrodes; e – O-rings.

Regardless of the chosen geometry, K_{cell} is determined by means of accurate measurements of the cross sectional area A and the length l of the inner hole of the glass tube separating the platinum electrodes, as expressed in (2.7).

Electrolytic conductivity is determined by means of two measurement steps and the differential measurement principle is shown in the following equation:

$$\kappa = \frac{K_{\text{cell}}}{R_{\text{W}} - R_{\text{N}}}\,, \tag{2.26}$$

where K_{cell} is the geometric cell constant, R_{W} and R_{N} are the resistance values measured with and without the central section, respectively.

Since K_{cell} is accurately determined by dimensional measurements of the central section and resistance measurements are traceable to SI, κ is absolutely determined.

Measurements have to be performed at the reference temperature of 25 °C [36], but practically, they are carried out at temperature values very close to, so, κ values have to be referred to it.

Then, primary measurement of κ is obtained by:

$$\kappa = \frac{K_{\text{cell}}}{\left[\overline{R}_{\text{W}}(1+\alpha_{\text{T}}(T_{\text{W}}-T_{\text{ref}})) - \overline{R}_{\text{N}}(1+\alpha_{\text{T}}(T_{\text{N}}-T_{\text{ref}}))\right]} + \delta\kappa_{\text{W}} + \delta\kappa_{\text{N}}\,, \qquad (2.27)$$

where K_{cell} is the geometric cell constant of the primary cell, $\overline{R}_{\text{W}}$ and $\overline{R}_{\text{N}}$ are the average of n resistance measurements ($j = 1, \ldots, n$) carried out by means of the cell in configuration with and without the central section respectively, T_{W} and T_{N} are the corresponding temperature values of measurements carried out using the cell with and without the central section respectively, T_{ref} is the reference temperature, α_{T} is the temperature coefficient which value has been obtained by the literature [37], $\delta\kappa_{\text{W}}$ and $\delta\kappa_{\text{N}}$ are additional terms concerning the variations of electrolytic conductivity due to the solution contamination, considering the cell with and without the central section.

Afterwards, this solution with known conductivity, is employed to determine the geometric constant of a secondary device K_2.

2.5 Secondary method of electrolytic conductivity measurement

The process of determining the cell constant under specified conditions (that is, with a working solution having a specified conductivity value and with the cell at a specified temperature [38]) is called cell calibration. In cell with fixed geometry the cell constant is not accurately definable using dimensional measurements and it should be thus determined by calibration against a reference cell:

$$K_2 = \frac{R_2}{R_1} K_1\,, \qquad (2.28)$$

where K_1 and K_2 are the constants of the reference and the cell under calibration, respectively, and R_1 and R_2 are the resistances of the two cells.

At high conductivity values, calibration is commonly performed by means of a substitution method [311-02-04] [39]. However, at low conductivity values, this method is no longer accurate because air carbon dioxide CO_2 causes a drift of the solution conductivity which is unpredictable and different among the two cells. Therefore, K_2 is determined by comparison against K_1 using a solution that continuously flows throughout an hydraulic system connecting the cells (see Sec. 2.6).

The new calibrated cell is used to develop reference solutions (prepared dissolving weighed amounts of KCl salt in ultra pure water, depending on the required conductivity value) and it is used to calibrate commercial cells and conductivity probes.

Electrolytic conductivity values obtained with secondary method are based on the following equation:

$$\kappa_2 = \frac{K_2}{[R_2(1 + \alpha_T(T_2 - T_{ref}))]} + \delta\kappa\,, \tag{2.29}$$

where K_2 is the geometric constant of the secondary cell, R_2 is the resistance value measured by the secondary cell, T_2 is the temperature value corresponding to secondary measurements, T_{ref} is the reference temperature α_T is the temperature coefficient, which value has been obtained by the literature [37], $\delta\kappa$ is an additional term which takes into account the variations of electrolytic conductivity due to the pollution of the solution.

κ_2 has an uncertainty which mainly takes account of the measurement repeatability, temperature, contamination and K_2 calibration.

2.6 Measurement of low electrolytic conductivity solutions

The measurement of samples at low electrolytic conductivity values is no longer accurate because significant difficulties arise from solution contamination by air carbon dioxide (CO_2) and other contaminants from the glass walls. Also temperature variations and parasitic phenomena affect resistance measurements and are sources of errors in the electrolytic conductivity determination. The indications reported in [13, 37] prescribe, for solutions with conductivity lower than $5\,\mathrm{mS\,m^{-1}}$, the use of a system with flowing solution to reduce CO_2 contamination.

For these reasons, it was developed a closed system to perform measurements with a flowing solution. This hydraulic system allows measurements of low electrolytic conductivity solutions and, at the same time, in-line secondary cell calibrations. By means of this circuit, since the two cells contain shares (at approximately equal temperatures) of the same solution, the drift is homogeneous throughout the two communicating cells and the effects of CO_2 cancel out because they are in common mode. This kind of system is used also for the calibration of commercial coaxial conductivity cells and it is described in [40, 41].

2.6.1 Hydraulic circuit

In order to have measurements with a flowing solution, the flow-through cells developed at INRIM (described in detail in Chapter 3) are inserted in a Pyrex®glass hydraulic circuit together with an expansion chamber and a peristaltic pump. The closed circuit is shown in Figg. 2.10 and 2.11.

The glass pipeline has a length of 183 cm and an inner diameter of 6 mm. It is connected to the cells and the expansion chamber by means of 6 cm silicone joints (Masterflex®Biopharm Plus). Moreover, cells and the expansion chamber have 6 Teflon® stopcocks (length 12 mm and inner diameter 4.2 mm). All the materials employed were chosen because of their high inertness, so that solution contamination could be kept to a minimum.

The expansion chamber is a Pyrex®glass cylindrical flask equipped with two bottom pipelines, to allow the solution flow, and two top ones to inject an inert gas (argon). This device is partially filled with the solution to be measured and partially with argon gas to avoid solution contamination with air CO_2 and to damp possible fast rises of the flow pressure. A commercial CO_2 probe (Testo 535) is inserted into the input pipeline of the expansion chamber to monitor the CO_2 concentration in the argon gas during the measurement period.

The solution flow (50 mL min^{-1}) is ensured by the Watson-Marlow Bredel Sci-Q 323 peristaltic pump [42].

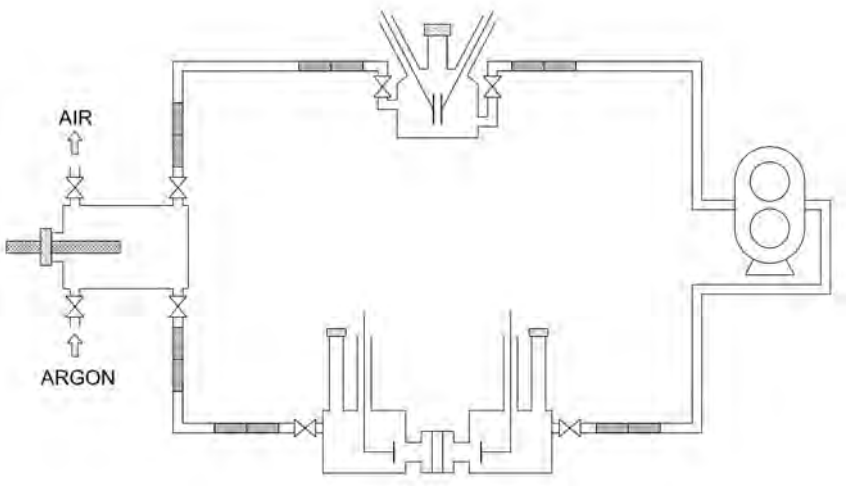

Figure 2.10: Graphic representation of the idraulic circuit

Since it is employed to perform κ measurements of low electrolytic solutions, the system has to be perfectly clean. So, before measurement, each circuit component is washed several times with ultra-pure water and left to rest at least 1 h. When the

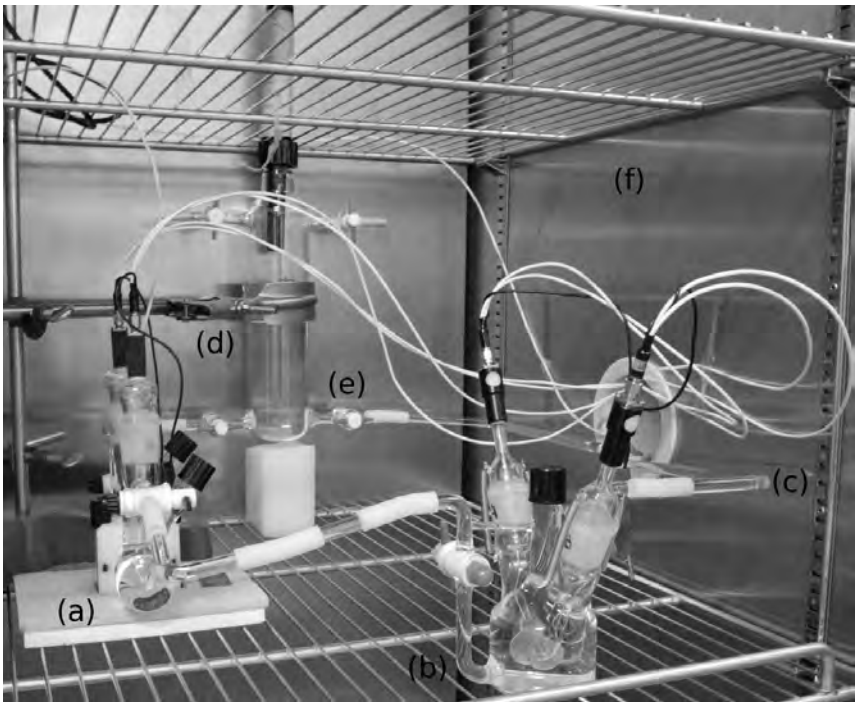

Figure 2.11: Picture of the circuit inserted in the thermostatic air chamber. The system includes (a) the reference cell, (b) the cell under calibration, (c) the glass pipes, (d) the expansion chamber, (e) stopcock, (f) thermostatic chamber.

circuit is considered clean and ready to be used, it is primed with the measurement solution.

To obtain conductivity values at the reference temperature of 25 °C, all the components of the circuit are assembled within the thermostatic air bath [29] with the exception of the peristaltic pump which could be a source of temperature instability. The Pt100 platinum resistance thermometer [43] is placed in contact with the cell wall and connected to a digital multimeter (Agilent Technologies 3458A [30]) to monitor the solution temperature.

Finally, the circuit is filled with the solution sample and the expansion chamber is loaded with argon gas.

The two cells are connected to a HP 3235 switch control unit which alternatively connects the two cells to an Agilent E4980A LCR meter [26] to perform impedance measurements. A complete cycle consists of two successive sweeps and it takes less than 2 min. Measurements are carried out overnight for about 15 h.

2.6.2 Measurements with the reference cell and flowing solution

The primary conductivity determination performed by means of the hydraulic circuit and flowing solution is estimated by the following equation:

$$\kappa = \frac{K_{\text{cell}}}{\overline{R}_{\text{W}} - \overline{R}_{\text{N}}} + \delta\kappa_{\text{W}} + \delta\kappa_{\text{N}}\,, \tag{2.30}$$

where:

- $\overline{R}_{\text{W}}$ is the average of n resistance measurements $R^{C}_{\text{W,j}}$ $(j = 1, \ldots, n)$ carried out on the cell with the central section and corrected for the temperature difference $T_{\text{W,j}} - T_{\text{ref}}$, where $T_{\text{W,j}}$ is the air bath temperature during the jth measurement. The correction is given by

$$R^{C}_{\text{W,j}} = R_{\text{W,j}}[1 + \alpha_{\text{T}}(T_{\text{W,j}} - T_{\text{ref}})]\,, \tag{2.31}$$

  where α_{T} is the temperature coefficient of the solution conductivity [44];

- $\overline{R}_{\text{N}}$ is the average of n resistance measurements $R^{C}_{\text{N,j}}$ $(j = 1, \ldots, n)$ carried out on the cell without the central section and corrected for the temperature difference $T_{\text{N,j}} - T_{\text{ref}}$, where $T_{\text{N,j}}$ is the air bath temperature during the jth measurement. The correction is given by

$$R^{C}_{\text{N,j}} = R_{\text{N,j}}[1 + \alpha_{\text{T}}(T_{\text{N,j}} - T_{\text{ref}})]\,, \tag{2.32}$$

- $\delta\kappa_{\text{W}}$ and $\delta\kappa_{\text{N}}$ are additional terms taking into account the resistance drift due to solution contamination

2.6.3 In-line calibration procedure

The hydraulic circuit for flowing solutions is also employed to perform secondary cell calibration by means of comparison method. The measurement system and procedure have been previously described in Sec. 2.6.1.

Since just one Pt100 thermometer is employed, temperature is measured positioning it on the reference cell, while the temperature of the cell under calibration is inferred from that of the reference cell by considering the chamber temperature inhomogeneity.

Measuring the resistance of the two cells yields, (according to Eq. (2.6)), two resistance values $R_1 = K_1/\kappa_1$ and $R_2 = K_2/\kappa_2$, where K_1 and K_2 are the two cell constants, and κ_1 and κ_2 are the conductivities of the solutions contained in the cells.

Ideally, a calibration should be carried out with $\kappa_1 = \kappa_2$ and with the cells at the specified temperature. When this condition is met, K_2 can be directly determined in terms of K_1 as shown in Eq. (2.28).

If contamination and temperature affect the conductivity (the temperature coefficient can range from $2\,\%\,^{\circ}\mathrm{C}^{-1}$ to $7\,\%\,^{\circ}\mathrm{C}^{-1}$ [13]), then $\kappa_1 \neq \kappa_2$. These effects can be modelled by the following equation:

$$\kappa_2(T_2) = \kappa_1(T_1)[1 + \alpha_T(T_2 - T_1)](1 + \delta\kappa_2 - \delta\kappa_1)\,, \tag{2.33}$$

where T_1 and T_2 are the cell temperatures; α_T is the temperature coefficient of the solution conductivity at the specified temperature; and $\delta\kappa_1$ and $\delta\kappa_2$ represent the relative change in the conductivity due to contamination in each cell.

Taking into account (2.33), K_2/K_1 becomes

$$\frac{K_2}{K_1} = \frac{R_2}{R_1}\frac{\kappa_2(T_2)}{\kappa_1(T_1)} \approx \frac{R_2}{R_1}(1 + \alpha_T\Delta T + \Delta\kappa_{\mathrm{pol}})\,, \tag{2.34}$$

where $\Delta T = T_2 - T_1$ and $\Delta\kappa_{\mathrm{pol}} = \delta\kappa_2 - \delta\kappa_1$. In the above equation, the expression within parentheses constitutes an error term.

With the substitution method, this error is not negligible because, even though the two cells are filled with shares of the same transfer solution, temperature and contamination drifts can be different. While the term $\alpha_T\Delta T$ can be corrected by measuring ΔT, $\Delta\kappa_{\mathrm{pol}}$ is unpredictable and cannot be corrected. Therefore, $\Delta\kappa_{\mathrm{pol}}$ is a non negligible source of uncertainty.

Instead, with the comparison method, the solution flows in both cells, so that both the temperature and the solution (though contaminated) are homogeneous throughout the circuit, $T_2 \approx T_1$ and $\delta\kappa_2 \approx \delta\kappa_1$, and the error term is negligible.

Results concerning calibration measurements of different electrolytic solutions performed by substitution and comparison methods are described in the Chapter 3.

2.7 An impedance spectrometer for ultra pure water measurements

Conductivity measurements of liquids ask for measurements of impedance in a wide frequency range to identify stray parameters caused by electrode-surface effects. As it was observed by preliminary measurements, on low-conductivity liquids (such as ultra-pure water), frequencies of interest range below those available on precision LCR meter (usually in the 10 Hz range). A dedicated impedance meter capable of extending the measurement bandwidth below hertz is necessary. Commercial instruments (impedance analyzers and dynamic potentiostats) devoted to electrochemical

impedance spectroscopy, capable of reaching the mHz or even µHz range, are available on the market; however, they usually have a relative uncertainty in the 1×10^{-3} range. Moreover, being "closed" instruments, the metrological traceability of their measurements can be difficult to assess. The impedance spectrometer proposed is based on a commercial analog–digital conversion (ADC)/digital–analog conversion (DAC) board, a simple custom-made analog frontend amplifier, and acquisition and processing software. An previous version of the spectrometer has been presented in [45].

2.7.1 Measurement set-up

A block schematic of the spectrometer is shown in Fig. 2.12. The measurement cell [44] (name code IRMMECEL002), is a flow-through secondary cell with $K_{\text{cell}} \approx 15\,\text{m}^{-1}$ and it is described in detail in the next chapter.

Electrically, the cell is a two-terminal impedance, connected with coaxial leads, as shown in Fig. 2.12. To measure ultra-pure water by avoiding contamination by air CO_2 and other contaminants, an in-flow setup becomes necessary. Then, the cell is directly connected to the ultra-pure water production system (Millipore®) as shown in Fig. 2.13.

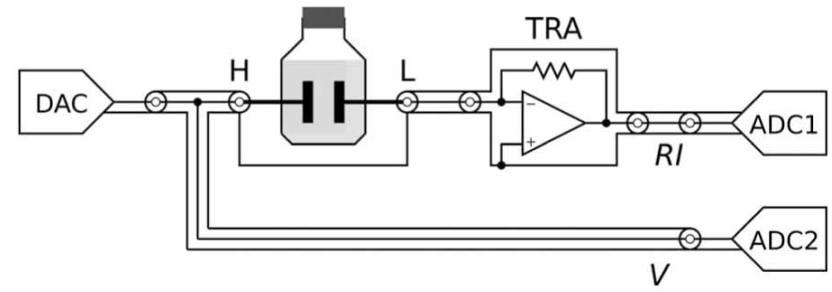

Figure 2.12: Simplified schematics of the spectrometer. ADC1, ADC2, and DAC are the ADCs and the DAC belonging to the acquisition board. DAC energizes the conductivity cell with voltage V at port H; V is measured by ADC2. Current I at port L is converted to voltage RI by TRA, a transresistance amplifier having gain R. RI is measured by ADC1.

2.7.2 Data acquisition and processing

The DAC is energized with a sampled frequency comb of sine waves, i.e.

$$s[j] = A \sum_{h \in H} \cos\left(2\pi h \frac{j}{n} + \phi_{\text{h}}\right) \quad j = 0, \ldots, 2^n\,. \tag{2.35}$$

Figure 2.13: In-flow setup for the measurement of ultrapure water. The production unit employed (Millipore® mod. RiOs-Di and Milli-Q academic) is connected with Pyrex® pipelines to the measurement cell in Fig. 3.4. Water outlet is collected in a beaker for temperature measurement.

Each sine wave of the comb is an harmonic of index h, belonging to the harmonic set $H \subset 1 \dots 2^{n-2}$ of a fundamental having a period of 2^n samples. All harmonics have the same peak amplitude A and a random phase ϕ_h; if H is sufficiently large, set $s[k]$ approximately has a normal distribution [46]. A is chosen to achieve the desired root-mean-square value of s, i.e.

$$s_\mathrm{RMS} = \left(2^{-n} \sum_j s^2[j] \right)^{\frac{1}{2}} . \tag{2.36}$$

Samples $v_1[j]$ and $v_2[j]$, $j = 1 \dots 2^n$, are acquired at the sampling frequency f_S and processed with discrete Fourier transform (DFT) to obtain amplitude spectra $V_1[k]$ and $V_2[k]$, where $k = 0 \dots 2^{n-2}$ and $f_\mathrm{k} = k(f_\mathrm{S}/2^n)$. Impedance $Z(f)$ can be

estimated [47], [48] at all frequencies f_h with the DFT ratio, i.e.

$$Z(f_\mathrm{h}) = R(f_\mathrm{h})\frac{V_2[h]}{V_1[h]}\,, \tag{2.37}$$

where $R(f_\mathrm{h})$ is the gain of the transresistance amplifier (see Fig. 2.12) at frequency f_h. Eq. (2.37) can be rewritten in terms of the auto and cross power spectral densities P_1 and C_{12} (of v_1 and between v_1 and v_2, respectively) for which functions that are more convenient than the bare fast Fourier transform may be available in the programming environment, i.e.

$$Z(f_\mathrm{h}) = R(f_\mathrm{h})\frac{C_{12}[h]}{P_1[h]}\,. \tag{2.38}$$

The choice of set H is arbitrary; for a given s_RMS value, its numerosity n_H influences the signal to-noise ratio (SNR) of readings $Z(f_\mathrm{h})$. As a rule of thumb, the SNR is proportional to $(n_\mathrm{H})^{-1}$. A method for the optimal choice of set H has been published [49]. Presently, the software allows selecting between two possible combs:

1. Linear comb: $H = 1 \ldots 2^{n-2}$; all possible harmonics [50] are present in s.
2. Log comb: H includes approximately the same number of harmonics per frequency octave.

Typical sampling parameters are $n = 18$, $f_\mathrm{S} = 2\,\mathrm{kHz}$. The resulting minimum frequency (and frequency spacing between harmonics) is $\approx 7.63\,\mathrm{mHz}$; for a linear comb $n_\mathrm{H} = 2^{16} \approx 6 \times 10^{-4}$ frequencies, a log comb with ten frequencies per octave results in $n_\mathrm{H} = 153$.

Measurement results on pure-water samples and a comparison with measurements performed with an LCR meter are reported in Chapter 3.

Chapter 3

Measurement results

3.1 Introduction

During Ph.D. research activity, my attention was focused on the implementation of devices for the ultra pure water conductivity determination. The starting point was to create a set of electrolytic cells suitable for the measurement of low electrolytic conductivity solutions. All the cells were especially built by the glass blowers Disa Raffaele e F.lli.

On the basis of the experience and needs encountered during the work, I also designed a closed hydraulic system which allows to perform measurements of low κ and cell calibrations by means of a solution which continuously flows through the system.

In this chapter, the results obtained by using the instrumentation and measurement procedures previously described are reported.

3.2 Electrolytic cells

3.2.1 Primary cells

The primary cell permits to obtain electrolytic conductivity values traceable to SI unit. Each NMI chooses its primary device: at INRIM two Jones-type primary cells, according to the differential measurements firstly conceived by NIST [34, 35], were developed.

By means of these two cells, it is possible to carry out measurements in $0.005\,\mathrm{S\,m^{-1}}$ to $2\,\mathrm{S\,m^{-1}}$ range.

Both cells are composed of two Pyrex®glass half-cells and a removable hollow cylindrical central section. Each half-cell contains a smooth round planar platinum

electrode (thickness 0.5 mm, diameter 20 mm) [51], which guarantees chemical inertness and minimizes the permeability to impurities [37]. Each electrode, embedded into a glass bar, is removable to allow thorough cleaning. A platinum wire, spot-welded to the back of the electrode, connects the electrode to a coaxial connector.

Each half-cell is equipped with two pipes: a filling pipe with an SVL®cap to avoid solution contamination and a valve pipe to allow solution flow by means of the connection to the hydraulic circuit (described in Sec. 2.6.1) to perform measurement with a flowing solution and, at the same time, in-line calibration measurements.

The removable central section is made of Pyrex®glass. It has a length $l \approx 10\,\mathrm{mm}$ and an inner hole with a nominal diameter $d \approx 15\,\mathrm{mm}$. The dimensions were accurately characterized by the INRIM Mechanical Division, by means of a coordinate measuring machine (CMM). To take into account the inhomogeneity of d along the hole in the K_{cell} evaluation, the central section is considered to be a series of N slices with diameter d_i and the cell constant is estimated with the following equation:

$$K_{\mathrm{cell}} = \frac{4l}{\pi N} \sum_{i=1}^{N} \left(\frac{1}{d_i}\right)^2 . \tag{3.1}$$

A special quick closure system in Delrin®(polyoxymethylene) homogeneously distributes mechanical stresses around the glass flanges (Fig. 3.2) and it tightens the glass flanges preventing lateral and rotational movements of the two half-cells. The cell was designed with a volume of about 160 mL in order to have a good thermal capacity.

The main difficulties in the use of primary cells concern the measurement repeatability due to difference in final assembly and the possible contamination of the cell. The cell differential design allows highly accurate evaluation of the geometric constant, but it is necessary to disassemble and clean the cell before each measurement, continuously changing the alignment of the cell parts.

IRMMECEL001

The primary cell named with code IRMMECEL001 is shown in Fig. 3.1.

The estimated cell constant is:

$$K_{\mathrm{cell}} = 55.8703\,\mathrm{m}^{-1} \quad \text{with} \quad U(K_{\mathrm{cell}})_{(k=2)} = 0.0305\,\mathrm{m}^{-1} . \tag{3.2}$$

In Table 3.1 on page 61 the uncertainty budget for a solution with nominal conductivity of $5\,\mathrm{mS\,m}^{-1}$ is reported. In the treatment of the measurement uncertainty the relevant international documents [52, 53] were followed and the corresponding uncertainties were combined by applying the uncertainty propagation law, where the input quantities are considered uncorrelated.

In the following, details about the uncertainty contributions are reported:

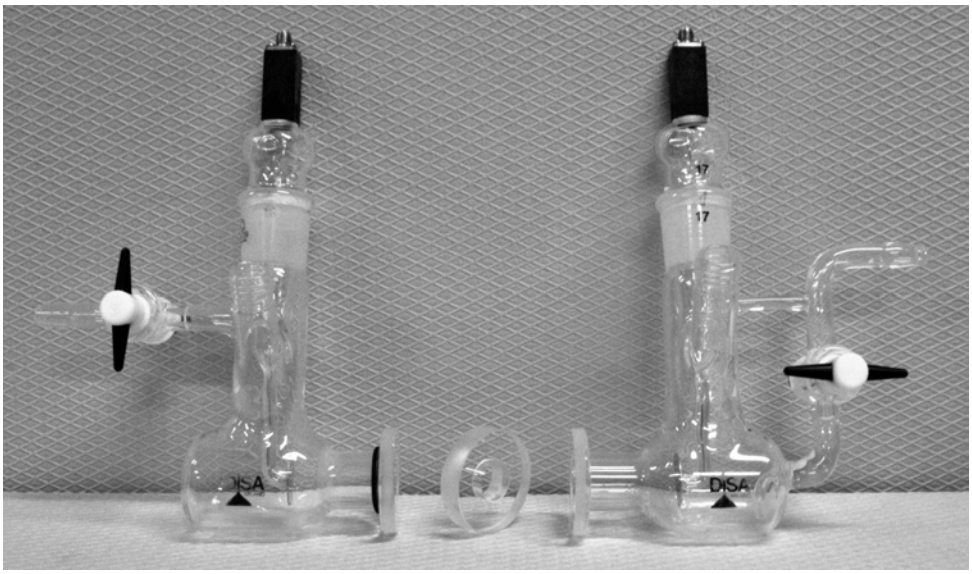

Figure 3.1: Picture of the flow-through primary cell IRMMECEL001 developed at INRIM

Figure 3.2: Delrin®closure system

- The combined standard uncertainty $u(K_{\text{cell}})$ associated with the cell constant and obtained by the certificate was $1.53 \times 10^{-2}\,\text{m}^{-1}$.

- The uncertainty $u(\overline{R}_{\text{W}})$ associated with resistance of the cell in configuration with the central tube was given by three contributions. The uncertainty contribution due to the LCR bridge was evaluated from its calibration with a Tinsley standard AC resistors having resistance value similar to the one obtained with the solution ($100\,\text{k}\Omega$). The resulting standard uncertainty contribution was $0.7\,\Omega$ for which a normal distribution was assumed. The uncertainty contribute due to the LCR bridge resolution was evaluated $0.029\,\Omega$. For

the estimation of the type A contribution obtained by the repetition of the measurements a different aqueous solution with a similar conductivity value was prepared and three repetitions were carried out. The standard uncertainty associated with this repetition was 13.0 Ω. The combined standard uncertainty $u(\overline{R}_{\mathrm{W}})$ due to the three contributions was 13.1 Ω.

- The uncertainty $u(T_{\mathrm{W}})$ associated with temperature when the cell is in configuration with the central section is given by four contributions. The first corresponds to the calibration uncertainty of the platinum resistance thermometer. The calibration certificate issued by INRIM was referred to the international temperature scale of 1990 (ITS-90) [54]. At 25 °C the calibration expanded uncertainty is $U = 0.002\,^{\circ}\mathrm{C}$ with a rectangular distribution. The second contribution was given by the uncertainty of the multimeter, which corresponds to an expanded uncertainty for temperature of 0.003 K. Moreover, the resolution of the system thermometer/multimeter was 0.001 K and a rectangular distribution was associated. The fourth contribution was due to the variation of temperature obtained during the measurements. The associated standard uncertainty was $2.75 \times 10^{-2}\,^{\circ}\mathrm{C}$. The combined standard uncertainty for $u(T_{\mathrm{W}})$ was $2.77 \times 10^{-2}\,^{\circ}\mathrm{C}$.

- The uncertainty $u(\overline{R}_{\mathrm{N}})$ associated with resistance of the cell in configuration without the central section is given by three contributions. The uncertainty contributions due to the LCR meter calibration and to the LCR meter resolution was evaluated as for $u(\overline{R}_{\mathrm{W}})$. For the estimation of the type A contribution obtained by the repetition of the measurements a different aqueous solution with a similar conductivity value was prepared and two repetitions were carried out. The combined standard uncertainty $u(\overline{R}_{\mathrm{N}})$ was 17.9 Ω.

- The uncertainty $u(T_{\mathrm{N}})$ associated with temperature when the cell is in configuration without the central section was given by the same four contributions of $u(T_{\mathrm{W}})$. The combined uncertainty standard uncertainty $u(T_{\mathrm{N}})$ was $4.70 \times 10^{-3}\,^{\circ}\mathrm{C}$.

- The uncertainty $u(\alpha_{\mathrm{T}})$ associated with temperature coefficient was considered of 10% considering a rectangular distribution. The uncertainty contribution was $2.89 \times 10^{-4}\,^{\circ}\mathrm{C}^{-1}$.

- $\delta\kappa_{\mathrm{W}}$ corresponded to the variation of conductivity value during the measurement with the cell with the central section due to the contamination of the solution. It was evaluated considering the resistance at a specific frequency value for 100 frequency sweeps. The resistance difference was determined and it was transformed in a conductivity value considering a cell constant specific

of the cell with the central tube. This cell constant was evaluated by the average of other conductivity measurements with the primary cell with solution at different concentrations. The variation resulted of $1.37 \times 10^{-5}\,\mathrm{S\,m^{-1}}$. A rectangular distribution was associated.

- $\delta\kappa_\mathrm{N}$ corresponds to the variation of conductivity value during the measurement with the cell without the central tube due to the pollution of the solution. It has been evaluated as for $\delta\kappa_\mathrm{W}$. It was transformed from a resistance value in a conductivity one considering a cell constant specific of the configuration without the central tube. The variation resulted of $9.40 \times 10^{-6}\,\mathrm{S\,m^{-1}}$. A rectangular distribution was associated.

The reliability of the results obtained with IRMMECEL001 has been evaluated by means of the participation in the international measurement comparison CCQM-K92 on a solution with electrolytic conductivity value of $50\,\mathrm{mS\,m^{-1}}$ [55], whose results will be presented in Chapter 4 and the technical report is presented in Appendix.

IRMMECEL003

IRMMECEL003 was built following the same design of the previous primary cell. However, the new cell has been equipped with some technical improvements:

(i) the electrodes are held in place by means of an anchoring system realized through metal springs and hooks in glass, in order to prevent changes in geometry as a consequence of electrodes displacements (Fig. 3.3a);

(ii) valve pipes are located laterally in order to minimize the cell size (Fig. 3.3b);

(iii) the removable central section has a more regular central hole, in order to reduce diameter inhomogeneities along the hole which affect the imperfect definition of the K_cell.

In IRMMECEL003,

$$K_\mathrm{cell} = 56.312\,\mathrm{m^{-1}} \quad \text{with} \quad U(K_\mathrm{cell})_{(k=2)} = 0.0239\,\mathrm{m^{-1}}\,. \tag{3.3}$$

Unfortunately, I have not been able to test the traceability of this cell in any international comparison.

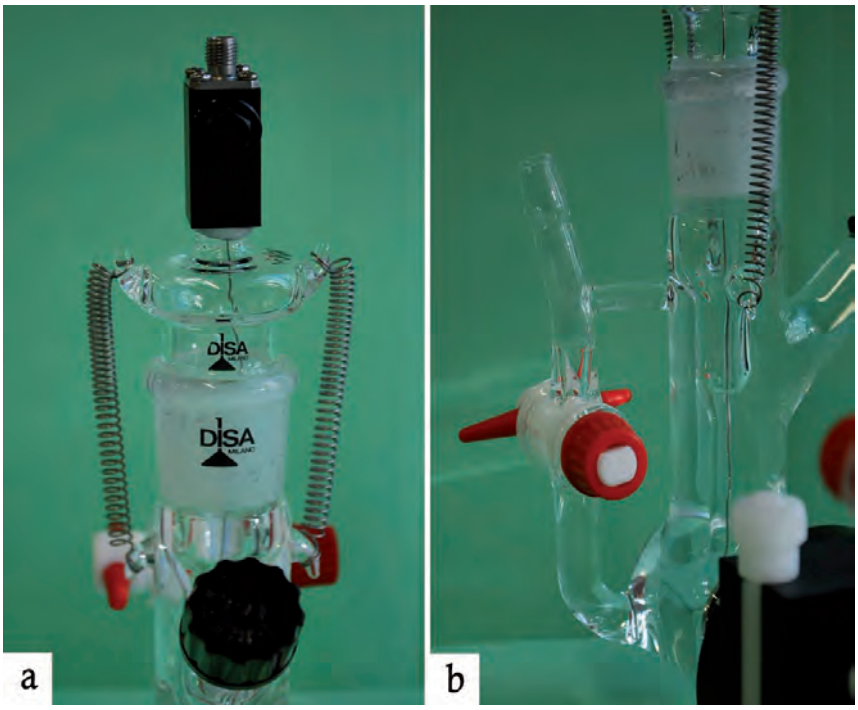

Figure 3.3: Picture of the flow-through primary cell IRMMECEL003

3.2.2 Secondary cells

Secondary cells have a fixed geometry and their cell constants are not determined using dimensional measurements because the accuracy would be too low. They are determined by calibration (Sec. 2.4).

Secondary cells are more easily applied for routine measurements. They are employed for the production of certified reference materials and calibration of commercial conductivity meters.

At INRIM, different types of secondary cells were developed and used to carry out dissemination and research activities. The most suitable geometry of the cell is chosen depending on the conductivity of the solution: high conductivity solutions (e.g. seawater) require cells with large K_2. On the contrary, to perform conductivity measurement of ultra pure water, it is necessary to employ cells with small K_2.

In the following, the main characteristics of the secondary cells developed at INRIM and their uncertainty evaluation are presented.

IRMMECEL002

IRMMECEL002 (Fig. 3.4) has a single chamber with 180 mL capacity with round and facing electrodes of thickness 0.5 mm and diameter 1.5 cm, positioned at a distance of about 15 mm. The electrodes are connected to coaxial connectors with platinum wires and they are fixed by means of an anchoring system with metal springs which prevents electrodes displacements.

The cell can be connected to the closed hydraulic circuit (Sec. 2.6.1) by means of two pipelines (outer diameter 9 mm) that allow the solution flow. The cell constant K_2 was estimated by in-line calibration procedure (described in Sec. 2.6.3):

$$K_2 = 15.753\,\mathrm{m}^{-1} \quad \text{with} \quad U(K_2)_{(k=2)} = 0.012\,\mathrm{m}^{-1}\,. \tag{3.4}$$

Figure 3.4: Picture of the flow-through secondary cell IRMMECEL002 developed at INRIM

IRMMECEL002 can be employed for conductivity measurements of aqueous solutions in the range 0.15 mS m^{-1} to 100 mS m^{-1}, which corresponds to the R range from 96 kΩ to 150 Ω and f^* range from 50 Hz to 60 kHz.

To perform κ determinations of KCl solutions, the used measurement method is described in Sec. 2.5. In model equation (2.29), the term $\delta\kappa$ is relative to the solution

conductivity drift due to contamination and it has not taken into consideration; because a solution with a value of $\kappa > 5\,\mathrm{mS\,m^{-1}}$ is considered stable [37].

In Table 3.2 on page 62 the uncertainty budget for a solution with nominal conductivity of $15\,\mathrm{mS\,m^{-1}}$ is reported.

In the following, details about the uncertainty contributions are reported:

- The combined standard uncertainty $u(K_2)$ associated with the cell constant and obtained by calibration was $6.00 \times 10^{-3}\,\mathrm{m^{-1}}$.
- The type A uncertainty $u(R_2)$ was obtained by the measurement repetition on the aqueous solution.
- The type B uncertainty $u(R_{\mathrm{sys}})$ was due to the LCR bridge calibration, which was carried out against standard resistors with $1\,\mathrm{k\Omega}$ value. Uncertainty of the standard, AC errors and LCR bridge linearity were the evaluated contributions.
- The uncertainty $u(T_2)$ was associated with the variation of temperature obtained during the measurements.
- The type B contribution $u(T_{\mathrm{sys}})$ was due to three contributions. The first corresponded to the calibration uncertainty of the platinum resistance thermometer. The calibration certificate issued by INRIM was referred to the international temperature scale of 1990 (ITS-90) [54]. At 25 °C the calibration expanded uncertainty is $U = 0.003\,^{\circ}\mathrm{C}$ with a rectangular distribution. The second contribution was given by the uncertainty of the multimeter, which corresponds to an expanded uncertainty for temperature of 0.003 K. Moreover, the resolution of the system thermometer/multimeter was 0.001 K and a rectangular distribution was associated.
- The uncertainty $u(\alpha_{\mathrm{T}})$ associated with temperature coefficient was considered of 10% considering a rectangular distribution.

IRMMECEL002 has been employed to perform measurements on bioethanol during the participation in EURAMET Study 1202 international comparison (see Chapter 4, Sec. 4.4), which technical report is included in Appendix.

IRMMECEL004

With the aim to perform conductivity measurement of ultra pure water, secondary cells require K_2 in the order of magnitude of $1\,\mathrm{m^{-1}}$, i.e. large electrode surface areas and small distance between the electrodes.

According to that, IRMMECEL004 was designed and built. The cell is shown in Fig. 3.5.

It has a single chamber of about 200 mL volume and two coaxial electrodes of 3 cm length and 0.25 mm thickness. The inner electrode has a diameter of 4 cm while the outer electrode has diameter of 5 cm. The distance between the electrodes is 5 mm. The cell can be connected to the flowing system or directly to the ultrapure water production system Millipore®by means of two pipelines (outer diameter 9 mm).

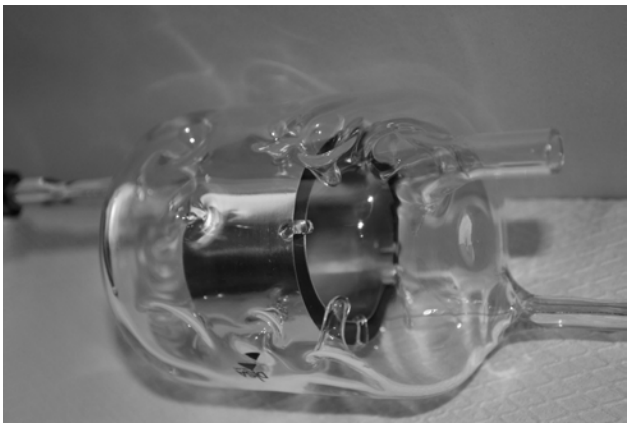

Figure 3.5: Picture of the flow-through secondary cell with coaxial electrodes IRMMECEL004

The cell constant K_2 is:

$$K_2 = 0.938\,\mathrm{m}^{-1} \quad \text{with} \quad U(K_2)_{(k=2)} = 0.016\,\mathrm{m}^{-1}\,. \tag{3.5}$$

The operating κ range is from $0.1\,\mathrm{mS\,m}^{-1}$ to $30\,\mathrm{mS\,m}^{-1}$, with measured $R_{\max}$ values of 9 kΩ and $R_{\min}$ of about 30 Ω, corresponding to $f^* = 50$ Hz and $f^* = 74$ kHz respectively.

A first preliminary study about this cell capability was carried out using a KCl aqueous solution with nominal conductivity of $1\,\mathrm{mS\,m}^{-1}$: measurements were performed including IRMMECEL004 in the hydraulic circuit, with the peristaltic pump set at 10 rpm speed. Measurements were carried out following Eq. (2.29) and the corresponding uncertainty budget is reported in Table 3.3 on page 63. The uncertainty components related to model equation are evaluated on the basis of the reported considerations:

- The combined standard uncertainty $u(K_2)$ associated with the cell constant and obtained by calibration was $8.00 \times 10^{-3}\,\mathrm{m}^{-1}$.

- The type A uncertainty $u(R_2)$ was obtained by the measurement repetition on the aqueous solution.
- The type B uncertainty $u(R_{\text{sys}})$ was due to the LCR bridge calibration, which was carried out against standard resistors with 1 kΩ value. Uncertainty of the standard, AC errors and LCR bridge linearity are the evaluated contributions.
- The uncertainty $u(T_2)$ was associated with the variation of temperature obtained during the measurements.
- The type B contribution $u(T_{\text{sys}})$ was due to three contributions. The first corresponds to the calibration uncertainty of the platinum resistance thermometer. The calibration certificate issued by INRIM was referred to the international temperature scale of 1990 (ITS-90) [54]. At 25 °C the calibration expanded uncertainty is $U = 0.002\,°\text{C}$ with a rectangular distribution. The second contribution is given by the uncertainty of the multimeter, which corresponds to an expanded uncertainty for temperature of 0.003 K. Moreover, the resolution of the system thermometer/multimeter was 0.001 K and a rectangular distribution has been associated.
- The uncertainty $u(\alpha_{\text{T}})$ associated with temperature coefficient was considered of 10% considering a rectangular distribution.
- $\delta\kappa$ corresponded to the variation of conductivity value during the measurement due to the solution contamination. It was evaluated considering the resistance at a specific frequency value for 100 frequency sweeps. The resistance difference was determined and it was transformed in a conductivity value considering K_2 The variation resulted of $3.26 \times 10^{-8}\,\text{S}\,\text{m}^{-1}$. A rectangular distribution was associated.

Future studies on IRMMECEL004 will focus on the improvement of measurement uncertainty for solutions with values of $\kappa < 1\,\text{mS}\,\text{m}^{-1}$, in order to participate in an upcoming international comparison on ultra-pure water measurement.

IRMMECEL005

IRMMECEL005 has a small chamber of 20 mL capacity and it is provided of two small platinum electrodes with diameter of 0.5 cm at a distance of 2.5 cm. The cell is shown in Fig. 3.6 and it has been designed for conductivity measurement of concentrated solution ($\kappa > 100\,\text{mS}\,\text{m}^{-1}$).

The cell constant K_2 has been estimated from calibration by substitution:

$$K_2 = 212.526\,\text{m}^{-1} \quad \text{with} \quad U(K_2)_{(k=2)} = 1.36\,\text{m}^{-1}\,. \tag{3.6}$$

The operating κ range is from $0.1\,\mathrm{mS\,m^{-1}}$ to $500\,\mathrm{mS\,m^{-1}}$, with measured $R_{\max}$ values of $1.6\,\mathrm{M\Omega}$, corresponding to $f^* \approx 40\,\mathrm{Hz}$ and $R_{\min}$ of about $450\,\Omega$ at $f^* = 620\,\mathrm{kHz}$.

Figure 3.6: Picture of the secondary cell IRMMECEL005 employed for salinity measurements

The cell was used to perform measurement (described in Sec. 2.5, by using the equation model (2.29)) of a solution with a nominal conductivity of $\kappa = 1\,\mathrm{mS\,m^{-1}}$.

The uncertainty evaluation is reported in Table 3.4 on page 64 and the considered contributions are reported as follows:

- The combined standard uncertainty $u(K_2)$ associated with the cell constant and obtained by calibration by substitution was $6.78 \times 10^{-1}\,\mathrm{m^{-1}}$.
- The type A uncertainty $u(R_2)$ is due to the measurement repetition on the KCl solution.
- The type B uncertainty $u(R_{\mathrm{sys}})$ is due to the LCR bridge calibration, which was carried out against standard resistors with $1\,\mathrm{k\Omega}$ value. Uncertainty of the standard, AC errors and LCR bridge linearity are the evaluated contributions.
- The uncertainty $u(T_2)$ is associated with the variation of temperature obtained during the measurements.
- The type B contribution $u(T_{\mathrm{sys}})$ is due to three contributions which correspond to the calibration uncertainty of the platinum resistance thermometer [43]

with a rectangular distribution, to the uncertainty of the multimeter and to the resolution of the system thermometer/multimeter to which a rectangular distribution has been associated.

- The uncertainty $u(\alpha_T)$ associated with temperature coefficient has been considered of 10% considering a rectangular distribution.

- $\delta\kappa$ corresponded to the variation of conductivity value during the measurement due to the solution contamination. It was evaluated considering the resistance at a specific frequency value for 100 frequency sweeps. The resistance difference was determined and it was transformed in a conductivity value considering K_2 The variation resulted of $1.49 \times 10^{-7}\,\mathrm{S\,m^{-1}}$. A rectangular distribution was associated.

The major contribution to $u_c(\kappa_2)$ is due to $u(K_2)$ because of K_2 determination has been carried out by means of calibration by substitution method despite of the reference solution has a low conductivity value. Moreover, also $u(R_2)$ is a significant contribution. It is associate to resistance measurements performed on a solution with a conductivity value close to the lower limit of the measurement cell capability.

Besides, IRMMECEL005 has been employed on CCQM-K105 and P142 international comparison on seawater samples (see Chapter 4, Sec. 4.1, 4.3) to perform measurement of solutions with electrolytic conductivity values higher than the upper measurement limit of the cell. It has been a forced choice because, during the measurements campaign, air thermostatic chamber has broken and we were obliged to employ an oil bath, giving up to perform measurements with primary cells. The technical reports with detailed descriptions about these activities will be presented in Chapter 4 and in Appendix.

IRMMECEL007

On the basis of found experience and difficulties during EURAMET International Comparison on bioethanol measurements [56], IRMMECEL007 has been designed and realized to perform electrolytic conductivity measurement of bioethanol samples. Since bioethanol has very low electrolytic conductivity values ($1\,\mu\mathrm{S\,m^{-1}}$ to $500\,\mu\mathrm{S\,m^{-1}}$) [57], measurements are affected not only by drifts due to sample contamination but also by evaporation phenomena. For that reasons, it has been decided to develop a secondary cell with a small chamber ($\approx 15\,\mathrm{mL}$) equipped by two wide platinum parallel electrodes (thickness 0.5 mm, diameter 2.5 cm) at a narrow distance (2 mm). A picture of the cell is shown in Fig. 3.7.

The cell constant K_2 has been estimated:

$$K_2 = 5.092\,\mathrm{m^{-1}} \quad \text{with} \quad U(K_2)_{(k=2)} = 1.07\,\mathrm{m^{-1}}\,. \tag{3.7}$$

The operating κ range is from $0.05\,\mathrm{mS\,m^{-1}}$ to $50\,\mathrm{mS\,m^{-1}}$, with measured $R_{\max}$ values of $70\,\mathrm{k\Omega}$, corresponding to $f^* \approx 50\,\mathrm{Hz}$ and $R_{\min}$ of about $100\,\Omega$ at $f^* = 36\,\mathrm{kHz}$.

Unfortunately, at the end of calibration measurements, one of the cell electrodes has desoldered: we suspect that probably it was already partially disconnected from the platinum wire, therefore resistance measurements are not completely accurate. This is the reason why $U(K_2)$ is so large and the cell has not been tested so far by appropriate measurements.

Figure 3.7: Picture of the secondary cell IRMMECEL007 developed for bioethanol measurements

3.3 The flowing solution system - results

Preliminary measurements on a $3\,\mathrm{mS\,m^{-1}}$ solution were performed to compare the stability of the hydraulic system with flowing solution (whose set-up and procedure were been previously discussed in Sec. 2.6.1 and 2.6.2) and without the closed system.

Moreover, to check the efficiency of the system, measurements on a $5\,\mathrm{mS\,m^{-1}}$ solution were carried out: this is the border conductivity value for a stable electrolytic solution.

Finally, electrolytic conductivity measurements on a $1\,\mathrm{mS\,m^{-1}}$ solution were realized, which is not possible to determine without the flowing system.

3.3.1 $3\,\mathrm{mS\,m^{-1}}$ solution

For the measurement on the $3\,\mathrm{mS\,m^{-1}}$ solution, the system with a flowing solution described in Chapter 2 was used.

Figure 3.8 shows the results of (i) a measurement with the system containing a static solution (circles); (ii) a measurement with flowing solution without argon buffer gas (diamonds) and (iii) a measurement with flowing solution and argon buffer gas injected into the expansion chamber (triangles). Each curve represents a time series of resistance values measured at f^*.

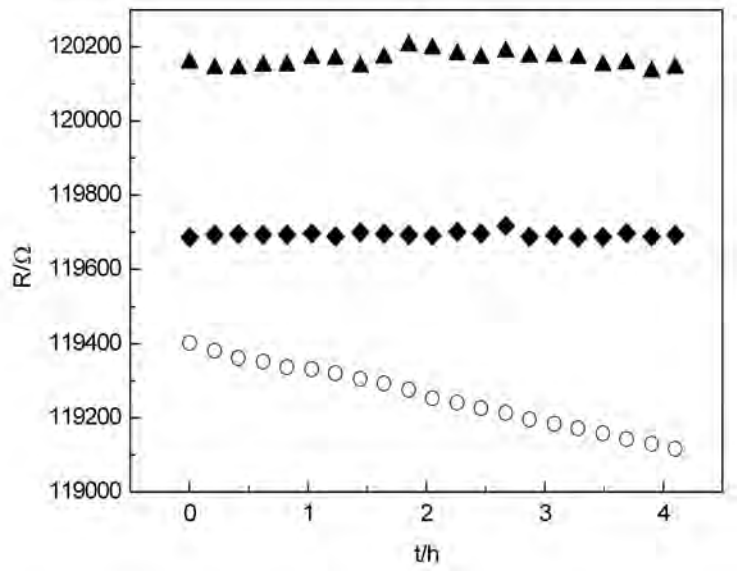

Figure 3.8: Drift of resistance measurements of a $3\,\mathrm{mS\,m^{-1}}$ solution, using the primary cell without central section: (i) static solution (circles); (ii) flowing solution without argon buffer gas (diamonds); and (iii) flowing solution with argon buffer gas (triangles).

Figure 3.8 clearly shows that without flowing solution the resistance drifts significantly (drift coefficient $\approx -1.4 \times 10^{-4}$), whereas with flowing solution the stability of the resistance is much higher (drift coefficient $\approx -2.0 \times 10^{-7}$).

Argon gas was also used with flowing solution to try to further reduce contamination from air CO_2: in this case, however, Fig. 3.8 does not show any significant improvement with respect to the measurement carried out without argon gas. Probably, at lower conductivity values, where CO_2 contamination is relatively higher, argon gas might help to reduce such contamination.

According to these preliminary stability results, the measurements described below were taken with flowing solution and argon gas.

3.3.2 $5\,\mathrm{mS\,m^{-1}}$ solution

Figure 3.9 shows an example of three impedance measurements on a $5\,\mathrm{mS\,m^{-1}}$ solution carried out on the cell without the central section. (The set-up with the flowing solution was used). The minimum value of the reactance can be identified at a frequency $f^* = 424\,\mathrm{Hz}$.

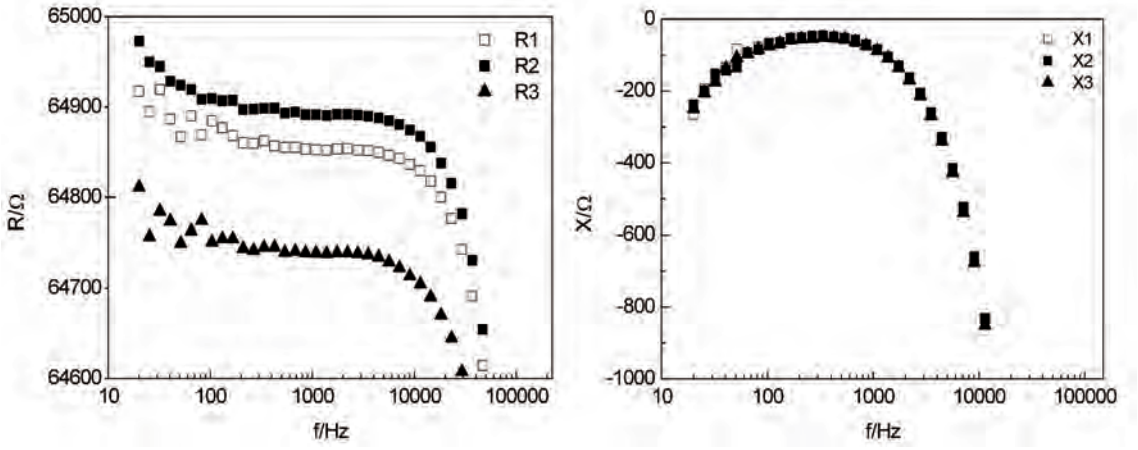

Figure 3.9: Example of raw impedance measurements carried out on the primary cell without the central section: a) Real component (resistance) and b) Imaginary component (reactance).

Following the primary method of measurement with flowing solutions, reported in 2.6.2, the electrolytic conductivity of the examined solution is determined by (2.30). In the measurement model all quantities were considered uncorrelated and in the treatment of the measurement uncertainty, the relevant international documents [52, 53] were followed. The uncertainty budget for the solution with a nominal conductivity of $5\,\mathrm{mS\,m^{-1}}$ is reported in Table 3.5 on page 65. Remarks are as follows.

1. The uncertainties $u(\overline{R}_\mathrm{W})$ and $u(\overline{R}_\mathrm{N})$ are obtained by considering the following contributions: (i) LCR meter calibration against a $100\,\mathrm{k\Omega}$ Tinsley standard AC resistor, (ii) LCR meter resolution, (iii) temperature correction and (iv) the type A uncertainty resulting from repeatability.

2. $u(\delta\kappa_\mathrm{W})$ and $u(\delta\kappa_\mathrm{N})$ are estimated from the conductivity drift of representative measurements taken respectively with and without the cell central section over a period of 10 h at f^*.

The repeatability of the set-up with flowing solution and inert gas was compared with measurements performed by the primary cell without the closed system and inert gas, reported in Tab. 3.1. The new set-up achieved a repeatability of about $20\,\Omega$ which compares favourably with the $52\,\Omega$ achieved by the static set-up.

3.3.3 $1\,\mathrm{mS\,m^{-1}}$ solution

With the $1\,\mathrm{mS\,m^{-1}}$ solution the resistance values at $f^* = 81.9\,\mathrm{Hz}$ were identified as corresponding to the minimum of the impedance imaginary component. The estimated α_T is $3\,\%\,^\circ\mathrm{C}^{-1}$ with an uncertainty of 10% [13].

Uncertainty contributions and calculation procedure for this solution were the same as in the $5\,\mathrm{mS\,m^{-1}}$ case.

The obtained conductivity value is $\kappa = 1.215 \times 10^{-3}\ \mathrm{S\,m^{-1}}$, the combined standard uncertainty is $u_\mathrm{c}(\kappa) = 1.1 \times 10^{-4}\ \mathrm{S\,m^{-1}}$ and the expanded uncertainty with $k = 2$ is $U(\kappa_2) = 2.2 \times 10^{-4}\ \mathrm{S\,m^{-1}}$.

3.3.4 Conclusions

Conductivity measurements performed with KCl aqueous solutions of 5, 3, 1 $\mathrm{mS\,m^{-1}}$ have produced good results. They confirmed that $5\,\mathrm{mS\,m^{-1}}$ is the threshold value for the use of the hydraulic circuit. At the same time, these measurements pointed out some weaknesses of the system.

Filling operation is a delicate phase that has to be accomplished as fast as possible. The hydraulic circuit is filled with the measurement solution and Ar gas is insuflated contemporaneously in the expansion chamber in order to avoid solution contamination. The expansion chamber has valves that are not appropriate for the gas conservation inside the vessel and it is necessary to monitor the gas pressure inside the circuit. High solution speeds are suitable to better homogenize the solution, but peristaltic pump imparts mechanical vibrations to the entire system.

Then, future work will be mainly devoted to (i) build a new central section with a more accurate cylindrical hole, with the aim of improving the corresponding uncertainty contribution; (ii) substitute the peristaltic pump with a magnetic one, with the aim of improving flow stability; (iii) reduce the number of silicone joints used to connect the glass pipes and the cells,with the aim of reducing solution contamination and (iv) improve argon monitoring to prevent gas leakage in the system.

The final goal is to obtain a system for conductivity measurements of ultra-pure water with a target uncertainty lower than 1%.

3.4 In-line calibration system - results

A working solution of $3\,\mathrm{mS\,m^{-1}}$ was used to compare the calibration by substitution with the one by comparison. In addition, a calibration by comparison was performed with a working solution of $0.3\,\mathrm{mS\,m^{-1}}$. In this case, calibration by substitution is infeasible because of the high contamination drift.

3.4.1 Substitution method

Table 3.6 on page 66 reports the uncertainty budget for K_2/K_1 in the case of calibration by substitution with a $3\,\mathrm{mS\,m^{-1}}$ solution. The uncertainty components related to (2.34) were evaluated on the basis of the following considerations:

1. R_1 and R_2 were measured by employing the sequence described in Sec. 2.6.3. Fig. 3.10 shows the behaviour of repeated measurements of K_2/K_1 estimated according to model (2.34). The origin of the time axis corresponds to the time when the cells are laid in the chamber after being filled. Since their initial temperature differs from that of the chamber, there is an initial transient to reach thermal equilibrium. This transient has a duration of about $3 \times 10^4\,\mathrm{s}$ and has to be skipped. Data analysis starts at time $t_0 \approx 3 \times 10^4\,\mathrm{s}$, as highlighted in Fig. 3.10. Starting from t_0, the behaviour of K_2/K_1 clearly shows a drift which is actually due to the different contamination of the two solutions. From t_0 to t_1, the drift is linear and can be easily modelled. The least-square estimate of K_2/K_1 at t_0 is $4.479\,906 \times 10^{-2}$ with a type A uncertainty $u(K_2/K_1) = 1.2 \times 10^{-7}$.

2. The Type-B uncertainties of R_1 and R_2 depend on the LCR bridge calibration. This was carried out against standard resistors in the range from $1\,\mathrm{k\Omega}$ to $1\,\mathrm{M\Omega}$. The following contributions were taken into account: uncertainty of the standards, AC errors and LCR bridge linearity [58].

3. According to [37], $\alpha_T \approx 2\,\%\,^{\circ}\mathrm{C}^{-1}$; for this quantity, it has been assumed a rectangular distribution with a relative half-width of $10\,\%$, considering the wide spread of the measurements described in this work.

4. As described in Sec. 2.6.3, the temperature is measured on the reference cell, only; thus, the temperature difference $\Delta T = T_2 - T_1$ in Eq. (2.34) can be written as $\Delta T = \Delta T_\mathrm{m} + \Delta T_\mathrm{b}$, where ΔT_m is the temperature difference measured by the thermometer between two successive sweeps and ΔT_b is the temperature bias which takes into account the chamber temperature inhomogeneity. ΔT_b was independently estimated to be $0.11\,^{\circ}\mathrm{C}$; for this quantity, it has been assumed a rectangular distribution with a half-width of $0.05\,^{\circ}\mathrm{C}$. ΔT_m, instead, has zero average value along the measurement cycles, with negligible uncertainty.

5. As pointed out in point 1, before t_0, thermal equilibrium is not yet established among the solution, the cells and the chamber. During this transient, solution conductivity changes in an unpredictable way because both of contamination drift and temperature variations. This behaviour is shown in Fig. 3.11 for several solution samples at $3\,\mathrm{mS\,m^{-1}}$. Between time 0 and t_0 the drift due to

contamination is masked by the effect of the wide temperature changes. After t_0, contamination becomes the main source of drift and conductivity shows a substantially linear drift. The two dash-dot lines visible in Fig. 3.11 bound the spread of the drifts of different solution samples between $d_{\min} = -3 \times 10^{-8}\,\mathrm{s}^{-1}$ and $d_{\max} = 3 \times 10^{-8}\,\mathrm{s}^{-1}$. Assuming that between time 0 and t_0 contamination drift is bounded by the same limits, a rectangular distribution with zero mean and half-width $(d_{\max} - d_{\min})t_0 = 1.8 \times 10^{-3}$ was assigned to the differential change $\Delta\eta$.

Thus, in the calibration by substitution with a solution of $3\,\mathrm{mS\,m^{-1}}$, K_2/K_1 was equal to $4.479\,906 \times 10^{-2}$ with an expanded uncertainty $U_{(\mathrm{k}=2)}(K_2/K_1) = 1.2 \times 10^{-4}$.

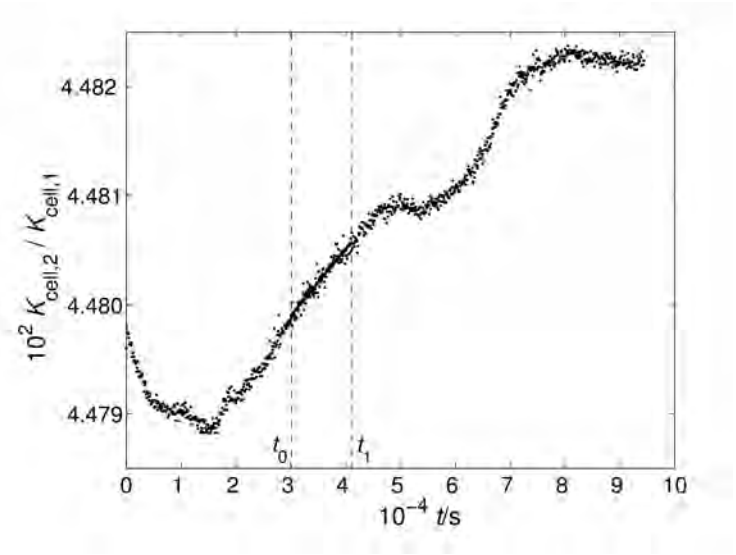

Figure 3.10: Example of measurement with the substitution method: K_2/K_1 versus time. The data employed in the estimation of K_2/K_1 are taken in the interval from t_0 to t_1. During the transient from time 0 to t_0, thermal equilibrium is not yet established; after t_1 drift cannot be modelled easily.

3.4.2 Comparison method

Table 3.7 on page 67 reports the uncertainty budget of K_2/K_1 in the case of calibration by comparison with the $3\,\mathrm{mS\,m^{-1}}$ working solution. The uncertainty components related to (2.33) were evaluated on the basis of the following considerations:

1. Fig. 3.12 shows the behaviour over time, after the initial transient, of K_2/K_1 with a $3\,\mathrm{mS\,m^{-1}}$ flowing solution. Analysis of the corresponding time-series

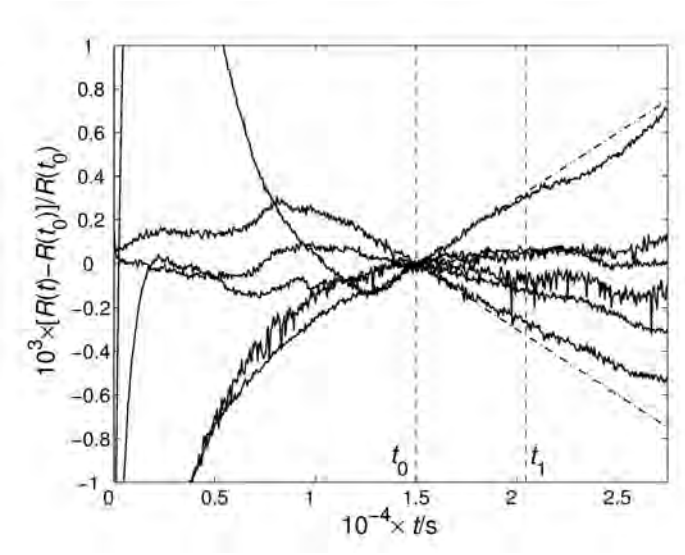

Figure 3.11: Relative change of cell resistance with respect to the value at t_0 for several solution samples at $3\,\mathrm{mS\,m^{-1}}$. Before t_0, the thermostatic chamber and the cells are not yet in thermal equilibrium and the resistance change is unpredictable. After t_0 resistance shows a substantially linear drift, bounded by the two dash-dot lines.

shows a negligible drift over more than 7 h of measurement time. This implies that the solution is homogeneous among the two cells; that the error term due to ΔT and $\Delta\eta$ can be neglected and that (2.33) is a suitable measurement model.

2. The Type-B uncertainties of R_1 and R_2 which come from LCR bridge calibration were evaluated as in point 2 of Sec. 3.4.1.

3. In the calibration by comparison, there can be an additional source of error associated to resistance measurement, not present when the two cells are separated. In fact, when the LCR meter is connected to one of the cells, the measured impedance is actually affected by the rest of the circuit. This causes a systematic error which is of difficult estimation because it depends in a somewhat complicated way on the circuit impedance and on its distributed capacitance toward the ground. When the LCR meter is measuring the impedance between the terminals of one of the cells, the terminals of the other cell should then be grounded. In this way, no current is injected through the circuit to the low side of the LCR meter and the above described error becomes negligible.

In the calibration by comparison case, considering a $3\,\mathrm{mS\,m^{-1}}$ solution, K_2/K_1 is equal to $4.480\,380 \times 10^{-2}$ with an expanded uncertainty $U_{(\mathrm{k=2})}(K_2/K_1) = 6.2 \times 10^{-6}$.

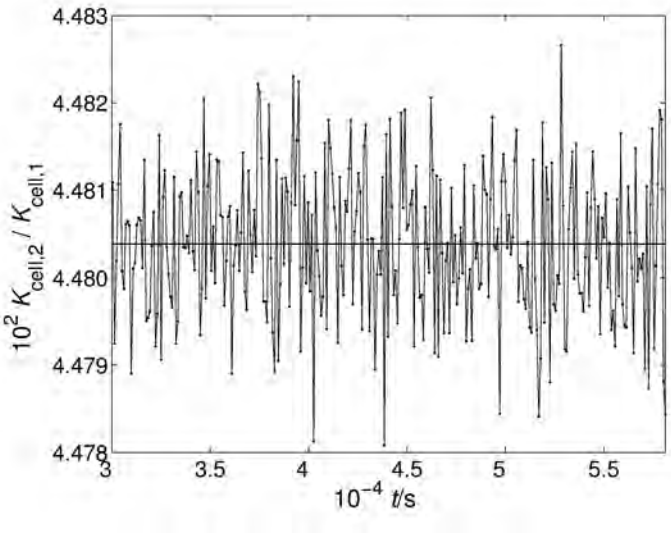

Figure 3.12: Ratio of resistances measured with the reference cell and with the flow-through cell at the same time for a $3\,\mathrm{mS\,m^{-1}}$ solution. The thick solid line marks the mean value of K_2/K_1.

Thus, comparing Sec. 3.4.1 and 3.4.2, calibration by comparison shows an uncertainty which is one order of magnitude better than that obtained with the substitution method.

Tab. 3.8 on page 68 reports the uncertainty budget of K_2/K_1 in the case of calibration by comparison with the $0.3\,\mathrm{mS\,m^{-1}}$ working solution. In this case, the uncertainty components are the same described in the above for the $3\,\mathrm{mS\,m^{-1}}$ solution. Fig. 3.13 shows the behaviour over time, after the initial transient, of K_2/K_1: also in this case the ratio is stable and the effects of temperature and contamination are negligible. The uncertainty obtained with the $0.3\,\mathrm{mS\,m^{-1}}$ is comparable to that achieved in the case of the $3\,\mathrm{mS\,m^{-1}}$.

3.4.3 Conclusion

In this section, a comparison calibration system for conductivity cells working at low conductivity values has been described. The system allows the rejection of drifts caused by solution contamination and the homogenization of the temperature in the reference cell and in the cell under calibration. A comparison between two calibration methods, substitution and comparison, was carried out with a $3\,\mathrm{mS\,m^{-1}}$ working solution. This showed that the uncertainty achieved with the comparison method is one order of magnitude better than that obtained by the substitution one. The result of a calibration by comparison with a $0.3\,\mathrm{mS\,m^{-1}}$ working solution

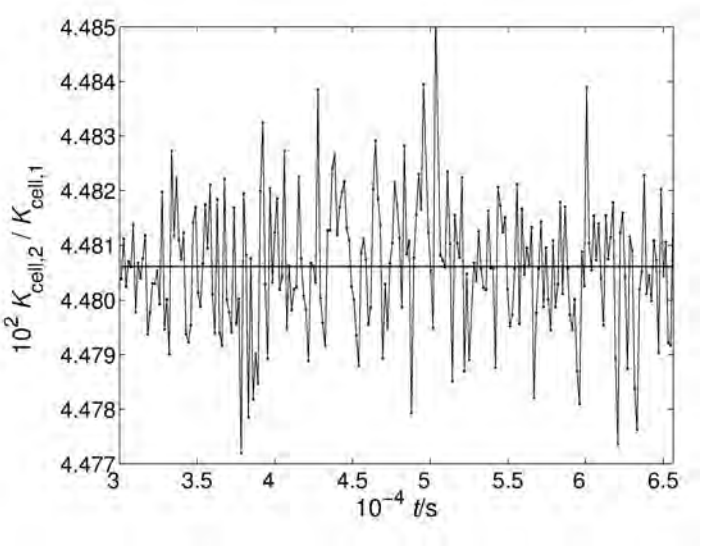

Figure 3.13: Ratio of resistances measured with the reference cell and the flow-through cell at the same time for a $0.3\,\mathrm{mS\,m^{-1}}$ solution. The thick solid line marks the mean value of K_2/K_1.

is also reported. All the calibration results are compatible within the uncertainties.

The use of this system could be extended, with little technical modifications, to the in-line calibration of a generic commercial conductivity probe. In addition, the calibration range could be extended to conductivities ranging down to those of ultra pure water values.

3.5 Impedance spectrometer measurements

In the following measurement results on pure-water samples are reported considering the instrumentation and the measurement system described in Chapter 2, Sec. 2.7. Moreover, a comparison with measurements performed with an LCR meter is reported.

3.5.1 Resistance standard

A first test of the spectrometer was conducted on a calibrated resistor having nominal value of $100\,\mathrm{k\Omega}$. Fig. 3.14 shows the deviation of the spectrometer readings with respect to the calibrated resistor value, when a nominal gain value of $R(f) = 100\,\mathrm{k\Omega}$ is employed in Eq. (2.37). The measurement outcome can be employed as an input of adjustment procedures of the spectrometer [59].

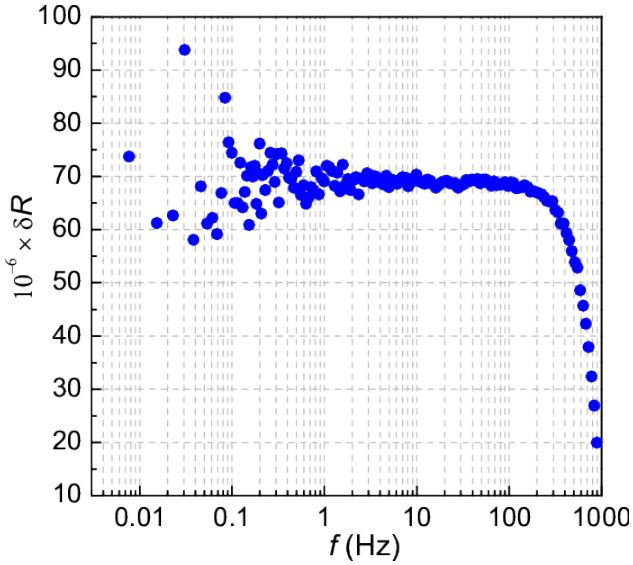

Figure 3.14: Deviation of the spectrometer resistance readings from the calibrated impedance value of a 100 kΩ resistor (ESI mod. SR1 - 100 kΩ, with adapters for two-port measurements).

3.5.2 Water contaminated with CO_2

The investigated sample is ultrapure water contaminated by exposure to atmospheric CO_2, whose dissociation increases conductivity (to a maximum of about 1 µS cm^{-1}). The measurements are performed at 25 °C in a thermostated environment. Results of impedance measurements with spectrometer $Z^{IS} = R^{IS} + jX^{IS}$ and with a commercial LCR meter $Z^{LCR} = R^{LCR} + jX^{LCR}$ are reported in Figs. 3.15 and 3.16. For this sample, $f^* \approx 10$ Hz cannot be reached by the particular LCR meter employed. The maximum relative difference $\delta = |Z^{IS} - Z^{LCR}|/|Z^{LCR}|$ in the superposition frequency range (20 Hz-1 kHz)) is 0.2%.

3.5.3 Pure water, in-Flow

First measurements on ultrapure water not contaminated by exposure to air have been conducted with the system shown in Fig. 2.13. A theoretical conductivity value of 0.055 µS cm^{-1} at 25 °C is expected [41, 60]. Results of the measurements are shown in Fig. 3.17. The estimated conductivity value is 0.053 µS cm^{-1} at 21 °C, compatible with the absence of contamination. For this sample, $f^* \approx 1$ Hz, which is well beyond the inferior frequency limit of the LCR meter.

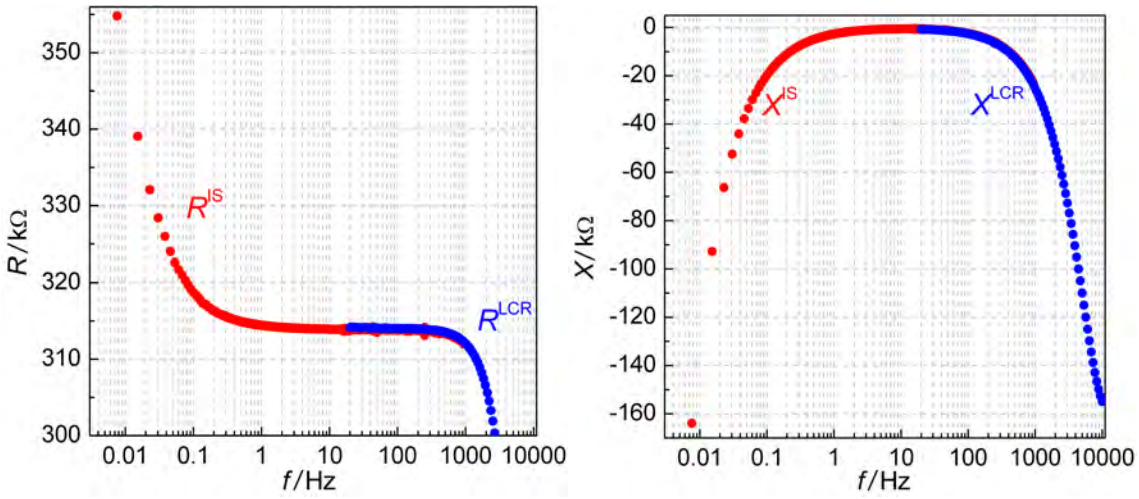

(a) (b)

Figure 3.15: Comparison of impedance measurement performed with the impedance spectrometer (IS) and the LCR meter (LCR). (a) Series resistance (R^{IS}, R^{LCR}) measurement versus frequency f. (b) Series reactance (X^{IS}, X^{LCR}).

3.5.4 Uncertainty

A detailed expression of measurement uncertainty will be a matter of future work; it will involve an analysis under *GUM Supplement 2* [61] and will be cumbersome because of the presence of DFT calculations in the measurement model. An estimate for $Z = 100\,\mathrm{k\Omega}$ resistive is reported in Table 3.9 on page 69.

The measurement accuracy can be substantially improved by the calibration of the spectrometer components, particularly the transresistance amplifier gain $R(f)$ and the ADC mismatch, and by adjusting the corresponding numerical constants in the software. An alternative route for accuracy improvement is to implement adjustment methods (improperly called *calibrations*) typical of LCR meters and network analyzers, such as short–open–load calibration [59].

3.5.5 Conclusion

The described spectrometer, based on multifrequency excitation and DFT analysis, allows to perform measurements of impedance spectra in a bandwidth extended down to the mHz range. The accuracy of the spectrometer has been confirmed by comparison with the resistance standard calibrated value and with LCR meter measurements for pure water equilibrated with air.

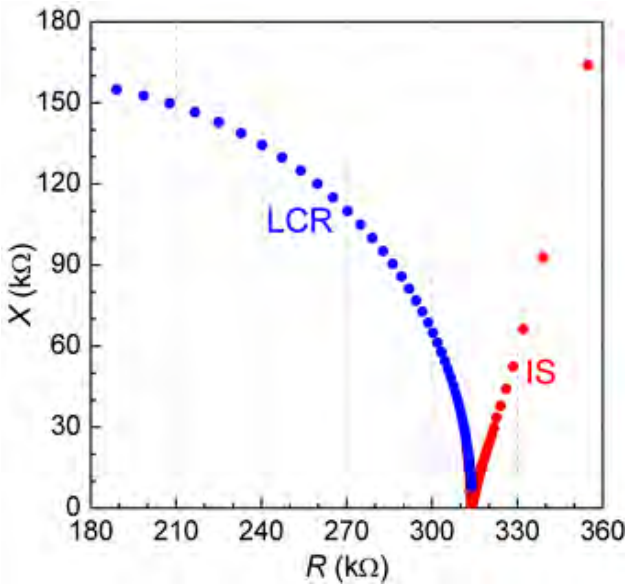

Figure 3.16: Same data in Fig. 3.15, here shown as an R-X Nyquist diagram. Only the measurements conducted with the impedance spectrometer (IS), at variance with those of the LCR meter, allow the observation of data at frequency ω^* (corresponding to $X(\omega^*) = 0$) and the effect of the electrode impedance Z_e, which gives the straight line on the right-hand side of the graph.

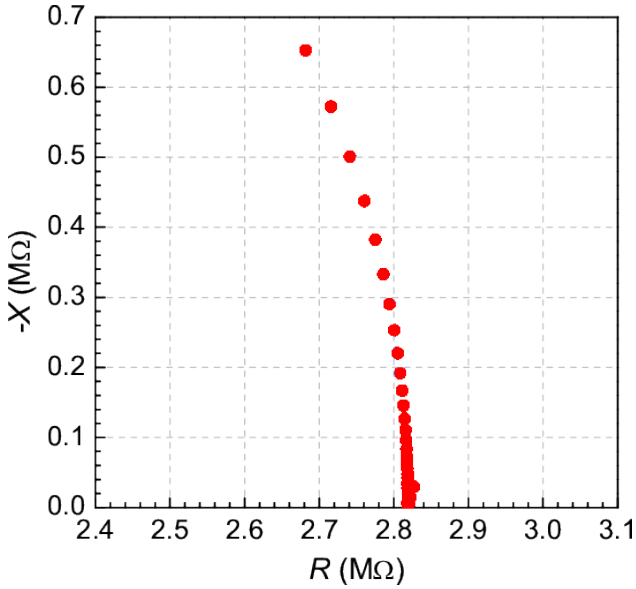

Figure 3.17: R-X Nyquist diagram of measurement performed on in-flow pure water with the impedance spectrometer

3.6 Preliminary measurement on UPW at DFM

During a brief sojourn at the Danmarks Nationale Metrologiinstitut (DFM), preliminary measurements were carried out to realize a flow system for ultra pure water. Several set-up were tested using different cells, flowing water at different rates and bubbling argon gas.

Measurements with different cells The electrolytic conductivity of ultra pure water, directly from Millipore® system, has been measured by means of three different conductivity measurement cells: a four-port temperature stabilized cell of glass, $K_{\text{cell}} = 10\,\text{m}^{-1}$, a two-port cell of glass, $K_{\text{cell}} = 10\,\text{m}^{-1}$, and a two-port cell of stainless steel, $K_{\text{cell}} = 1\,\text{m}^{-1}$.

The quality of employed water is critical for performed measurements: the Millipore® water purification system is composed of three parts. First pretreatment stage (RiOs-DI 3 UV) utilizes a unique filtering cartridge pack, including the pretreatment and the reverse osmosis membranes, and, by a mercury-vapour UV light source, it assures an efficient removal of $> 94\%$ of ionic contaminants and $> 99\%$ of other contaminants (organics, bacteria, particles). A 60 L central reservoir allows to maintain the purified water over some weeks, for the laboratory needs. A final purification stage (Milli-Q Academic), carries out a final filtration by using a specific cartridges which remove ionic and inorganic contaminants; the packs contain a microfilter for particulate removal, activated carbon for organics adsorption and mixed-bed ion-exchange resin for ion removal. The ultra-pure water which comes out by the outlet gun has a conductivity value $< 0.05\,\mu\text{S}\,\text{cm}^{-1}$ [62].

Measurement at different flow rate Measurements were carried out with Millipore® operating at different speed. At high flow-rates ($\approx 1\,\text{L}\,\text{min}^{-1}$), conductivity data close to the theoretical limit of $5.5\,\mu\text{S}\,\text{m}^{-1}$ at 25 °C was achieved for each of the three measurement cells. At lower flow rates ($4\,\text{mL}\,\text{min}^{-1}$ to $50\,\text{mL}\,\text{min}^{-1}$), conductivity data in the range $7\,\mu\text{S}\,\text{m}^{-1}$ to $20\,\mu\text{S}\,\text{m}^{-1}$ was achieved.

Measurement with argon gas In addition, tests using argon gas were carried out: bubbling Ar-gas in the 500 mL bottle, from where liquid was pumped into the cell, did not lower the measured conductivity value compared to the case with no Ar-gas. Argon gas had an observable effect on lowering the conductivity value measured when flowing into the measurement cell, but the gas bubbles also might have an effect on the cell itself.

Table 3.10 on page 70 provides an overview of conductivity measurement performed.

Table 3.1: Uncertainty budget for a solution with nominal conductivity $5\,\mathrm{mS\,m^{-1}}$ at 25 °C. Measurements were carried out by means of primary cell IRMMECEL001.

Uncertainty source	**Estimate**	**Standard uncertainty**	**Assumed distribution /Type A,B**	**Sensitivity coefficient**	**Contribution to standard uncertainty** ($\mathrm{S\,m^{-1}}$)
X_i	x_i	$u(x_\mathrm{i})$		c_i	$u_\mathrm{i}(y)$
K_cell	55.870 $\mathrm{m^{-1}}$	1.53×10^{-2} $\mathrm{m^{-1}}$	Norm./B	1.02×10^{-4} S	1.55×10^{-6}
$\overline{R}_\mathrm{W}$	73 248.4 Ω	13.1 Ω	Norm./A	-5.75×10^{-7} $\mathrm{S^2\,m^{-1}}$	7.52×10^{-6}
T_W	24.937 °C	2.77×10^{-2} °C	Rect./B	-8.44×10^{-4} $\mathrm{S\,m^{-1}\,°C^{-1}}$	2.33×10^{-5}
$\overline{R}_\mathrm{N}$	63 458.2 Ω	17.9 Ω	Norm./A	-5.75×10^{-7} $\mathrm{S^2m^{-1}}$	1.03×10^{-5}
T_N	24.881 °C	4.70×10^{-3} °C	Rect./B	-7.31×10^{-4} $\mathrm{S\,m^{-1}\,°C^{-1}}$	3.44×10^{-6}
$\delta\kappa_\mathrm{W}$	0 $\mathrm{S\,m^{-1}}$	3.95×10^{-6} $\mathrm{S\,m^{-1}}$	Rect./B	1	3.95×10^{-6}
$\delta\kappa_\mathrm{N}$	0 $\mathrm{S\,m^{-1}}$	2.71×10^{-6} $\mathrm{S\,m^{-1}}$	Rect./B	1	2.71×10^{-6}
α_T	0.02 $\mathrm{°C^{-1}}$	2.89×10^{-4} $\mathrm{°C^{-1}}$	Rect./B	1.69×10^{-3} $\mathrm{°C\,S\,m^{-1}}$	4.88×10^{-7}
Electrolytic conductivity $\kappa = 5.68 \times 10^{-3}$ $\mathrm{S\,m^{-1}}$					
Combined uncertainty $u_\mathrm{c}(\kappa) = 2.73 \times 10^{-5}$ $\mathrm{S\,m^{-1}}$					
Expanded uncertainty ($k = 2$) $U(\kappa) = 5.46 \times 10^{-5}$ $\mathrm{S\,m^{-1}}$					

Table 3.2: Uncertainty budget for a solution with nominal conductivity of $15\,\mathrm{mS\,m^{-1}}$ at $25\,^{\circ}\mathrm{C}$; measurements were performed with IRMMECEL002.

Uncertainty source	**Estimate**	**Standard uncertainty**	**Assumed distribution /Type A,B**	**Sensitivity coefficient**	**Contribution to standard uncertainty** ($\mathrm{S\,m^{-1}}$)
X_i	x_i	$u(x_\mathrm{i})$		c_i	$u_\mathrm{i}(y)$
K_2	$15.753\ \mathrm{m^{-1}}$	$6.00 \times 10^{-3}\ \mathrm{m^{-1}}$	Norm./B	$1.02 \times 10^{-3}\ \Omega^{-1}$	6.11×10^{-6}
R_2	$981.535\ \Omega$	$3.44 \times 10^{-1}\ \Omega$	Norm./A	$-1.63 \times 10^{-5}\ \Omega^{-2}\,\mathrm{m^{-1}}$	5.62×10^{-6}
R_sys	$0\ \Omega$	$2.50 \times 10^{-1}\ \Omega$	Rect./B	$-1.63 \times 10^{-5}\ \Omega^{-2}\,\mathrm{m^{-1}}$	4.09×10^{-6}
T_2	$24.995\ ^{\circ}\mathrm{C}$	$5.20 \times 10^{-3}\ ^{\circ}\mathrm{C}$	Norm./A	$-3.21 \times 10^{-4}\ \Omega^{-1}\,\mathrm{m^{-1}}\,^{\circ}\mathrm{C^{-1}}$	1.67×10^{-6}
T_sys	$0\ ^{\circ}\mathrm{C}$	$3.14 \times 10^{-3}\ ^{\circ}\mathrm{C}$	Rect./B	$-3.21 \times 10^{-4}\ \Omega^{-1}\,\mathrm{m^{-1}}\,^{\circ}\mathrm{C^{-1}}$	1.01×10^{-6}
α_T	$0.02\ ^{\circ}\mathrm{C^{-1}}$	$2.89 \times 10^{-4}\ ^{\circ}\mathrm{C^{-1}}$	Rect./B	$8.02 \times 10^{-5}\ ^{\circ}\mathrm{C}\,\Omega^{-1}\,\mathrm{m^{-1}}$	2.32×10^{-8}
Electrolytic conductivity $\kappa_2 = 1.6094 \times 10^{-2}\ \mathrm{S\,m^{-1}}$					
Combined uncertainty $u_\mathrm{c}(\kappa_2) = 9.5 \times 10^{-6}\ \mathrm{S\,m^{-1}}$					
Expanded uncertainty ($k = 2$) $U(\kappa_2) = 1.9 \times 10^{-5}\ \mathrm{S\,m^{-1}}$					

Table 3.3: Uncertainty budget of a solution with nominal conductivity $1\,\mathrm{mS\,m^{-1}}$ at 25 °C. Measurement performed with IRMMECEL004.

Uncertainty source	**Estimate**	**Standard uncertainty**	**Assumed distribution /Type A,B**	**Sensitivity coefficient**	**Contribution to standard uncertainty** ($\mathrm{S\,m^{-1}}$)
X_i	x_i	$u(x_\mathrm{i})$		c_i	$u_\mathrm{i}(y)$
K_2	0.938 $\mathrm{m^{-1}}$	8.00×10^{-3} $\mathrm{m^{-1}}$	Norm./B	1.33×10^{-3} Ω^{-1}	1.06×10^{-5}
R_2	757.552 Ω	1.34 Ω	Norm./A	-1.63×10^{-6} $\Omega^{-2}\,\mathrm{m^{-1}}$	2.19×10^{-6}
R_sys	0 Ω	2.50×10^{-1} Ω	Rect./B	-1.63×10^{-6} $\Omega^{-2}\,\mathrm{m^{-1}}$	4.09×10^{-7}
T_2	25.010 °C	3.77×10^{-3} °C	Norm./A	-3.72×10^{-5} $\Omega\,\mathrm{m^{-1}\,°C^{-1}}$	1.40×10^{-7}
T_sys	0 °C	3.14×10^{-3} °C	Rect./B	-3.72×10^{-5} $\Omega\,\mathrm{m^{-1}\,°C^{-1}}$	1.17×10^{-7}
α_T	0.03 $\mathrm{°C^{-1}}$	2.89×10^{-4} $\mathrm{°C^{-1}}$	Rect./B	-1.25×10^{-5} $\mathrm{°C\,\Omega^{-1}\,m^{-1}}$	3.62×10^{-9}
$\delta\kappa$	0 $\Omega^{-1}\,\mathrm{m^{-1}}$	9.43×10^{-9} $\Omega^{-1}\,\mathrm{m^{-1}}$	Rect./B	1	9.43×10^{-9}
Electrolytic conductivity $\kappa_2 = 1.24 \times 10^{-3}$ $\mathrm{S\,m^{-1}}$					
Combined uncertainty $u_\mathrm{c}(\kappa_2) = 1.1 \times 10^{-5}$ $\mathrm{S\,m^{-1}}$					
Expanded uncertainty ($k = 2$) $U(\kappa_2) = 2.2 \times 10^{-5}$ $\mathrm{S\,m^{-1}}$					

Table 3.4: Uncertainty budget of a solution with nominal conductivity $1\,\mathrm{mS\,m^{-1}}$ at $25\,^{\circ}\mathrm{C}$: measurements were carried out by IRMMECEL005.

Uncertainty source	**Estimate**	**Standard uncertainty**	**Assumed distribution /Type A,B**	**Sensitivity coefficient**	**Contribution to standard uncertainty** ($\mathrm{S\,m^{-1}}$)
X_i	x_i	$u(x_\mathrm{i})$		c_i	$u_\mathrm{i}(y)$
K_2	$212.526\ \mathrm{m^{-1}}$	$6.78 \times 10^{-1}\ \mathrm{m^{-1}}$	Norm./B	$5.84 \times 10^{-6}\ \Omega^{-1}$	3.96×10^{-6}
R_2	$171\,161.209\ \Omega$	$6.83 \times 10^{2}\ \Omega$	Norm./A	$-7.27 \times 10^{-9}\ \Omega^{-2}\,\mathrm{m^{-1}}$	4.96×10^{-6}
R_sys	$0\ \Omega$	$5.60\ \Omega$	Rect./B	$-7.27 \times 10^{-9}\ \Omega^{-2}\,\mathrm{m^{-1}}$	4.07×10^{-8}
T_2	$25.052\ ^{\circ}\mathrm{C}$	$4.66 \times 10^{-2}\ ^{\circ}\mathrm{C}$	Norm./A	$-3.74 \times 10^{-5}\ \Omega^{-1}\,\mathrm{m^{-1}}\,^{\circ}\mathrm{C^{-1}}$	1.16×10^{-6}
T_sys	$0\ ^{\circ}\mathrm{C}$	$3.14 \times 10^{-3}\ \Omega$	Rect./B	$-3.74 \times 10^{-5}\ \Omega^{-1}\,\mathrm{m^{-1}}\,^{\circ}\mathrm{C^{-1}}$	1.17×10^{-7}
α_T	$0.03\ ^{\circ}\mathrm{C^{-1}}$	$2.89 \times 10^{-4}\ ^{\circ}\mathrm{C^{-1}}$	Rect./B	$-6.40 \times 10^{-5}\ ^{\circ}\mathrm{C}\,\Omega^{-1}\,\mathrm{m^{-1}}$	1.85×10^{-8}
$\delta\kappa$	$0\ \Omega^{-1}\,\mathrm{m^{-1}}$	$3.99 \times 10^{-8}\ \Omega^{-1}\,\mathrm{m^{-1}}$	Rect./B	1	3.99×10^{-8}
Electrolytic conductivity $\kappa_2 = 1.242 \times 10^{-3}\ \mathrm{S\,m^{-1}}$					
Combined uncertainty $u_\mathrm{c}(\kappa_2) = 6.6 \times 10^{-6}\ \mathrm{S\,m^{-1}}$					
Expanded uncertainty ($k = 2$) $U(\kappa_2) = 1.3 \times 10^{-5}\ \mathrm{S\,m^{-1}}$					

Table 3.5: Uncertainty budget of a solution with nominal conductivity $5\,\mathrm{mS\,m^{-1}}$ at 25 °C: hydraulic circuit was used to perform measurements.

Uncertainty source	**Estimate**	**Standard uncertainty**	**Assumed distribution /Type A,B**	**Sensitivity coefficient**	**Contribution to standard uncertainty** ($\mathrm{S\,m^{-1}}$
X_i	x_i	$u(x_\mathrm{i})$		c_i	$u_\mathrm{i}(y)$
K_cell	55.870 $\mathrm{m^{-1}}$	1.53×10^{-2} $\mathrm{m^{-1}}$	Norm./B	9.58×10^{-5} S	1.46×10^{-6}
$\overline{R}_\mathrm{W}$	75 144.40 Ω	13.96 Ω	Norm./A	-5.13×10^{-7} $\mathrm{S^2\,m^{-1}}$	7.16×10^{-6}
$\overline{R}_\mathrm{N}$	64 705.60 Ω	11.09 Ω	Norm./A	5.13×10^{-7} $\mathrm{S^2 m^{-1}}$	5.69×10^{-6}
$\delta\kappa_\mathrm{W}$	0 $\mathrm{S\,m^{-1}}$	5.20×10^{-7} $\mathrm{S\,m^{-1}}$	Rect./B	1	5.20×10^{-7}
$\delta\kappa_\mathrm{N}$	0 $\mathrm{S\,m^{-1}}$	4.04×10^{-7} $\mathrm{S\,m^{-1}}$	Rect./B	1	4.04×10^{-7}
Electrolytic conductivity $\kappa = 5.350 \times 10^{-3}$ $\mathrm{S\,m^{-1}}$					
Combined uncertainty $u_\mathrm{c}(\kappa) = 9.3 \times 10^{-6}$ $\mathrm{S\,m^{-1}}$					
Expanded uncertainty ($k = 2$) $U(\kappa) = 1.9 \times 10^{-5}$ $\mathrm{S\,m^{-1}}$					

Table 3.6: Uncertainty budget for the calibration by substitution of K_2/K_1 with a $3\,\mathrm{mS\,m^{-1}}$ working solution.

Uncertainty source	**Estimate**	**Standard uncertainty**	**Assumed distribution /Type A,B**	**Sensitivity coefficient**	**Contribution to standard uncertainty** ($\mathrm{S\,m^{-1}}$
X_i	x_i	$u(x_\mathrm{i})$		c_i	$u_\mathrm{i}(y)$
K_2/K_1	$4.479\,906 \times 10^{-2}$	1.2×10^{-7}	Norm./A	1.0	1.2×10^{-7}
R_1	$1.12 \times 10^{5}\ \Omega$	$5.6\ \Omega$	Rect./B	$-4.0 \times 10^{-7}\ \Omega^{-1}$	2.2×10^{-6}
R_2	$5.01 \times 10^{3}\ \Omega$	$0.25\ \Omega$	Rect./B	$8.9 \times 10^{-6}\ \Omega^{-1}$	2.2×10^{-6}
α_T	$2.00 \times 10^{-2}\ \Omega$	$1.2 \times 10^{-3}\ ^\circ\mathrm{C}^{-1}$	Rect./B	$4.9 \times 10^{-3}\ ^\circ\mathrm{C}$	5.9×10^{-6}
ΔT	$0.110\ ^\circ\mathrm{C}$	$3.0 \times 10^{-2}\ ^\circ\mathrm{C}$	Rect./B	$-1.3 \times 10^{-3}\ ^\circ\mathrm{C}^{-1}$	3.9×10^{-5}
$\Delta\eta T$	$0\ \mathrm{S\,m^{-1}}$	$1.0 \times 10^{-3}\ \mathrm{S\,m^{-1}}$	Rect./B	$-4.5 \times 10^{-2}\ \mathrm{m\,S^{-1}}$	4.5×10^{-5}
Combined uncertainty $u_\mathrm{c}(K_2/K_1) = 6.0 \times 10^{-5}$					
Expanded uncertainty ($k = 2$) $U(K_2/K_1) = 1.2 \times 10^{-4}$					

Table 3.7: Uncertainty budget for the calibration by comparison with a $3\,\mathrm{mS\,m^{-1}}$ working solution.

Uncertainty source	**Estimate**	**Standard uncertainty**	**Assumed distribution /Type A,B**	**Sensitivity coefficient**	**Contribution to standard uncertainty** ($\mathrm{S\,m^{-1}}$
X_i	x_i	$u(x_\mathrm{i})$		c_i	$u_\mathrm{i}(y)$
K_2/K_1	$4.480\,380 \times 10^{-2}$	4.9×10^{-7}	Norm./A	1.0	4.9×10^{-7}
R_1	$1.09 \times 10^{5}\ \Omega$	$5.5\ \Omega$	Rect./B	$-4.1 \times 10^{-7}\ \Omega^{-1}$	2.2×10^{-6}
R_2	$4.89 \times 10^{3}\ \Omega$	$0.24\ \Omega$	Rect./B	$9.2 \times 10^{-6}\ \Omega^{-1}$	2.2×10^{-6}
Combined uncertainty $u_\mathrm{c}(K_2/K_1) = 3.1 \times 10^{-6}$					
Expanded uncertainty ($k = 2$) $U(K_2/K_1) = 6.2 \times 10^{-6}$					

Table 3.8: Uncertainty budget for the calibration by comparison with a $0.3\,\mathrm{mS\,m^{-1}}$ working solution.

Uncertainty source	**Estimate**	**Standard uncertainty**	**Assumed distribution /Type A,B**	**Sensitivity coefficient**	**Contribution to standard uncertainty** ($\mathrm{S\,m^{-1}}$
X_i	x_i	$u(x_\mathrm{i})$		c_i	$u_\mathrm{i}(y)$
K_2/K_1	$4.480\,605 \times 10^{-2}$	8.1×10^{-7}	Norm./A	1.0	8.1×10^{-7}
R_1	$1.10 \times 10^{6}\ \Omega$	$55\ \Omega$	Rect./B	$-4.1 \times 10^{-8}\ \Omega^{-1}$	2.2×10^{-6}
R_2	$4.93 \times 10^{4}\ \Omega$	$2.5\ \Omega$	Rect./B	$9.1 \times 10^{-7}\ \Omega^{-1}$	2.2×10^{-6}
Combined uncertainty $u_\mathrm{c}(K_2/K_1) = 3.2 \times 10^{-6}$					
Expanded uncertainty ($k = 2$) $U(K_2/K_1) = 6.4 \times 10^{-6}$					

Table 3.9: Preliminary uncertainty budget for the measurement of resistive $Z = 100\,\mathrm{k}\Omega$ impedance. $s_{\mathrm{RMS}} = 0.5\,\mathrm{V}$, sampling parameters as in Sec. 2.7.2, log comb, one single acquisition.

Uncertainty source	$f = 10\,\mathrm{mHz}$ $u_{\mathbf{R}} \times 10^6$	$f = 100\,\mathrm{Hz}$ $u_{\mathbf{R}} \times 10^6$
TRA gain error *a*	60	70
TRA & ADC intermod. distortion *b*	30	30
ADC channel mismatch *c*	100	100
ADC channel separation *d*	1	1
Noise	50	5
Combined uncertainty	130	126

a Deviation from nominal due to feedback resistor tolerance and open-loop finite gain.
b Evaluated from specifications for large signals.
c From direct measurement.
d From specifications.

Table 3.10: Summary of measurement configurations performed at Danmarks Nationale Metrologiinstitut

Date	**Description**	T (°C)	K_{cell} (m^{-1})	q ($\mathrm{mL\,min}^{-1}$)	**Cell type**	κ ($\mu\mathrm{S\,m}^{-1}$)
10/5/12	UPW left exposed to air for several hours	25	10	4	4 port glass, temp. Stab.	76
	Fresh UPW flowing from Millipore to a bottle and subsequently to the cell	25	10	4	4 port glass, temp. Stab.	55
15/5/12	UPW left exposed to air for days	24	10	4	4 port glass, temp. Stab.	102
	UPW left exposed to air for days	25	10	4	4 port glass, temp. Stab.	104
	UPW left exposed to air for days	26	10	4	4 port glass, temp. Stab.	106
	Fresh UPW in a loop	25	10	4	4 port glass, temp. Stab.	36
	Fresh UPW in a loop. Water overflowed bottle for several minutes	25	10	4	4 port glass, temp. Stab.	21
16/5/12	UPW direct from Millipore	23.5	10	2000	2 port glass cell	4.7
18/5/12	UPW direct from Millipore	25	10	2000	4 port glass, temp. Stab.	5.9
	UPW direct from Millipore	23.5	1	2000	2 port glass cell	4.7
	UPW from Millipore to bottle to MasterFlex pump to cell. Water overflowed bottle for several minutes	25	10	50	4 port glass, temp. Stab.	10
21/5/12	Ar-gas flowing to cell. UPW from Millipore to bottle to MasterFlex pump to cell. Water overflowed bottle for several minutes	25	10	50	4 port glass, temp. Stab.	10
	Ar-gas flowing to bottle. UPW from Millipore to bottle to MasterFlex pump to cell. Water overflowed bottle for several minutes	23.2	10	50	2 port glass cell	13
22/5/12	Ar-gas flowing to bottle. UPW from Millipore to bottle to MasterFlex pump to cell. Water overflowed bottle for several minutes	23.2	10	50	2 port glass cell	13
	Ar-gas flowing to bottle. UPW from Millipore to bottle to MasterFlex pump to cell. Water overflowed bottle for several minutes	23.2	10	4	2 port glass cell	18
	UPW direct from Millipore through 1.5 m PVDF tube	23.2	10	2000	2 port glass cell	5.1
	UPW direct from Millipore through MasterFlex tubings and 1.5 m PVDF tube	23.2	10	1000	2 port glass cell	5.3
	Ar-gas flowing to bottle. UPW from Millipore to bottle to MasterFlex pump to cell. Water overflowed bottle for several minutes. Measurement cell immersed in water	23.2	10	50	2 port glass cell	7.6
	UPW from Millipore to bottle to Airpax magnetic pump to cell. Water overflowed bottle for several minutes	23.2	10	1000	2 port glass cell	5.4
	UPW from Millipore to bottle to Airpax magnetic pump to cell. Water overflowed bottle for several minutes	23.2	10	200	2 port glass cell	7.3
	UPW from Millipore to bottle to Airpax magnetic pump to cell. Water overflowed bottle for several minutes. Ar -gas bubbling	23.2	10	1000	2 port glass cell	5.8

Chapter 4

International Comparisons

NMIs test their best measurement capabilities in international comparisons. On the basis of the Mutual Recognition Arrangement (MRA) [63], these comparisons are used to establish the worldwide compatibility of the measurements. The key-comparisons can be proposed by CCs or by EURAMET.

On the basis of the results obtained in the comparisons, NMIs can declare to EURAMET their calibration and measurement capabilities.

During my Ph.D. activity, I had the opportunity to take part in two CCQM key comparisons (CCQM-K105 and CCQM-K92), in one CCQM pilot comparison on seawater samples (CCQM-P142) and in one EURAMET study 1202 on bioethaol measurements. I dealt with the experiments, the data evaluations and measurement technical reports.

Furthermore, since INRIM was the coordinating laboratory for CCQM-K105, I was involved in the estimation of the key comparison reference value (KCRV) of the results reported by NMIs.

The technical reports of these measurement comparisons are reported in Appendix.

4.1 Key comparison CCQM-K105 "Electrolytic conductivity at $5.3\,\mathrm{S\,m^{-1}}$"

CCQM-K105 comparison was carried out in 2012 in the framework of the EMRP project ENV05 "Ocean metrology". It was coordinated by INRIM and supported by the Physikalisch-Technische Bundesanstalt (PTB). The comparison aimed to demonstrate the calibration and measurement capabilities of the participating institutes with respect to the conductivity of multi-component aqueous salt solutions.

The solution used in the comparison was a natural seawater taken from the North Atlantic ocean and diluted with water to a Pratical Salinity value of 35

which corresponded to a nominal conductivity value around $5.3\,\mathrm{S\,m^{-1}}$ at 25 °C and $4.3\,\mathrm{S\,m^{-1}}$ at 15 °C.

The seawater sample was provided by OSIL which guarateed for batch homogeneity. However, homogeneity and stability tests were also performed by the support laboratory. Batch homogeneity was taken into account in the evaluation of the uncertainty of the KCRV.

Measurements had to be carried out preferably by means of a primary measurement system. It was asked to participants to perform measurement both at 25 °C and 15 °C and to correct the results to exactly 25.000 °C and 15.000 °C.

4.1.1 KCRV and uncertainty evaluation

Originally, 15 NMIs were involved in measurement campaign, but two of them withdrew form the comparison. Then, after receiving the measurement results by each participant, the KCRV, the associated uncertainty and the degree of equivalence of the results were calculated by applying the guidelines proposed by Cox in [64].

Firstly Procedure A was applied and the weighted mean was calculated considering the measurements from each institute. This procedure assumes that the seawater sample is stable, measurements from each institute are mutually independent and Gaussian distributions are assigned to the results.

To carry out an overall consistency check to the results, the chi-square test was applied but it failed.

Consequently, Procedure B reported in [64], which is based on the Monte Carlo method, was employed. A random sample of 10^6 trials for each temperature was used. Each random sample was the sum of two other random samples: the one first was associated with the uncertainties of the institutes' results and the second one was associated with the inhomogeneity of the seawater sample. These two random samples were generated according to the following: i) the measurements were considered independent; ii) a Gaussian probability distribution was associated with the measurements of the institutes which declared a coverage factor of 2; iii) a t-student distribution with appropriate degrees of freedom was associated with the measurements of the NMI which declared a coverage factor of 2.87 at 25 °C ($\nu = 4$) and 2.65 at 15 °C ($\nu = 5$); iv) a Gaussian probability distribution with a standard deviation of $6.60 \times 10^{-5}\,\mathrm{S\,m^{-1}}$ was associated with the inhomogeneity of the sample.

For the evaluation of the median and the associated uncertainty, the algorithm at points 3-10 of procedure B was applied. $d_{\mathrm{i\ low}}$ and $d_{\mathrm{i\ up}}$ are the lower and the upper endpoints of the 95.45% interval of confidence of d_{i}.

Table 4.1 and Fig. 4.1 show the results for the degree of equivalence of each institute for the seawater sample at 25 °C using median as an estimator.

In the case of the seawater sample at 15 °C the same procedure A was applied. However, also in this case, the chi-squared test failed. Consequently, procedure B

Table 4.1: Results for the degree of equivalence of NMIs for the seawater sample at 25 °C. Estimator: median.

Institute	d_i $\mathrm{S\,m^{-1}}$	$d_{i\ \mathrm{low}}$	$d_{i\ \mathrm{up}}$
1	−0.024	−0.030	−0.019
2	−0.011	−0.049	0.026
3	−0.0065	−0.015	0.0012
4	−0.0064	−0.024	0.011
5	−0.0035	−0.012	0.0050
6	−0.0034	−0.0088	0.0012
7	−0.0014	−0.0039	0.000 72
8	0.0003	−0.0033	0.0040
9	0.0012	−0.0020	0.0050
10	0.0016	−0.000 85	0.0044
11	0.0016	−0.0013	0.0051
12	0.0045	0.000 55	0.0084
13	0.0089	0.0055	0.012

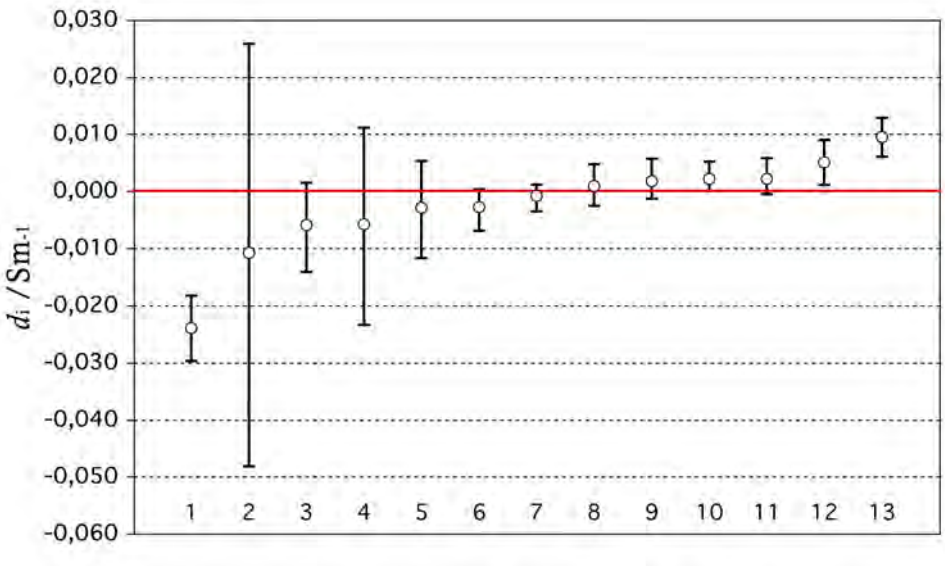

Figure 4.1: Seawater sample at 25 °C. Plot of the degrees of equivalence and 95.45% interval of confidence according to Cox Procedure B. Estimator: median.

was considered. A random sample of 10^6 trials was used.

Table 4.2 and Fig. 4.2 show the results for the degree of equivalence of NMIs for seawater sample at 15 °C using median as the estimator.

An alternative procedure for the evaluation of the KCRV by searching a consistent subset was proposed by Nielsen [65]: the weighted mean of data at 25 °C

Table 4.2: Results for the degree of equivalence of NMIs for the seawater sample at 15 °C. Estimator: median.

Institute	$d_{\mathbf{i}}$ $\mathrm{S\,m^{-1}}$	$d_{\mathbf{iLOW}}$	$d_{\mathbf{iUP}}$
1	−0.013	−0.018	−0.0072
2	−0.012	−0.020	−0.0041
3	−0.0062	−0.022	0.0086
4	−0.0043	−0.0082	−0.000 036
5	−0.0038	−0.013	0.0048
6	−0.0036	−0.030	0.022
7	−0.000 82	−0.0031	0.0010
8	−0.000 12	−0.0022	0.0019
9	0.000 78	−0.0010	0.0029
10	0.0021	−0.000 85	0.0055
11	0.0022	−0.000 55	0.0052
12	0.0026	−0.000 60	0.0062
13	0.0027	0.000 013	0.0052

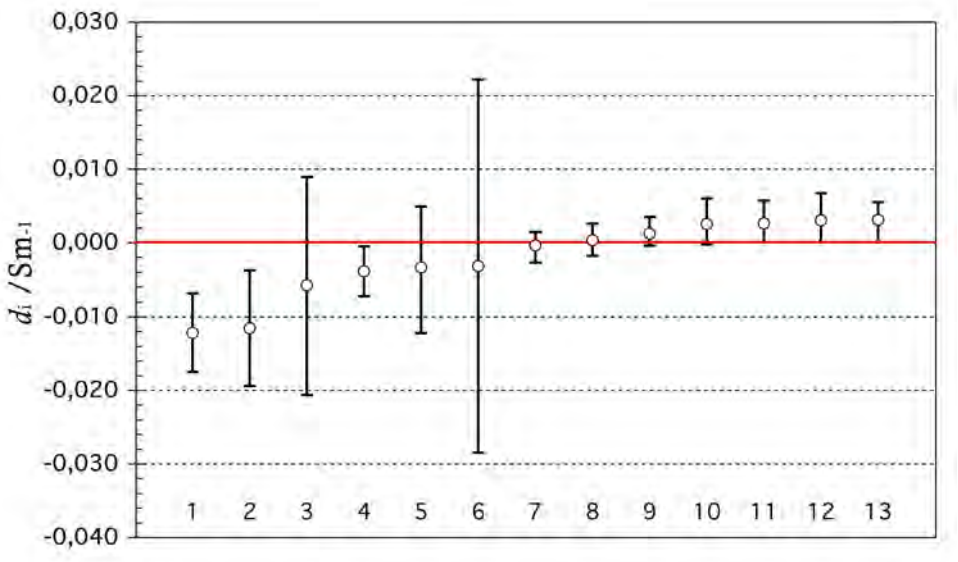

Figure 4.2: Seawater sample at 15 °C. Plot of the degrees of equivalence and 95.45% interval of confidence according to Cox procedure B. Estimator: median.

and 15 °C was calculated. In this process procedure A [64] was iteratively applied by excluding for each iteration the more discrepant datum, and by recomputing the weighted mean and performing a chi-square test on the remaining result subset until a consistent subset was obtained.

The results from NMI 1, 12 and 13 were removed from the dataset and Table 4.3

and Fig. 4.3 show the results for the degree of equivalence of institutes for seawater sample at 25 °C using weighted mean as an estimator.

Table 4.3: Results for the degree of equivalence of NMIs for the seawater sample at 15 °C. Estimator: weighted mean.

Institute	d_i / S m^{-1}	$U(d_i)$
1	−0.024	0.0055
2	−0.011	0.0382
3	−0.0061	0.0081
4	−0.0060	0.0180
5	−0.0031	0.0089
6	−0.0030	0.0035
7	−0.0010	0.0012
8	0.000 65	0.0035
9	0.0015	0.0032
10	0.0019	0.0019
11	0.0019	0.0028
12	0.0048	0.0035
13	0.0092	0.0029

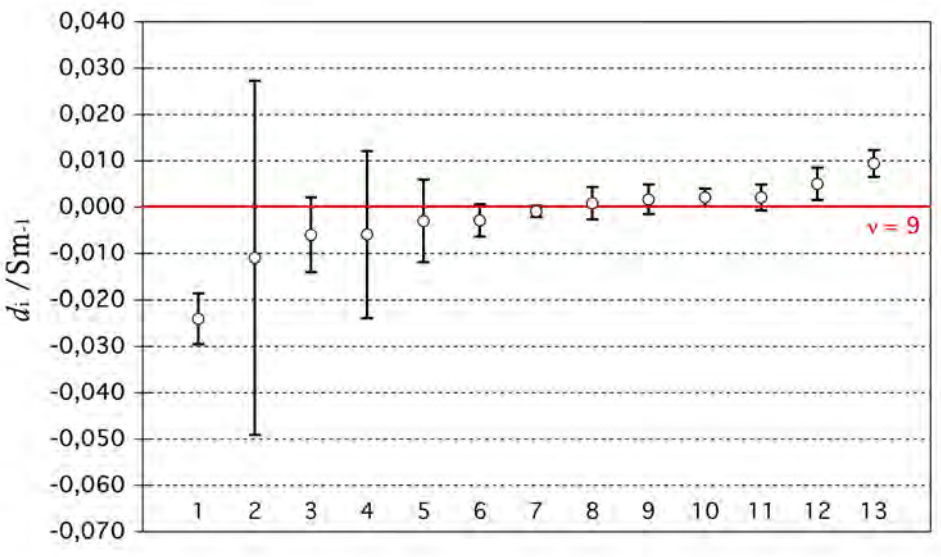

Figure 4.3: Seawater sample at 25 °C. Plot of the degrees of equivalence and 95% interval for the consistent subset obtained according to Nielsen. Estimator: weighted mean.

The same procedure for seawater sample at 15 °C was applied. The results purged from the dataset were those of NMI 1, 2 and 4. Table 4.4 and Fig. 4.4 show the

results for the degree of equivalence of institutes for seawater sample at 15 °C using weighted mean as an estimator.

Table 4.4: Results for the degree of equivalence of NMIs for the seawater sample at 15 °C. Estimator: weighted mean.

Institute	d_i / S m^{-1}	$U(d_i)$
1	−0.013	0.0053
2	−0.013	0.0078
3	−0.0070	0.0154
4	−0.0051	0.0031
5	−0.0046	0.0090
6	−0.0044	0.0262
7	−0.0016	0.0016
8	0.000 87	0.0016
9	2.5×10^{-5}	0.0014
10	0.0013	0.0031
11	0.0014	0.0027
12	0.0018	0.0033
13	0.0019	0.0021

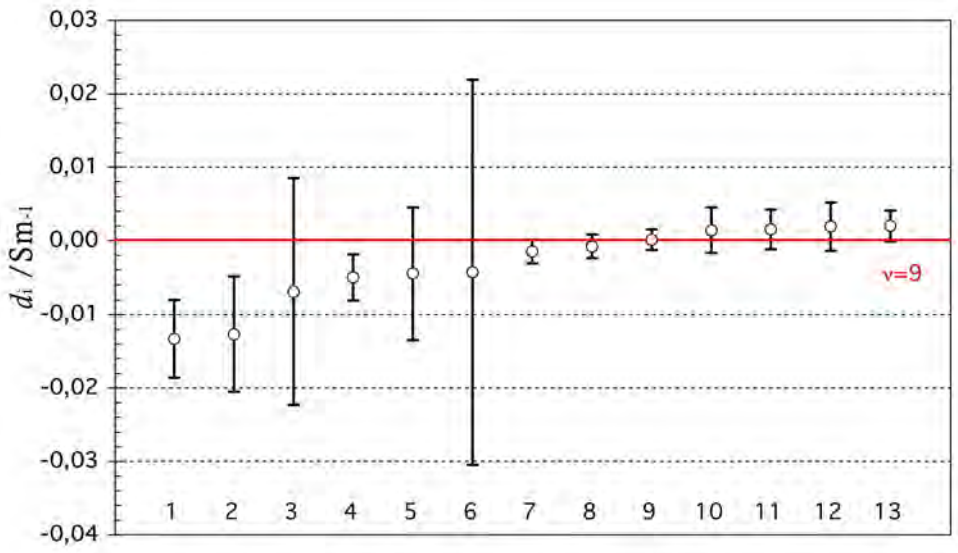

Figure 4.4: Seawater sample at 15 °C. Plot of the degrees of equivalence and 95% interval for the consistent subset obtained according to Nielsen. Estimator: weighted mean.

When Procedure A failed, there was no general consensus between NMIs about the choice of the proper algorithm for the determination of a reference value, its

uncertainty and the interval of confidence of the degrees of equivalence. On the basis of the large number of results that need to be purged from largest-consistent subset procedure, and some theoretical criticism of the method itself [66], Cox Procedure B [64] was considered preferable for stating the final comparison result. NMI 1 requested to be excluded from the KCRV determination because of problems by using its measurement cell during the comparison.

Therefore, after approval from all participating NMIs, final results and KCRV determination will be available in Draft B of the key comparison report.

4.2 Key comparison CCQM-K92 "Electrolytic conductivity at $0.05\,\mathrm{S\,m^{-1}}$"

CCQM-K92 was carried out in 2011, proposed by CCQM-EAWG. The electrolytic conductivity values of $20\,\mathrm{S\,m^{-1}}$ and $0.05\,\mathrm{S\,m^{-1}}$ where chosen in this comparison. It was coordinated by the Slovak Institute of Metrology (SMU). INRIM participated only in $0.05\,\mathrm{S\,m^{-1}}$ measurement. The report describing the measurement procedure and the obtained result is reported in Appendix.

4.3 Pilot comparison CCQM-P142

CCQM-P142 "Equivalence conductance ratio measurement results of seawater" was carried out under the EMRP project ENV05 "Ocean metrology".

Salinity is the total portion of dissolved salts in a seawater sample and, according to the Pratical Salinity Scale (PSS-78), it is determined in terms of the ratio K_{15} (at temperature of 15 °C) of electrolytic conductivity of seawater to that of a defined potassium chloride solution [67]:

$$K_{15} = \frac{\kappa(S,15,0)}{\kappa(\mathrm{KCl},15,0)}\,, \tag{4.1}$$

where $\kappa(S,15,0)$ is the conductivity of seawater sample and $\kappa(\mathrm{KCl},15,0)$ is the conductivity of the standard KCl solution, both at 15 °C and at atmospheric pressure (which is expressed by 0).

At present, Pratical Salinity results are not traceable to metrological references consistent with the SI but, since it is an important input quantity to oceanographic models, there is a strong interest to establish the traceability to SI units of practical salinity values [67],[68],[69].

The Pilot Study CCQM-P142 aimed at investigating the equivalence of conductance ratio measurements in order to quantify the reproducibility of independent

measurement results. Each participating NMI had to measure and report the conductance values of three different seawater samples ($4.3\,\mathrm{S\,m^{-1}}$, $2.5\,\mathrm{S\,m^{-1}}$, $1\,\mathrm{S\,m^{-1}}$ at 15 °C) and of one KCl aqueous solution with an approximate conductivity of $4.3\,\mathrm{S\,m^{-1}}$ at 15 °C.

From NMIs data, the coordinating laboratory (PTB) calculated the conductance ratios of the seawater samples.

4.4 EURAMET Study 1202

The 2011 EURAMET Study 1202 "Electrolytic conductivity of bioethanol" was a preliminary and informal measurement comparison on synthetic ethanol and bioethanol samples. The objective o f this comparison was the analysis of the difficulties related to the measurement of conductivity of a volatile substances like ethanol and bioethanol. The study was related to the EMRP project ENG09 "Metrology for biofuels" and was proposed by EURAMET Sub-Committee Electrochemical Analysis of TC-MC. This comparison was pushed by the automotive and aviation industry.

Results of primary and secondary electrolytic conductivity values of bioethanol were compared and stability problems were observed.

Chapter 5

Conclusions

The research activity in electrolytic conductivity described in this thesis is part of an INRIM program on electrical measurements which started in 2003. Moreover, it is considered as an important starting point for the development of new metrological references in the field of electrochemical analysis.

This research activity was focused on improving the existing system for intermediate conductivity values and on developing new systems and devices for very low and high values. In fact, low conductivity values are of fundamental importance in many industrial applications (pharmaceutical, microelectronics, environmental), while high conductivity values are significant for the oceanographic community.

The developed primary system allows conductivity measurements in the range from $0.005\,\mathrm{S\,m^{-1}}$ to $2\,\mathrm{S\,m^{-1}}$ with an associated relative uncertainty better than 0.7%.

This system employs a primary cell with a removable central section, having a simple, cylindrical geometry which is characterisable with high accuracy. To test the measurement capability, the methodology and the measurement system, I participated in the international key comparison CCQM-K92 on "Electrolytic Conductivity at $0.05\,\mathrm{S\,m^{-1}}$".

For low and high conductivity values I designed secondary cells with fixed geometry, adapting electrodes size and shape to obtain optimal resistance values. In particular, for pure water values, I designed and characterised a secondary flow-through cell with coaxial electrodes; for biofuels characterization, I designed a secondary cell with large electrodes at a very small distance which was inspired by the participation in the EURAMET Study 1202 "Electrolytic conductivity of bioethanol". Finally, for high conductivity solutions, a specific cell was designed and employed in the CCQM-K105 Key Comparison "Electrolytic conductivity at $5.3\,\mathrm{S\,m^{-1}}$" and in the CCQM-P142 Pilot study "Equivalence ratio of conductance measurement results of seawater". The CCQM-K105 comparison was coordinated by INRIM and I took part in data analysis and in the estimation of the reference values.

I worked on the development of a new measurement system suitable for measurements of low conductivity solutions ($< 1\,\mathrm{mS\,m^{-1}}$). By performing measurements of such electrolytic solutions (down to ultra pure water), significant difficulties mainly arise from the solution contamination due to air carbon dioxide, temperature control and resistance measurement which are strongly affected by parasitic phenomena.

For these reasons, I developed a closed glass hydraulic circuit to carry out measurements on flowing solutions. This circuit includes flow-through reference and secondary cells. This hydraulic circuit allows to low conductivity measurements and calibration of secondary cells by comparison. This circuit contains also a specifically designed expansion vessel.

The flowing solution avoids air contact and prevents air CO_2 absorption. Measurements were performed with three different solutions with conductivity values of $5\,\mathrm{mS\,m^{-1}}$, $3\,\mathrm{mS\,m^{-1}}$ and $1\,\mathrm{mS\,m^{-1}}$. Measurements carried out by all the solutions showed an effective positive improvement due to the closed circuit, in particular for the solution of lower conductivity value ($1\,\mathrm{mS\,m^{-1}}$) which could not be measured without flowing system.

Finally, I worked at the implementation of an impedance spectrometer for ultra pure water measurements because commercial RLC meters do not reach frequency values lower than 20 Hz useful for conductivity measurements of ultra pure water.

For the future, the main objectives include the improvement of the measuring system in order to extend the measurement capability to lower conductivity values. These improvements consist in a better control of the inert gas inside the circuit, the achievement of higher speed flow through a magnetic pump, avoiding mechanical vibrations in the system. Moreover, the hydraulic circuit has to be adapted to perform calibration by comparison method of commercial conductivity probes. On the basis of the experiences maturated through preliminary measurements on ultra pure water, a circuit directly connected to Millipore system and to an impedance spectrometer has to be developed.

Appendix A

Technical reports

Istituto Nazionale di Ricerca Metrologica

E. Orrù, F. Durbiano

CCQM-K105 Key Comparison
Electrolytic conductivity at 5.3 S/m,
INRIM Measurement Report

RT 6/2013 Marzo 2013

INRIM TECNICHAL REPORT

Abstract
Salinity is a measure of dissolved material in water. It is expressed in terms of a conductance ratio between a seawater sample and a defined potassium chloride solution at atmospheric pressure and at the temperature of 15 °C. Practical Salinity results are currently not traceable to metrological references consistent with the International System of Units (SI).
A first Pilot Study (CCQM-P111) was carried out, but the calculated uncertainty associated with the conductivity values resulted too large. So another comparison has been organised to underpin the SI traceability of the results. It is a follow-up the Pilot Study CCQM P111. This comparison helps to establish a metrological infrastructure for oceanography. It was coordinated by INRiM and supported by PTB. This report describes the measurement procedure and the results obtained at INRiM.

Sommario
La salinità è una misura del sale disciolto in acqua. Essa è espressa come il rapporto tra la conduttanza di un campione di acqua di mare e quella di una soluzione acquosa con massa nota di cloruro di potassio alla pressione atmosferica e alla temperatura di 15 °C. Siccome i valori della Salinità Pratica attualmente non sono riferibili alle unità del Sistema Internazionale (SI) è stato effettuato uno Studio Pilota, ma i valori di incertezza ottenuti, associati ai valori di conducibilità, sono risultati troppo grandi. Di conseguenza è stato organizzato un altro confronto, CCQM-K105, di interesse soprattutto per la comunità marina. Il confronto è stato coordinato dall'INRiM e supportato dal PTB. Questo rapporto tecnico descrive la procedura di misura e i risultati ottenuti all'INRiM.

Summary Measurement Report
CCQM-K105

Laboratory: Istituto Nazionale di Ricerca Metrologica – INRiM-
Electromagnetism Division
Electrochemical measurements laboratory
Strada delle Cacce 91
10135, Torino
Italy

Contact person: Dr. Francesca Durbiano
Tel: 00-39-011-3919-316
Fax: 00-39-011-346384
E-mail: f.durbiano@inrim.it;

Measuring Setup

The measuring cell

Conductivity measurements were performed with the secondary cell (cod. IRMMECEL003) developed at INRiM. It has a single glass chamber, holding two parallel platinum electrodes that face each other. The capacity of the cell is about 15 mL. The geometric constant of this cell was estimated by calibrating it by substitution against the INRiM primary cell (cod. IRMMECEL001). A photograph of the secondary cell is shown in Figure 1. For the calibration a KCl aqueous solution of 5 S/m at 25 °C was used.

Fig. 1: Secondary cell for high conductivity values

Impedance measurement

Impedance measurements were realized using a high precision commercial LCR-meter (Agilent 4980A). The meter was connected to the secondary cell by means of Teflon-insulated BNC terminated coaxial cables, using a four terminals configuration. An open/short procedure

was applied to the LCR meter to compensate for cable effects. The applied excitation is a sine wave with an rms value of 0.5 V.

Temperature measurement
The cell was placed in a high precision oil bath (Hart Scientific Model 7008), which was set to 25 °C and 15 °C respectively. The temperature measurements were performed using a Pt-100 platinum resistance thermometer, which was placed in contact with the cell wall. Temperature measurements were carried out simultaneously with the impedance ones using a digital multimeter (Agilent Technologies 3458A).

Data acquisition system
Data acquisition was managed by a software developed at INRiM in LabWindows/CVI.
Conductivity values and their respective uncertainty were determined using Microsoft Excel.

Measurement procedure

After removing the bottles from their packaging, an inspection for damage, leakage, deposit or visible contamination in the solution was performed, with negative results. The bottles were then stored in a cabinet at room temperature. Before breaking the seal and uncapping the bottles, these were weighed and correction for the buoyancy was calculated. The corrected values are reported in Table 1.
Before using the cell, it was cleaned with ultra pure water (from MilliQ) and "primed" with measurement solution. The cell was then filled with fresh solution and it was dipped into the oil bath. Measurement lasted at least 12-15 hours in order to be sure that solution temperature reached that of the bath oil.

Table 1: **Sample data of CCQM-K105 solutions**

Bottle N°	Date received	Date measured	Corrected mass co-ordinating lab, g	Corrected mass after receipt, g
8	2012.10.15	2012.11.12	364.842	364.847
9		2012.11.20	372.308	372.315
10		2012.11.26	357.486	357.480
11		2012.12.03	374.041	374.036

Conductivity determination

Electrolytic conductivity of each sample was determined by repetition of impedance measurements of the solution included in the secondary cell. In this case, the corresponding impedance spectra of the solution is characterized by three frequency regions: at low frequencies resistance increases because of the double layer, at high frequencies it decreases because of capacitive effects, at intermediate frequencies resistance is approximately constant. The resistance in the bulk of the solution corresponds to the value in the transition region which is located at a frequency f^*, where the modulus of the reactance has a minimum close to zero.

In the following, on the basis of the resistance value, the electrolytic conductivity and the measurement uncertainty were calculated.
The conductivity . of the solution contained in the secondary cell was estimated using the following equation:

$$\kappa = \frac{C_{II}}{\left(R\left(1+\alpha_{\mathrm{T}}\left(T-T_{ref}\right)\right)\right)} \qquad (1)$$

where:

C_{II} is the geometric constant of the secondary cell which was estimated by calibration against the primary cell;
R is the resistance value located in the impedance spectra at f* measured by the LCR bridge; α_{T} is the temperature coefficient of the solution; T is the measuring temperature and T_{ref} the reference temperature (25 °C and 15 °C).

Although the conductivity values are stated to be 25 °C and 15 °C, resistances were not measured at the exact temperature. Consequently, the bulk resistance R was corrected to its value at 25 °C and 15 °C using the temperature coefficients $\alpha_{25°C}$ = 0.0197 °C^{-1} and $\alpha_{15°C}$ = 0.0229 °C^{-1} [1].

Uncertainty determination

In the treatment of the measurement uncertainty the relevant international documents [2] and [3] were followed. The corresponding uncertainties were combined by applying the uncertainty propagation law, where the input quantities are considered uncorrelated. In the following, details about the uncertainty contributions are reported.

- The secondary cell was calibrated against the primary cell on a KCl solution. Two characteristic constants C_{II15} and C_{II25} were obtained at 15 °C and 25 °C. Two combined standard uncertainties associated with the cell constants were evaluated at 15 °C and 25 °C: $u(C_{II15})$ and $u(C_{II25})$.
- The uncertainty $u(R)$ (Type A) was calculated by the repetition of several measurements of the sample. A normal distribution was considered. The number of repetitions of resistance measurements carried out on the sample at each temperature was respectively 6 for the sample at 25 °C and 4 for the sample at 15 °C.
- The uncertainty $u(R_{sys})$ (Type B) is given by the calibration of the LCR bridge with a Tinsley standard AC resistor having resistance value similar to the ones obtained with the solution (100 Ω) and a rectangular distribution was considered.
- The uncertainty $u(T_{sys})$ associated with temperature is given by the convolution of three systematic contributions (Type B). The first one corresponds with the calibration uncertainty of the platinum resistance thermometer. The calibration certificate issued by INRiM refers to the international temperature scale of 1990 (ITS-90), and the calibration uncertainty is $u(Pt100)$ = 0.003 °C with a rectangular distribution. The second uncertainty contribution is given by the digital multimeter, which corresponds with an uncertainty

$u(DMM)$ = 0.003 °C. Moreover, the resolution of the system thermometer/multimeter was 0.001 K and a rectangular distribution was deduced.

- The contribution $u(T)$ was due to the temperature repeatability of the impedance measurements (Type A). A normal distribution was considered.
- The uncertainty $u(\alpha_T)$ associated with temperature coefficient was reckoned to be 5 % considering a rectangular distribution.

The results found at INRiM are reported in Table 2

Table 2: **Sample results of CCQM-K105 solutions**

Reference Temperature	**Electrolytic Conductivity (κ)**	$u(\kappa)$	$U(\kappa)_{k=2}$
15.000 °C	4.2856 S/m	0.0131 S/m	0.0261 S/m
25.000 °C	5.2910 S/m	0.0191 S/m	0.0382 S/m

The uncertainty budget of sample at 25 °C and 15 °C are reported in Tables 3-4. The conductivity value, its composed uncertainty and expanded uncertainty are reported below each table.

Table 3: **Calculation of uncertainty budget of the CCQM-K105 solution at nominal temperature 25°C**

Uncertainty source	**Estimate**	**Assumed distribution /Type A,B**	**Standard uncertainty**	**Sensitivity coefficient**	**Contribution to standard uncertainty (S/m)**
X_i	x_i		$u(x_i)$	c_i	$u_I(y)$
C_{II}	223.596 m^{-1}	Norm./ A	6.78E-01 m^{-1}	2.37E-02	1.60E-02
R	42.259 Ω	Norm./ A	7.60E-02 Ω	-1.25E-01	9.52E-03
R_{sys}	0 Ω	Rect./ B	2.89E-02 Ω	-1.25E-01	3.61E-03
T	25.000 °C	Norm./ A	2.00E-02 °C	-1.04E-01	2.07E-03
T_{sys}	0 °C	Rect./ B	3.14E-03 °C	-1.04E-01	3.25E-04
α_T	0.0196 $°C^{-1}$	Rect./ B	2.89E-04 $°C^{-1}$	5.29E-03	1.53E-06

Electrolytic conductivity: 5.2910 S/m
Composed uncertainty $u_c(y)$: 1.91E-02 S/m
Expanded uncertainty (k = 2) : 3.82E-02 S/m

Table 4: **Calculation of uncertainty budget of the CCQM-K105 solution at nominal temperature 15°C**

Uncertainty source	**Estimate**	**Assumed distribution /Type A,B**	**Standard uncertainty**	**Sensitivity coefficient**	**Contribution to standard uncertainty (S/m)**
X_i	x_i		$u(x_i)$	c_i	$u_I(y)$
C_{II}	221.045 m^{-1}	Norm./ A	6.60E-01 m^{-1}	1.94E-02	1.28E-02
R	51.578 Ω	Norm./ A	1.09E-02 Ω	-8.31E-02	9.02E-04
R_{sys}	0 Ω	Rect./ B	2.89E-02 Ω	-8.31E-02	2.40E-03
T	15.000 °C	Norm./ A	1.43E-02 °C	-9.81E-02	1.40E-03
T_{sys}	0 °C	Rect./ B	3.14E-03 °C	-9.81E-02	3.08E-04
α_T	0.0229 $°C^{-1}$	Rect./ B	2.89E-04 $°C^{-1}$	4.29E-03	1.24E-06

Electrolytic conductivity: 4.2856
Composed uncertainty $u_c(y)$: 1.31-02 S/m
Expanded uncertainty (k = 2) : 2.61-02 S/m

References

[1] Seitz S, Spitzer P, Brown RJC, CCQM-P111 study on traceable determination of pratical salinity and mass fraction of major seawater components, (2010) Accred Qual Assur 15:9-17. doi:10.1007/s00769-009-0578-8.
[2] European Co-operation for Accreditation, EA 4/02, Expression of the Uncertainty of Measurement in Calibration. Dec. 1999.
[3] JCGM 100:2008, GUM 1995 with minor corrections. Evaluation of measurement data - Guide to the expression of uncertainty in measurement, First edition 2008.

CCQM-K105 Key Comparison
Electrolytic conductivity at 5.3 S/m

Technical protocol

Introduction

Salinity is a measure of dissolved material in water. Practical Salinity is currently the world wide accepted measure for the content of dissolved salt in seawater. It is expressed in terms of a conductance ratio between a seawater sample and a defined potassium chloride solution at atmospheric pressure and at the temperature of 15 °C. Practical Salinity results are currently not traceable to metrological references consistent with the International System of Units (SI).
Nevertheless, salinity is one of the most important input quantities for oceanographic models, which measuring data must be comparable on very long time scales. Thus, there is a major interest of oceanographic research to determine the equivalence of SI traceable conductivity measurements for the determination of practical salinity.
To face this topic a first Pilot Study (CCQM-P111) was carried out, but the conductivity uncertainty resulted large. So another comparison has been organised to underpin the SI traceability of the results. This comparison helps to establish a metrological infrastructure for oceanography. It is a follow-up comparison of CCQM Pilot Study P111.
The KC addresses to EAWG members. It will be coordinated by INRiM and is supported by PTB.

Purpose of the comparison

The proposed key comparison aims to demonstrate the calibration and measurement capabilities of the participating institutes with respect to the conductivity of multi-component aqueous salt solutions.
Furthermore, the KC additionally aims to provide an SI traceable conductivity reference value for standard seawater and its corresponding uncertainty.
To this end the conductivity of a standard seawater sample, provided by the support laboratory, have to be measured traceable to the SI, preferably by means of a primary conductivity measurement system. The nominal conductivity value of the solution will be around 5.3 S/m at 25 °C. The measurements will be performed at 25 °C and 15 °C (if possible).

Time schedule

September 2012	Technical protocol, approval and solution preparation
October 2012	Dispatch of the samples
November 2012	Measurement period
January 2013	Deadline for receipt of the report
April 2013	(EAWG at BIPM) Discussion of results and Draft A

CCQM-K105 Key Comparison: Electrolytic conductivity at 5.3 S/m,

Description of the samples

The solution used in this comparison is a standard seawater samples from OSIL. It is natural seawater taken from the North Atlantic and diluted with water to a Practical Salinity value of 35 (which corresponds to around 5.3 S/m at 25 °C and around 4.3 S/m at 15 °C).

The solution was bought by Physikalisch-Technische Bundesanstalt PTB, who, without further solution treatments, distributes it to the participants. Standard seawater is contained in 200 ml bottles of boresilicate, numbered and labelled with the filling date. The bottles lids were crimped with a tamper-evident closure, which are brake by first opening. Participating laboratories receive the number of bottles they have indicated in their submission.

Shipment to all participants will be performed at the same time. The bottles will be shipped in a cardboard box by courier. The contents will be labelled “seawater sample” with no commercial value. Please be attentive of possible customs delays, etc. Participants will be informed about the date of dispatching the samples, and are asked to confirm the receipt of the samples by email or fax.

Each participant will receive:

- the technical protocol,
- a number of 200 ml bottles the participating NMI has requested in its submission,
- data sheet listing the bottle masses.

Actions at receipt

Inspect the received bottles for damage, leakage or visible deposits in the solution. Weigh each bottle and compare the bottle masses (corrected for air buoyancy) with the values measured by the coordinating laboratory. Do not remove the label! Also report the ambient atmospheric pressure, relative humidity and temperature at the time the bottle was weighed. Use 1000 kg/m^3 for the density of the bottles filled with sample solution. If the discrepancy between your bottle mass and the mass reported in the datasheet by the coordinating laboratory is larger than 0.2 g, please look for possible leakage and inform the coordinating laboratory.

Do not immediately uncap the solution. Store the bottles in a dark and cool place. Avoid storage at temperatures higher than 25 °C! Please inform the contact person of receipt and report any mishaps. If the appearance or contents of a bottle seems suspicious, please report and a replacement bottle will be sent.

Measurement conditions

Keep the bottles at room temperature for two days right before the measurement. Turn the bottles carefully upside-down several times before opening. If there are visible deposits, please report and await a replacement bottle. Beware of possible bubble formation, which may distort the measurement results.

The measurements should be performed within one month after shipment of the solutions.

Participating NMIs are requested to measure the conductivity of the sample in the range around 25 °C and, if possible, additionally around 15 °C. Afterwards, correct the results to exactly 25 °C and 15 °C respectively. To this behalf please use a temperature coefficient α_{25} = 1.97 %/°C for the reference to 25 °C and α_{15} = 2.29 %/°C for the reference to 15 °C, according to:

$$\kappa_{25} = \kappa(t)(1+\alpha_{25}\,(t - 25°C))^{-1}\,, \qquad \kappa_{15} = \kappa(t)(1+a_{15}\,(t - 15°C))^{-1}.$$

where $\kappa(t)$ is the conductivity at the actual measuring temperature t, $\kappa_{25/15}$ are the conductivity values at 25 °C and 15 °C respectively.

Reporting

Participants must submit a measurement report including at least the following information:

- Name and address of the laboratory performing the measurements.
- Date of receipt of solutions.
- Identification of the samples (bottles) measured.
- Date(s) of measurement(s).
- Results from weighing the bottles.
- Measurement results, including standard and expanded uncertainties (k=2).
- Description of the measurement method and measuring procedure.
- Route of traceability.
- The uncertainty budget in accordance with GUM[1]. The calculations should be verifiable on the basis of the description and the submitted data.

The participating institutes should report their measurement results by email to the coordinating laboratory as soon as possible but no later than 15 January 2013. The coordinating laboratory will confirm the receipt of each report. If the confirmation does not arrive within 1 week, please contact the coordinating laboratory to identify the problem.

Participants are requested to use the summary report form in the annex prepared by the coordinating laboratory. All other information requested can be attached in a suitable manner.

A draft report will be sent to the participants for comments and discussion at the CCQM EAWG meeting in April 2013. During the meeting the determination of the key comparison reference value will be agreed upon. A reviewed Draft B report will be sent to the participants afterwards.

Principal uncertainty components:

The following uncertainty components should be considered by the participants.

- Repeatability and reproducibility of the conductivity measurements.
- Uncertainty of the cell constant. (calibration solution, reference value, geometric measurements).
- Uncertainty of the resistance/conductance measurements.
- Uncertainty of temperature measurement, temperature tracking, bath–cell offset and corrections.
- Other contributions, which may arise from the specific measuring set-up.

How Far the Light Shines statement

The results are considered representative for conductivity measurement of multi-component aqueous salt solutions in the range from 0.1 S/m and 10 S/m. In particular they cover the conductivity range of natural seawater.

[1] http://www.bipm.org/utils/common/documents/jcgm/JCGM_100_2008_E.pdf

CCQM-K105 Key Comparison: Electrolytic conductivity at 5.3 S/m,

Coordinating laboratory and contact person:

Francesca Durbiano
Istituto Nazionale di Ricerca Metrologica (INRiM)
Electromagnetism Division
Strada delle Cacce 91
10135 Torino
Italy
Tel.: +39 011 3919316
Fax: +39 011 346384
Email: f.durbiano@inrim.it

Supporting laboratory and contact person:

Steffen Seitz
Physikalisch-Technische Bundesanstalt (PTB)
Working Group 3.13
Bundesallee 100
D-38116 Braunschweig
Germany
Tel.: +49 531 592 3019
Fax: +49 531 592 3015
Email: steffen.seitz@ptb.de

Summary Measurement Report Form

Laboratory:
Contact person:
Institute:
Address:
Country:
Tel:
Fax:
E-mail:

Sample data:

Bottle numbers					
Date received					
Date measured					
mass (g)					

Measurement results:

Reference temperature	Electrolytic conductivity (S/m)	Standard uncertainty (S/m)	Coverage factor	Expanded uncertainty *(S/m)*
25 °C				
15 °C				
(other)				

Measurement report

Please, describe the measurement methods and procedure used, the calibration method(s) and route of traceability. Give details of the actual measurement results, measuring temperatures, ambient pressure, etc. and other observations. List all contributions to the uncertainty of the measurement result and report the calculation of its standard uncertainty.

Key Comparison CCQM-K92:
Electrolytic Conductivity at 0.05 S/m
INRIM Measurement Report

F. Durbiano, E. Orrù

Index

1) Information on Laboratory

Istituto Nazionale di Ricerca Metrologica – INRIM,
Electromagnetism Division
Strada delle Cacce 91,
I - 10135, Turin, Italy

Contact person: dr. Francesca Durbiano
e-mail: f.durbiano@inrim.it
Tel 0039 011 3919316
Fax 0039 011 346384

2) Introduction

In the recent years pilot comparisons have been carried out under the auspices of the CCQM working group on electrochemical analysis. In 2001 the pilot comparison CCQM-P22 of conductivity at 1.28 S/m and 0.1 S/m was conducted with 13 participants, organized by *Danish Institute of Fundamental Metrology* - DFM, Denmark. In 2003, the pilot comparison CCQM-P47 of conductivity was performed at 0.05 S/m and 0.005 S/m with 17 participants, organized by *Neederlands Meetinstituut – Van Swinden Laboratorium* - NMi-VSL, Netherlands. In 2005 the first key international comparison on electrolytic conductivity was conducted. It was the CCQM-K36 on nominal conductivity of 0.5 S/m and 0.005 S/m and it was organized by DFM with the bearing of *Physikalisch-Technische Bundesanstalt* - PTB and *National Institute of Standards and Technology* - NIST. 13 national laboratories took part. In 2008 comparison CCQM-P111 on Traceable determination of Practical Salinity and mass fraction of major seawater components, and consequently on a nominal conductivity of 5 S/m, has been organized by PTB. 13 national laboratories took part. The *Istituto Nazionale di Ricerca Metrologica* - INRiM results of these comparisons are reported in [1-4].
During the October CCQM EAWG meeting a new key international comparison, CCQM-K92, on conductivity of 20 S/m and 0.05 S/m has been planned. The *Slovak Institute of Metrology* - SMU plays the role of pilot laboratory. Aims of this Key Comparison is to establish the equivalence of measurement of electrolytic conductivity at national metrology institutes at the values of 20 S/m and 0.05 S/m. INRiM decided to take part to the comparison only for what concern the 0.05 S/m value. This report describes the measurements carried out at INRiM.
In the following the expanded uncertainty corresponds to an interval of confidence having a coverage probability of 95 %.

2.1) Samples

The KCl solution in water was prepared at SMU aiming at a nominal conductivity of 0.05 S/m. A copy of the measurement protocol was sent by e-mail to the participants.
On 14th February 2011, INRiM received two bottles of KCl solution in water (samples n. 6 and 7). On the 9th of March 2011 the solution was declared altered and so another solution was sent (samples n. 1B and 19B) by the pilot laboratory. The second shipment has been carried out on the 14th of March 2011 and the solution arrived on the 15th of March 2011. Hereafter the second solution will debate only.

2.2) Actions at receipt

After removal of the bottles from their packaging, an inspection for damage, leakage or visible

contamination in the solution was performed, with negative results. The bottles were then stored in a cabinet at room temperature. The pilot laboratory was informed by e-mail of receipt.

2.3) Test performed beforehand

Before breaking the seal and uncapping the bottles, these were weighed and the measured mass values were sent by e-mail to the comparison coordinator. The bottles were turned upside-down: there was no visible deposit. A technical balance with resolution of 0.01 g and standard uncertainty of 0.025 g was used. The conditions during weighing were:

- Air density: 1.2 kg/m^3
- Temperature during weighing = 23 °C
- Air pressure during weighing was about 991 mbar
- The apparent mass (in air) of the bottles is reported in Table 1.

Correction for the buoyancy has been made.

Table 1: Weights of the bottles containing the sample solution

Sample	INRiM measured mass *(g)*	INRiM value corrected for the buoyancy *(g)*	SMU data *(g)*
n. 1B – 0.05 S/m	557.58	558.14	558.18
n. 19B – 0.05 S/m	556.28	556.84	556.87

2.4) Measurement conditions

The measurements of the 0.05 S/m solution started on the 21st of March and went on until the 25th of March. INRiM determined the electrolytic conductivity value for the solution using a new primary cell kept in a thermostatic air bath at 25 °C. The laboratory temperature was of 23 °C.

3) Measurement method

3.1) Traceability route

The primary cell used at INRiM consists of three parts, two half cells with the electrodes and one removable central tube having nominal length of 10 mm and nominal diameter of 7.5 mm. The conductivity of the solution is determined from the difference of two AC resistance measurements taken with, R_W, and without, R_N, the central tube. These resistances are measured in a large frequency range and corrected to the reference temperature, T_{Ref}. The resistance values are selected where polarisation and parasite effects are minimised, where the resistance values doesn't change as a function of frequency. The conductivity k of the aqueous solution is given by Equation 1:

$$k = \frac{C_{cell}}{R_W \cdot \left[1 + \alpha_T \left(T_W - T_{\mathrm{Re}f}\right)\right] - R_N \cdot \left[1 + \alpha_T \left(T_N - T_{\mathrm{Re}f}\right)\right]} + k_{polW} + k_{polN} \quad (1)$$

where C_{cell} is the cell constant, defined by geometrical parameters of the central tube, α_T is the temperature coefficient of 0.02 K^{-1} and this value has been obtained by the literature [5], T_W and T_N are the temperature values of the measurements carried out respectively with and without the central tube, and k_{polW} and k_{polN} are additional terms concerning the solution change due to the pollution considering the cell in configuration with and without central tube respectively.
A picture of the primary cell and of the central tube are reported respectively in Fig. 1 and Fig. 2.

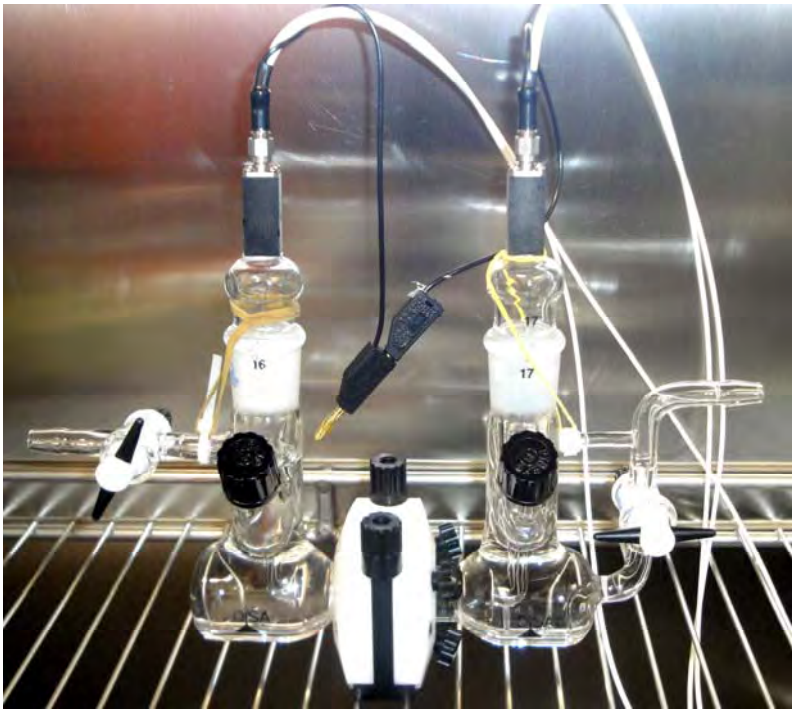

Figure 1: The INRiM primary cell for electrolytic conductivity measurements

The removable central tube is made of Pyrex®, and it is suitable for the measurements of diluted solutions.

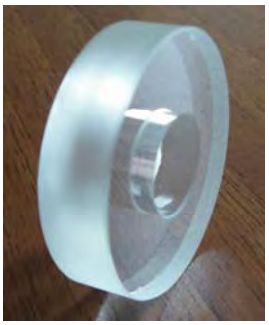

Figure 2: Central tube of the new INRiM primary cell

3.2) Measurement procedure with the primary cell

After every cell component was washed with ultra pure water, it was assembled. Figure 3 reports the closure system in Delrin® (polyoxymethylene), which homogeneously distributes the mechanical stress and tights the glass flanges of the cell.

Figure 3: Closure system for the new primary INRiM cell

Ultra pure water was then poured into the cell, which was then left at rest for at least two hours in order to verify leakage and to adsorb possible impurities from the cell surface and interstices. If the final conductivity value of the water is lower than 1 μS/cm the cell is considered ready to be filled. Then, the cell was washed three times with a small amount of sample solution. At the end the solution was poured into the cell and put in the thermostatic air bath. The thermostatic bath (Branca Ideal Air) has a fan for the air motion and a PID temperature controller. For temperature measurements a calibrated platinum resistance thermometer PT100 was located near the cell and measured by an Agilent Technologies 3458A multimeter.
Electrical resistance measurements were performed in alternating regime using a precision LRC meter (Agilent 4980A). The applied AC voltage was 0.5 V_{rms}. The solutions were measured in the largest frequency range allowed by the bridge (20 Hz – 2 MHz).
A software developed at INRiM in CVI was employed to measure the temperature, to set the applied voltage and the accuracy of the impedance measurements, to start the measurements and to store the data.
The resistance values R_x have been measured at temperatures very close to T_{ref}, and corrected to T_{ref}. The reference temperature required for the measurements was $T_{ref} = 25.000\,°C$. The temperature coefficient α_T = 0.02 K^{-1} was found in the literature [5] and also confirmed by measurements with the commercial probe plunged in the solution at different temperature.
The typical frequency response of an electrolytic cell, in which no chemical reactions occur, shows a low f_{low} and a high f_{high} cut-off frequency, respectively due to the predominance of double-layer effects at low frequencies and to the reduction of the impedance due to the electrode capacitance at high frequencies. The resistance value of the solution was deduced by referring to the frequency range between f_{low} and f_{high}, in correspondence of the minimum of the impedance imaginary component, where the cell has a predominantly resistive behaviour.
Then the conductivity value has been estimated by Equation (1).
In order to define the value of k_{polW} one of the measurement with the cell with the central tube carried out for the comparison has been chosen as representative: about this measurement the behaviour of the resistance at a specific frequency has been studied for about 10 hours. The same study was done on a measurement with the cell without the central tube for the evaluation of k_{polN}. In order to transform the resistance values in conductivity ones, the constants of the cell in configuration with and without the central tube have been evaluated, and the ratio between these cell constants and the resistance values has been considered. Moreover, no significant drift of the conductivity value was observed also considering measurements as a function of time carried out with a commercial probe (WTW InoLab TetraCon 325) on solution with similar conductivity.

4) Measurement results

Two resistance measurements were carried out with the primary cell equipped with the central tube, and two without.
The mean values of the corrected resistance values at the frequency of 3 kHz were taken.
The cell constant, defined by geometrical parameters of the central tube, has been accurately measured with a mechanical probe at INRiM. The calibration certificate of the cell constant reports the value:

$$C_{cell}\ 55.870\ m^{-1} \qquad \text{with } U_{(95\%)} = 3.06\ \text{E-02}\ m^{-1}$$

4.1) Uncertainty budget for the 0.05 S/m solution

In the treatment of the measurement uncertainty the relevant international documents [6] and [7] were followed. In model equation (1), corrections for errors of the measurements of the central tube length, of temperature *T*, of resistance *R* (error of the Agilent 4980A) and for the effect of the pollution in the solution, were assumed to be null. The corresponding uncertainties were combined by applying the uncertainty propagation law, where the input quantities are considered uncorrelated. In the following, details about the uncertainty contributions are reported.

- The combined standard uncertainty $u(C_{cell})$ associated with the cell constant and obtained by the certificate was 1.53 E-02 m^{-1}.
- The uncertainty $u(R_W)$ associated with resistance of the cell in configuration with the central tube is given by the convolution of three contributions. The uncertainty contribution due to the LCR bridge has been evaluated from its calibration with a Tinsley standard AC resistors having resistance value similar to the one obtained with the solution (10 kΩ). The resulting standard uncertainty contribution is 0.078 Ω for which a rectangular distribution has been assumed. The uncertainty contribute due to the LRC meter resolution has been evaluated of 0.029 Ω. For the estimation of the type A contribution obtained by the repetition of the measurements a different aqueous solution with a similar conductivity value has been prepared and five repetition has been carried out. The standard uncertainty was 0.53 Ω. The combined standard uncertainty $u(R_W)$ due to the three contributions was 0.54 Ω.
- The uncertainty $u(T_W)$ associated with temperature when the cell is in configuration with the central section is given by four contributions. The first corresponds to the calibration uncertainty of the platinum resistance thermometer. The calibration certificate issued by INRiM was referred to the international temperature scale of 1990 (ITS-90) [8]. At 25°C the calibration expanded uncertainty is U = 0.002 °C with a rectangular distribution. The second contribution is given by the uncertainty of the multimeter, which corresponds to an expanded uncertainty for temperature of 0.003 K. Moreover, the resolution of the system thermometer/multimeter was 0.001 K and a rectangular distribution has been associated. The fourth contribution was due to the variation of temperature obtained during the measurements. The value was 0.003 K and a rectangular distribution has been associated. At 25 °C the combined standard uncertainty for T_W was 1.35 E-03 °C.
- The uncertainty $u(R_N)$ associated with resistance of the cell in configuration without the central tube is given by the convolution of three contributions. The uncertainty contributions due to the LRC meter calibration and to the LRC meter resolution has been evaluated as for $u(R_W)$. For the estimation of the type A contribution obtained by the

repetition of the measurements a different aqueous solution with a similar conductivity value has been prepared and seven repetition has been carried out. The standard uncertainty was 0.34 Ω. The combined standard uncertainty $u(R_N)$ was 0.35 Ω.

- The uncertainty $u(T_N)$ associated with temperature when the cell is in configuration without the central section is given by the same four contributions of $u(T_W)$.
- The uncertainty $u(\alpha_T)$ associated with temperature coefficient has been considered of 5 % considering a rectangular distribution. The uncertainty contribution was 2.89 E-04 Ω.
- k_{polW} corresponds to the variation of conductivity value during the measurement with the cell with the central tube due to the pollution of the solution. It has been evaluated considering the resistance at a specific frequency value for 100 frequency sweeps. The resistance difference has been determined and it has been transformed in a conductivity value considering a cell constant specific of the cell with the central tube. This cell constant has been evaluated by the average of other conductivity measurements with the primary cell with solution at different concentrations. The variation resulted of 1.40E-06 S/m. A rectangular distribution has been associated.
- k_{polN} corresponds to the variation of conductivity value during the measurement with the cell without the central tube due to the pollution of the solution. It has been evaluated as for k_{polW}. It has been transformed from a resistance value in a conductivity one considering a cell constant specific of the configuration without the central tube. The variation resulted of 2.50E-06 S/m. A rectangular distribution has been associated.

The uncertainty budget is reported in Table 2.

Table 2: Uncertainty budget for nominal conductivity 0.05 S/m at 25 °C.

Uncertainty source	Estimate	Assumed distribution /Type A, B	Standard uncertainty	Sensitivity coefficient	Contribution to standard uncertainty *(S/m)*
X_I	x_I		$u(x_i)$	c_I	$u_I(y)$
C_{cell}	55.870 1/ m	Norm./ B	1.53E-02 1/m	8.938E-04 S	1.37E-05
R_W	8189.50 Ω	Norm./ A	0.54 Ω	-4.376E-05 S^2/m	-2.36E-05
T_W	25.067 °C	Rect./B	1.35E-03 °C	-7.158E-03 S/m°C	-9.69E-06
R_N	7070.65 Ω	Norm./ A	0.35 Ω	-4.370E-05 S^2/m	-1.51E-05
T_N	24.994 °C	Rect./ B	1.35E-03 °C	-6.180E-03 S/(m°C)	-8.37E-06
α_T	0.02 %/°C	Rect./ B	2.89E-04 1/°C	-0.026 °CS/m	-7.46E-06
k_{polW}	0 S/m	Rect./ B	8.08E-07 S/m	1	8.08E-07
k_{polN}	0 S/m	Rect./ B	1.44E-06 S/m	1	1.44E-06

Assigned value: 4.99355 E-02 S/m
Combined standard uncertainty: 3.45 E-05 S/m
Expanded uncertainty (k = 2): 6.9 E-05 S/m

The final result is also reported in Table 3.

Table 3: Result for the 0.05 S/m solution

Nominal Conductivity (S/m)	Result (assigned value) (S/m)	Standard uncertainty *(S/m)*	Coverage factor	Expanded Uncertainty *(S/m)*
0.05	4.99355 E-02	3.45 E-05	2	6.9 E-05

Table 4: Symbols

C_{cell}	Cell constant
k	Electrolytic conductivity
R_w	Resistance measured with the cell with the central tube
R_N	Resistance measured with the cell without the central tube
T_{ref}	Reference temperature
T_W	Temperature measured with the cell with the central tube
T_N	Temperature measured with the cell without the central tube
α_T	Temperature coefficient
k_{polW}	Variation of electrolytic conductivity due to the pollution with the cell with the central tube
k_{polN}	Variation of electrolytic conductivity due to the pollution with the cell without the central tube

Acknowledgements

The authors warmly thank D. Serazio (INRiM), for the development of the closure system of the primary cell.

References

[1] F. Durbiano, E. Ferrara, G. Marullo Reedtz, P. P. Capra, "*Pilot Study CCQM – P22 on Electrolytic Conductivity. IEN Measurement Report.*" Rapporto Tecnico IEN n. 629, maggio 2001.

[2] F. Durbiano, L. Callegaro, P. P. Capra, G. Marullo Reedtz, "Pilot Comparison CCQM-P47 on Electrolytic Conductivity of dilute solutions, IEN Measurement Report", Rapporto Tecnico IEN n. 666, ottobre 2003.

[3] F. Durbiano, L. Callegaro, P.P. Capra, and V. D'Elia, "Key Comparison CCQM-K36: Electrolytic Conductivity at 0.5 and 0.005 S/m, IEN Measurement Report", IEN Technical Report No. 694, October 2005.

[4] C. Boveri, F. Durbiano, "Pilot Study CCQM - P111: Traceable determination of Practical Salinity and mass fraction of major seawater components. INRiM Measurement Report", INRIM Technical Report no.136, August 2008.

[5] Standard Test Methods for the Electrical Conductivity and Resistivity of Water, ASTM-International, D 1125-91, 1991.

[6] European Co-operation for Accreditation, EA 4/02, Expression of the Uncertainty of Measurement in Calibration. Dec. 1999.

[7] JCGM 100:2008, GUM 1995 with minor corrections. Evaluation of measurement data - Guide to the expression of uncertainty in measurement, First edition 2008.

[8] H. Preston Thomas, *The International Temperature Scale of 1990 (ITS-90),* Metrologia 27, 3-10 (1990).

Istituto Nazionale di Ricerca Metrologica

E. Orrù, F. Durbiano

CCQM-P142 Pilot Study: Equivalence of conductance ratio measurement results of seawater, INRIM Measurement Report

RT 5/2013 Marzo 2013

INRIM TECNICHAL REPORT

Abstract
Pratical salinity is currently the world wide measure for the content of dissolved salt in seawater. According to the Pratical Salinity Scale from 1978 (PSS-78) it is expressed in terms of a conductance ratio between a seawater sample and a defined potassium chloride solution, both having conductivities around 4.3 S/m at 15°C.
The proposed pilot study aims to investigate the equivalence of such conductance ratio measurements in order to quantify the reproducibility of independent measurement results.
This pilot study has been carried out in the framework of the EMRP ENV05 project “Ocean metrology”.
This report describes the measurement procedure and the results obtained at INRiM.
The pilot study was co-coordinated by PTB and supported by INRIM.

Sommario
La salinità è una misura attualmente in uso per determinare il contenuto di sale disciolto in acqua. Essa è espressa come il rapporto tra la conduttanza di un campione di acqua di mare e quella di una soluzione acquosa con massa nota di cloruro di potassio con conducibilità pari a 4,3 S/m a 15 °C.
Con questo studio pilota si vuole verificare la riproducibilità del rapporto delle misure di conduttanza ottenuto attraverso misure indipendenti. Questo studio pilota è stato portato avanti nell’ambito del progetto EMRP ENV05 project “Ocean metrology”.
Questo rapporto tecnico descrive la procedura di misura e i risultati ottenuti all’INRiM.
Il confronto è stato coordinato dal PTB con il supporto dell’INRiM.

Summary Measurement Report
CCQM-P142

Laboratory: Istituto Nazionale di Ricerca Metrologica – INRiM-
Electromagnetism Division
Electrochemical measurements laboratory
Strada delle Cacce 91
10135, Torino
Italy

Contact person: Dr. Francesca Durbiano
Tel: 00-39-011-3919-316
Fax: 00-39-011- 346384
E-mail: f.durbiano@inrim.it;

Measuring Setup

The measuring cell

Conductivity measurements were performed with the secondary cell (cod. IRMMECEL003) developed at INRiM. It has a single glass chamber, holding two parallel platinum electrodes that face each other. The capacity of the cell is about 15 mL. The geometric constant of this cell was estimated by calibrating it by substitution against the INRiM primary cell (cod. IRMMECEL001). A photograph of the secondary cell is shown in Figure 1. For the calibration a KCl aqueous solution of 5 S/m at 25 °C was used.

Fig. 1: Secondary cell for high conductivity values

Impedance measurement

Impedance measurements were realized using a high precision commercial LCR-meter (Agilent 4980A). The meter was connected to the secondary cell by means of Teflon-insulated BNC terminated coaxial cables, using a four terminals configuration. An open/short procedure was applied to the LCR meter to compensate for cable effects. The applied excitation is a sine wave with an rms value of 0.5 V.

Temperature measurement
The cell was placed in a high precision oil bath (Hart Scientific Model 7008), which was set to 25 °C and 15 °C respectively. The temperature measurements were performed using a Pt-100 platinum resistance thermometer, which was placed in contact with the cell wall. Temperature measurements were carried out simultaneously with the impedance ones using a digital multimeter (Agilent Technologies 3458A).

Data acquisition system
Data acquisition was managed by a software developed at INRiM in LabWindows/CVI. Conductivity values and their respective uncertainty were determined using Microsoft Excel.

Measurement procedure

After removing the bottles from their packaging, an inspection for damage, leakage, deposit or visible contamination in the solution was performed, with negative results. The bottles were then stored in a cabinet at room temperature. Before breaking the seal and uncapping the bottles, these were weighed and correction for the buoyancy was calculated. The corrected values are reported in Table 1.

Before using the cell, it was cleaned with ultra pure water (from MilliQ) and "primed" with measurement solution. The cell was then filled with fresh solution and it was dipped into the oil bath. Measurement lasted at least 12-15 hours in order to be sure that solution temperature reached that of the bath oil.

Table 1: **Sample data of CCQM P142 solutions**

Sample	Bottle N°	Date received	Date measured	Corrected mass (g) co-ordinating lab	Corrected mass (g) after receipt
32 g/kg KCl	9	2012.10.15	2012.10.22	355.312	355.318
	29		2012.10.29	349.215	349.221
	44		2012.11.8	361.983	361.994
4.3 S/m	10		2013.01.10	359.680	359.682
	28		2013.01.16	372.753	372.765
	48		2013.01.24	359.629	359.632
2.5 S/m	4		2013.01.2	357.895	357.900
	32		2013.01.9	356.452	356.459
	47		-	362.048	362.054
1 S/m	14		2012.11.15	357.808	357.810
	25		2011.11.22	355.485	355.490
	47		2012.12.17	353.650	353.660

Conductivity determination

Electrolytic conductivity of each sample was determined by repetition of impedance measurements of the solution included in the secondary cell. In this case, the corresponding impedance spectra of the solution is characterized by three frequency regions: at low frequencies resistance increases because of the double layer, at high frequencies it decreases because of capacitive effects, at intermediate frequencies resistance is approximately constant. The resistance in the bulk of the solution corresponds to the value in the transition region which is located at a frequency f^*, where the modulus of the reactance has a minimum close to zero. In tables 2-5 temperatures and conductances (inverse values of measured resistances) at nominal temperature of 15 °C and 25 °C for each sample are reported. The repeatability of conductances were not evaluated.

Table 2: **KCl solution**

Nominal temperature 25°C		**Nominal temperature 15°C**	
Measured temperature *t*/°C	**Conductance *G* /S**	**Measured temperature *t*/°C**	**Conductance *G* /S**
25.004	0.023815	15.002	0.019726
25.014	0.023825	15.000	0.019725
24.993	0.023835	15.004	0.019726
24.997	0.023810	14.998	0.019723
24.998	0.023809	15.003	0.019722
24.999	0.023811	15.005	0.019718

Table 3: **4.3 Sm^{-1} seawater solution**

Nominal temperature 25°C		**Nominal temperature 15°C**	
Measured temperature *t*/°C	**Conductance *G* /S**	**Measured temperature *t*/°C**	**Conductance *G* /S**
25.003	0.023200	14.994	0.018951
25.001	0.023201	15.002	0.018956
24.999	0.023199	15.000	0.018948
25.003	0.023197	14.997	0.018953
25.003	0.023193	14.999	0.018960
25.000	0.023191	15.003	0.018952
24.997	0.023185	15.001	0.018950
24.997	0.023187	-	-
25.000	0.023184	-	-
25.005	0.023190	-	-

Table 4: **2.5 Sm^{-1} seawater solution**

Nominal temperature 25°C		**Nominal temperature 15°C**	
Measured temperature *t*/°C	**Conductance *G* /S**	**Measured temperature *t*/°C**	**Conductance *G* /S**
25.001	0.014025	14.996	0.011377
25.001	0.014028	14.996	0.011379
25.002	0.014025	15.000	0.011380
25.002	0.014027	14.999	0.011379
25.001	0.014023	-	-
25.003	0.014024	-	-

Table 5: **1 Sm^{-1} seawater solution**

Nominal temperature 25°C		**Nominal temperature 15°C**	
Measured temperature *t*/°C	**Conductance *G* /S**	**Measured temperature *t*/°C**	**Conductance *G* /S**
25.000	175.49190	14.998	0.004595
24.999	175.49103	15.001	0.004597
25.002	175.48890	15.002	0.004597
-	-	15.002	0.004595

In the following, the conductance of the samples is no longer taken into account and, on the basis of the resistance value, the electrolytic conductivity and the measurement uncertainty were calculated.
The conductivity . of the solutions contained in the secondary cell was estimated using the following equation:

$$\kappa = \frac{C_{II}}{\left(R\left(1+\alpha_{\mathrm{T}}\left(T-T_{ref}\right)\right)\right)} \qquad (1)$$

where:

C_{II} is the geometric constant of the secondary cell which was estimated by calibration against the primary cell;
R is the resistance value located in the impedance spectra at f* measured by the LCR bridge;
α_{T} is the temperature coefficient of the solution;
T is the measuring temperature and T_{ref} the reference temperature (25 °C and 15 °C).

Although the conductivity values are stated to be 25 °C and 15 °C, resistances were not measured at the exact temperature. Consequently, the bulk resistance R was corrected to its value at 25 °C and 15 °C using the temperature coefficients $\alpha_{25°C}$ = 0.0197 $°C^{-1}$ and $\alpha_{15°C}$ = 0.0229 $°C^{-1}$ [1].

Uncertainty determination

In the treatment of the measurement uncertainty the relevant international documents [2] and [3] were followed. The corresponding uncertainties were combined by applying the uncertainty propagation law, where the input quantities are considered uncorrelated. In the following, details about the uncertainty contributions are reported.

- The secondary cell was calibrated against the primary cell on a KCl solution. Two characteristic constants were obtained at 15 °C and 25 °C. Two combined standard uncertainties associated with the cell constants were evaluated at 15 °C and 25 °C: $u(C_{II15})$ and $u(C_{II25})$.
- The uncertainty $u(R)$ (Type A) was calculated by the repetition of several measurements of the sample solution. A normal distribution was considered. The number of repetitions of resistance measurements carried out on each sample at each temperature is reported in Tables 2-5.
- The uncertainty $u(R_{sys})$ (Type B) is given by the calibration of the LCR bridge with a Tinsley standard AC resistor having resistance value similar to the ones obtained with the solutions (100 Ω) and a rectangular distribution was considered.
- The uncertainty $u(T_{sys})$ associated with temperature is given by the convolution of three systematic contributions (Type B). The first one corresponds with the calibration uncertainty of the platinum resistance thermometer. The calibration certificate issued by INRiM refers to the international temperature scale of 1990 (ITS-90), and the calibration uncertainty is $u(Pt100)$ = 0.003 °C with a rectangular distribution. The second uncertainty contribution is given by the digital multimeter, which corresponds with an uncertainty $u(DMM)$ = 0.003 °C. Moreover, the resolution of the system thermometer /multimeter was 0.001 K and a rectangular distribution was deduced.
- The contribution $u(T)$ was due to the temperature repeatability of the impedance measurements (Type A). A normal distribution was considered.
- The uncertainty $u(\alpha_T)$ associated with temperature coefficient was reckoned to be 5 % considering a rectangular distribution.

The uncertainty budget of samples is reported in Tables 7-14. The conductivity value, its composed uncertainty and expanded uncertainty are reported below each table.

Table 7: **Calculation of uncertainty budget of the KCl solution at nominal temperature 25°C**

Uncertainty source	**Estimate**	**Assumed distribution /Type A,B**	**Standard uncertainty**	**Sensitivity coefficient**	**Contribution to standard uncertainty (S/m)**
X_i	x_i		$u(x_i)$	c_i	$u_I(y)$
C_{II25}	223.596 m^{-1}	Norm./ A	6.78E-01 m^{-1}	2.38E-02	1.61E-02
R	41.985 Ω	Norm./ A	8.16E-03 Ω	-1.27E-01	1.04E-03
R_{sys}	0 Ω	Rect./ B	2.89E-02 Ω	-1.27E-01	3.66E-03
T	25.000 °C	Norm./ A	2.86E-03 °C	-1.04E-01	2.98E-04
T_{sys}	0 °C	Rect./ B	3.14E-03 °C	-1.04E-01	3.27E-04
α_T	0.0196 $°C^{-1}$	Rect./ B	2.89E-04 $°C^{-1}$	-5.33E-03	1.54E-06

Electrolytic conductivity: 5.3256 S/m
Composed uncertainty $u_c(y)$: 1.66E-02 S/m
Expanded uncertainty (k = 2) : 3.32E-02 S/m

Table 8: **Calculation of uncertainty budget of the KCl solution at nominal temperature 15°C**

Uncertainty source	**Estimate**	**Assumed distribution /Type A,B**	**Standard uncertainty**	**Sensitivity coefficient**	**Contribution to standard uncertainty (S/m)**
X_i	x_i		$u(x_i)$	c_i	$u_I(y)$
C_{II15}	221.045 m^{-1}	Norm./ A	6.60E-01 m^{-1}	1.97E-02	1.30E-02
R	50.699 Ω	Norm./ A	3.27E-03 Ω	-8.60E-02	2.81E-04
R_{sys}	0 Ω	Rect./ B	2.89E-02 Ω	-8.60E-02	2.48E-03
T	15.000 °C	Norm./ A	1.06E-03 °C	-9.98E-02	1.06E-04
T_{sys}	0 °C	Rect./ B	3.14E-03 °C	-9.98E-02	3.13E-04
α_T	0.0229 $°C^{-1}$	Rect./ B	2.89E-04 $°C^{-1}$	-8.72E-03	2.52E-06

Electrolytic conductivity: 4.3599 S/m
Composed uncertainty $u_c(y)$: 1.33E-02 S/m
Expanded uncertainty (k = 2) : 2.65E-02 S/m

Table 9: **Calculation of uncertainty budget of seawater solution with nominal conductivity of 4.3 S/m at nominal temperature 25°C**

Uncertainty source	Estimate	Assumed distribution /Type A,B	Standard uncertainty	Sensitivity coefficient	Contribution to standard uncertainty (S/m)
X_i	x_i		$u(x_i)$	c_i	$u_I(y)$
$C_{\Pi 25}$	223.596 m^{-1}	Norm./ A	6.78E-01 m^{-1}	2.32E-02	1.57E-02
R	43.116 Ω	Norm./ A	4.11E-03 Ω	-2.36E-01	9.70E-04
R_{sys}	0 Ω	Rect./ B	2.89E-02 Ω	-2.36E-01	6.81E-03
T	25.000 °C	Norm./ A	9.49E-04 °C	-1.02E-01	9.64E-05
T_{sys}	0 °C	Rect./ B	3.14E-03 °C	-1.02E-01	3.19E-04
α_T	0.0196 $°C^{-1}$	Rect./ B	2.89E-04 $°C^{-1}$	-5.19E-03	1.50E-06

Electrolytic conductivity: 5.1859 S/m
Composed uncertainty $u_c(y)$: 1.72E-02 S/m
Expanded uncertainty (k = 2) : 3.43E-02 S/m

Table 10: **Calculation of uncertainty budget of seawater solution with nominal conductivity of 4.3 S/m at nominal temperature 15°C**

Uncertainty source	Estimate	Assumed distribution /Type A,B	Standard uncertainty	Sensitivity coefficient	Contribution to standard uncertainty (S/m)
X_i	x_i		$u(x_i)$	c_i	$u_I(y)$
$C_{\Pi 15}$	221.045 m^{-1}	Norm./ A	6.60E-01 m^{-1}	1.90E-02	1.25E-02
R	52.763 Ω	Norm./ A	4.54E-03 Ω	-1.21E-01	5.49E-04
R_{sys}	0 Ω	Rect./ B	2.89E-02 Ω	-1.21E-01	3.49E-03
T	15.000 °C	Norm./ A	1.17E-03 °C	-9.59E-02	1.12E-04
T_{sys}	0 °C	Rect./ B	3.14E-03 °C	-9.59E-02	3.01E-04
α_T	0.0229 $°C^{-1}$	Rect./ B	2.89E-04 $°C^{-1}$	4.19E-03	1.21E-06

Electrolytic conductivity: 4.1894 S/m
Composed uncertainty $u_c(y)$: 1.30E-02 S/m
Expanded uncertainty (k = 2) : 2.60E-02 S/m

Table 11: **Calculation of uncertainty budget of seawater solution with nominal conductivity of 2.5 S/m at nominal temperature 25°C**

Uncertainty source	**Estimate**	**Assumed distribution /Type A,B**	**Standard uncertainty**	**Sensitivity coefficient**	**Contribution to standard uncertainty (S/m)**
X_i	x_i		$u(x_i)$	c_i	$u_I(y)$
$C_{\Pi 25}$	223.596 m^{-1}	Norm./ A	6.78E-01 m^{-1}	1.40E-02	9.51E-03
R	71.296 Ω	Norm./ A	3.67E-03 Ω	-4.40E-02	1.62E-04
R_{sys}	0 Ω	Rect./ B	2.89E-02 Ω	-4.40E-02	1.27E-03
T	25.000 °C	Norm./ A	3.27E-04 °C	-6.15E-02	2.01E-05
T_{sys}	0°C	Rect./ B	3.14E-03 °C	-6.15E-02	1.93E-05
α_T	0.0196 $°C^{-1}$	Rect./ B	2.89E-04 $°C^{-1}$	-6.27E-03	1.81E-06

Electrolytic conductivity: 3.13625 S/m
Composed uncertainty $u_c(y)$: 9.60E-03 S/m
Expanded uncertainty (k = 2) : 1.92E-02 S/m

Table 12: **Calculation of uncertainty budget of seawater solution with nominal conductivity of 2.5 S/m at nominal temperature 15°C**

Uncertainty source	**Estimate**	**Assumed distribution /Type A,B**	**Standard uncertainty**	**Sensitivity coefficient**	**Contribution to standard uncertainty (S/m)**
X_i	x_i		$u(x_i)$	c_i	$u_I(y)$
$C_{\Pi 15}$	221.045 m^{-1}	Norm./ A	6.60E-01 m^{-1}	1.14E-02	7.51E-03
R	87.887 Ω	Norm./ A	5.00E-03 Ω	-4.36E-02	2.18E-04
R_{sys}	0 Ω	Rect./ B	2.89E-02 Ω	-4.36E-02	1.26E-03
T	15.000 °C	Norm./ A	1.05E-03 °C	-5.76E-02	6.05E-05
T_{sys}	0 °C	Rect./ B	3.14E-03 °C	-5.76E-02	1.81E-04
α_T	0.0229 $°C^{-1}$	Rect./ B	2.89E-04 $°C^{-1}$	5.03E-03	1.45E-06

Electrolytic conductivity: 2.5151 S/m
Composed uncertainty $u_c(y)$: 7.62E-03 S/m
Expanded uncertainty (k = 2) : 1.52E-02 S/m

Table 13: **Calculation of uncertainty budget of seawater solution with nominal conductivity of 1 S/m at nominal temperature 25°C**

Uncertainty source	Estimate	Assumed distribution /Type A,B	Standard uncertainty	Sensitivity coefficient	Contribution to standard uncertainty (S/m)
X_i	x_i		$u(x_i)$	c_i	$u_I(y)$
$C_{\Pi 25}$	223.596 m^{-1}	Norm./ A	6.78E-01 m^{-1}	5.70E-03	3.86E-03
R	175.489 Ω	Norm./ A	4.04E-03 Ω	-7.26E-03	2.93E-05
R_{sys}	0 Ω	Rect./ B	2.89E-02 Ω	-7.26E-03	2.10E-04
T	25.000 °C	Norm./ A	8.66E-04 °C	-2.50E-02	2.16E-05
T_{sys}	0 °C	Rect./ B	3.14E-03 °C	-2.50E-02	7.83E-04
α_T	0.0196 $°C^{-1}$	Rect./ B	2.89E-04 $°C^{-1}$	-1.27E-03	3.68E-07

Electrolytic conductivity: 1.2741 S/m
Composed uncertainty $u_c(y)$: 3.87E-03 S/m
Expanded uncertainty (k = 2) : 7.74E-03 S/m

Table 14: **Calculation of uncertainty budget of seawater solution with nominal conductivity of 1 S/m at nominal temperature 15°C**

Uncertainty source	Estimate	Assumed distribution /Type A,B	Standard uncertainty	Sensitivity coefficient	Contribution to standard uncertainty (S/m)
X_i	x_i		$u(x_i)$	c_i	$u_I(y)$
$C_{\Pi 15}$	221.045 m^{-1}	Norm./ A	6.60E-01 m^{-1}	4.60E-03	3.03E-03
R	217.581 Ω	Norm./ A	3.45E-02 Ω	-7.11E-03	2.45E-04
R_{sys}	0 Ω	Rect./ B	2.89E-02 Ω	-7.11E-03	2.05E-04
T	15.000 °C	Norm./ A	9.50E-04 °C	-2.33E-02	2.21E-05
T_{sys}	0 °C	Rect./ B	3.14E-03 °C	-2.33E-02	7.30E-05
α_T	0.0229 $°C^{-1}$	Rect./ B	2.89E-04 $°C^{-1}$	-1.02E-03	2.93E-07

Electrolytic conductivity: 1.0159 S/m
Composed uncertainty $u_c(y)$: 3.05E-03 S/m
Expanded uncertainty (k = 2) : 6.10E-03 S/m

References

[1] Seitz S, Spitzer P, Brown RJC, CCQM-P111 study on traceable determination of pratical salinity and mass fraction of major seawater components, (2010) Accred Qual Assur 15:9-17. doi:10.1007/s00769-009-0578-8.
[2] European Co-operation for Accreditation, EA 4/02, Expression of the Uncertainty of Measurement in Calibration. Dec. 1999.
[3] JCGM 100:2008, GUM 1995 with minor corrections. Evaluation of measurement data - Guide to the expression of uncertainty in measurement, First edition 2008.

EURAMET Study 1202:
Electrolytic Conductivity of Bioethanol
INRIM Measurement Report

F. Durbiano, E. Orrù

Index

1) Information on Laboratory

Istituto Nazionale di Ricerca Metrologica – INRIM,
Electromagnetism Division
Strada delle Cacce 91,
I - 10135, Turin, Italy

Contact person: dr. Francesca Durbiano
e-mail: f.durbiano@inrim.it
Tel 0039 011 3919316
Fax 0039 011 346384

2) Introduction

A preliminary, informal measurement comparison has been proposed under the auspices of the EURAMET electrochemical analysis Sub-Committee for analyzing possible comparability problems of electrolytic conductivity samples as synthetic ethanol and bioethanol. This comparison should be considered as preparatory to the actual measurement comparison that is a deliverable in the EMRP Project ENG09 "Metrology for biofuel".

2.1) Samples

Two solutions intended for the comparison were provided by the Physikalisch-Technische Bundesanstalt (PTB): bioethanol and synthetic, anhydrous ethanol from a commercial provider. On 14th December 2011 INRiM received:

Two 250 mL bottles of bioethanol sample (bottles n. 2 and 8);
Two 250 mL bottles of synthetic ethanol (bottles n. 4 and 9).

On 22nd December 2011 INRiM received:

A 250 mL bottle of bioethanol sample (bottles n. 5).

Table 1: Sample number and receipt date

Samples	Bottle number	Date received
Synthetic Ethanol	4 and 9	14 Dec 2011
Bioethanol	2* and 8	14 Dec 2011
Bioethanol	5	22 Dec 2011

2.2) Actions at receipt

After removal of the bottles from their packaging, an inspection for damage, leakage or visible contamination in the solution was performed. Sample n. 2 of bioethanol (marked with a * in Table 1) presented a leak of solution. The pilot laboratory was immediately informed and a new bottle of bioethanol (sample n. 5) was sent. INRiM informed by e-mail of the receipt. The

bottles were then stored in a cabinet at room temperature (24.2 °C).

2.3) Test performed beforehand

Before breaking the seal and uncapping the bottles, these were weighed and the measured mass values were sent by e-mail to the comparison coordinator. The bottles were turned upside-down: there was no visible deposit. A technical balance with resolution of 0.01 g and standard uncertainty of 0.025 g was used. The conditions during the weighing were:

- Air density: 1.2 kg/m^3
- Temperature during weighing = 24.2 °C
- Air pressure during weighing = 985 mbar

The apparent mass (in air) of the bottles and their values corrected for the buoyancy are reported in Table 2.

Table 2: Weights of the bottles containing the sample solution

Sample	**INRiM measured mass** ***(g)***	**INRiM value corrected for the buoyancy** ***(g)***	**PTB data** ***(g)***
Bottle # 4	475.41	476.05	476.061
Bottle # 9	478.01	478.65	478.692
Bottle # 2	473.04	473.68	477.023
Bottle # 8	477.28	477.92	477.935
Bottle # 5	478.24	478.88	478.891

2.4) Measurement conditions

The measurements of the synthetic ethanol solution started on the 19th of December and went on until the 21st of December. The measurements of the bioethanol solution started on the 22th of December and went on until the 24th of December. INRiM determined the electrolytic conductivity value for the solutions using the secondary cell kept in a thermostatic air bath at 25 °C. The laboratory temperature was 24,2 °C.

3) Measurement method

3.1) Traceability route

The secondary cell consists of a Pyrex® glass chamber holding two parallel, circular and faced electrodes (0.5 mm thickness and 20 mm diameter), positioned at a fixed distance of 10 mm. The cell chamber includes two valve pipelines for the potential circulation of the sample flux. The cell has a capacity of ~180 ml.
The conductivity of the solutions was determined through resistance measurements: these resistance values were measured in a large frequency range and corrected to the reference

temperature. The resistance values were selected where polarisation and parasite effects are minimised, that is where the resistance values doesn't change as a function of frequency. The conductivity k of the aqueous solution is given by Equation 1:

$$k = \frac{C_{II}}{R} + \delta k_T + \delta k_{pol} \qquad (1)$$

where C_{II} is the cell geometric constant of the secondary cell, δk_T is a very little contribution due to the temperature variation and δk_{pol} concerns the solution change due to the pollution. A picture of the secondary cell is reported in Fig. 1.

Figure 1: INRiM secondary cell for electrolytic conductivity measurements

3.2) Measurement procedure with the secondary cell

The cell was washed with ultra pure water, filled with it and left at rest for at least two hours in order to verify leakage and to adsorb possible impurities from the cell surface and interstices. If the final conductivity value of the water was lower than 1 μS/cm the cell was considered clean and ready to be filled. Then, it was primed for one hour with a synthetic ethanol from a commercial provider (99.8 % purity). After the priming step, the cell was washed three times with a small amount of sample solution (synthetic ethanol or bioethanol). At the end, the solution was poured into the cell and put in the air thermostatic bath. The solution was kept in contact with the laboratory air for a maximum of three minutes. The thermostatic bath (Branca Idealair Measure Box model 3715) has a fan for the air motion and a PID temperature controller. For temperature measurements a calibrated platinum resistance thermometer PT100 was located near the cell and measured by an Agilent Technologies 3458A multimeter.
Electrical resistance measurements were performed with a precision LRC meter (Agilent 4284A). The applied excitation was a sine wave with an rms value of 0.5 V assuming that the use of this low value of voltage avoids phenomena of ion discharge at the electrode surface. The solutions were measured in the largest frequency range allowed by the bridge (20 Hz – 1 MHz).
A software developed at INRiM in CVI was employed to measure the temperature, to set the applied voltage and the accuracy of the impedance measurements, to start the measurements

and to store the data. The resistance values R of the samples have been measured at temperatures very close to 25.000 °C.
The variation of conductivity due to temperature for the synthetic ethanol has been evaluated negligible by PTB experiments. For the bioethanol it has been evaluated 0.039 (µS/cm)/°C.
The typical frequency response of an electrolytic cell, in which no chemical reactions occur, shows a low f_{low} and a high f_{high} cut-off frequency, respectively due to the predominance of double-layer effects at low frequencies and to the reduction of the impedance due to the electrode capacitance at high frequencies. The resistance value of the solution was deduced by referring to the frequency range between f_{low} and f_{high}, in correspondence of the minimum of the impedance imaginary component, where the cell has a predominantly resistive behaviour.
Then the conductivity value has been estimated by Equation (1).
In order to define the value of δk_{pol}, one of the measurements carried out for the comparison was chosen as representative: the behaviour of the resistance at a specific frequency was studied for about 10 hours and transformed in a conductivity value.

The geometrical constant C_{II} was calibrated against the primary cell with an aqueous solution of KCl with nominal conductivity of 10 µS/cm. The obtained value is:

$$C_{II} = 16.215\ \text{m}^{-1} \qquad \text{with } U_{(95\%)} = 3.44\ \text{E-01 m}^{-1}$$

4) Measurement results

With the amounts of sample available two repetitions have been carried out.
Since for the synthetic ethanol two very different and inconsistent values were determined, both values are reported in this report.

4.1) Uncertainty budget for synthetic ethanol

In the treatment of the measurement uncertainty the relevant international documents [1] and [2] were followed. In model equation (1), corrections for errors of the measurements of the characteristic constant, temperature, resistance (error of the Agilent 4284A) and for the effect of the pollution in the solution were assumed to be null. The corresponding uncertainties were combined by applying the uncertainty propagation law, where the input quantities are considered uncorrelated. In the following, details about the uncertainty contributions are reported.

- The combined standard uncertainty $u(C_{II})$ associated with the cell constant and obtained by the certificate was 1.72 E-01 m^{-1}.
- The uncertainty $u(R)$ associated with resistance of the cell is given by the contribution due to the LCR bridge that was evaluated from its calibration with a Tinsley standard AC resistors having resistance value similar to the one obtained with the solution (1 MΩ); and due to the repetition of the measurements. For this last contribution in the case of the synthetic ethanol a different synthetic ethanol (anhydrous ethanol - Sigma Aldrich) was used and four repetitions were carried out. For the bioethanol sample the standard deviation was evaluated on the two repetitions.
- The uncertainty associated with variation of conductivity due to the variation of temperature δk_T refers to PTB experiments. For synthetic ethanol $u(\delta k_T)$ was considered negligible. In the case of bioethanol, since the highest variation of temperature during the measurements was 0.016 °C, δk_T was evaluated 6.24E-04 (µS/cm)/°C and a rectangular distribution was associated with its uncertainty.

- $u(\delta k_{pol})$ corresponds to the variation of conductivity value during the measurement due to the pollution of the solution. It was evaluated considering the conductivity at a specific frequency for ten hours. The conductivity difference was determined and a rectangular distribution was associated.

The uncertainty budgets for the two synthetic ethanol values are reported in Table 3 and in Table 4.

Table 3: Uncertainty budget for the synthetic ethanol (1) at 25 °C.

Uncertainty source	Estimate	Assumed distribution /Type A, B	Standard uncertainty	Sensitivity coefficient	Contribution to standard uncertainty *(S/m)*
X_I	x_I		$u(x_i)$	c_I	$u_I(y)$
C_{II}	16.215 1/ m	Norm./ A	1.72E-01 1/m	1.40E-07 S	2.41E-08
R	7142100 Ω	Norm./ A	42750 Ω	-3.18E-13 S^2/m	1.36E-08
δk_{pol}	0 S/m	Rect./ B	2.89E-08 S/m	1	2.89E-08

Assigned value: 2.272 E-06 S/m
Combined standard uncertainty: 4.00 E-08 S/m
Expanded uncertainty (k = 2): 8.0 E-08 S/m
Percentage expanded uncertainty: 3.5 %

Table 4: Uncertainty budget for the synthetic ethanol (2) at 25 °C.

Uncertainty source	Estimate	Assumed distribution /Type A, B	Standard uncertainty	Sensitivity coefficient	Contribution to standard uncertainty *(S/m)*
X_I	x_I		$u(x_i)$	c_I	$u_I(y)$
C_{II}	16.215 1/ m	Norm./ A	1.72E-01 1/m	1.69E-07 S	2.90E-08
R	5920780 Ω	Norm./ A	35441 Ω	-4.63E-13 S^2/m	1.64E-08
δk_{pol}	0 S/m	Rect./ B	2.89E-08 S/m	1	2.89E-08

Assigned value: 2.74 E-06 S/m
Combined standard uncertainty: 4.41 E-08 S/m
Expanded uncertainty (k = 2): 8.8 E-08 S/m
Percentage expanded uncertainty: 3.2 %

The uncertainty budget for the bioethanol is reported in Table 5.

Table 5: Uncertainty budget for the bioethanol at 25 °C.

Uncertainty source	Estimate	Assumed distribution /Type A, B	Standard uncertainty	Sensitivity coefficient	Contribution to standard uncertainty *(S/m)*
X_I	x_I		$u(x_i)$	c_I	$u_I(y)$
C_{II}	16.215 1/ m	Norm./ B	1.72E-01 1/m	1.14E-05 S	1.95E-06
R	87864.47 Ω	Norm./ A	163.17 Ω	-2.10E-09 S^2/m	3.43E-07
δk_T	0 S/m	Rect./ B	1.80E-08 S/m	1	1.80E-08
δk_{pol}	0 S/m	Rect./ B	2.89E-08 S/m	1	2.89E-08

Assigned value: 1.845 E-04 S/m
Combined standard uncertainty: 1.99 E-06 S/m
Expanded uncertainty (k = 2): 4.0 E-06 S/m
Percentage expanded uncertainty: 2.15 %

The final results are also reported in Table 6.

Table 6: Results of the Comparison

Sample	Result (assigned value) (S/m)	Standard uncertainty *(S/m)*	Coverage factor	Expanded Uncertainty *(S/m)*
Synthetic ethanol (1)	2.27 E-06	4.00 E-08	2	8.0 E-08
Synthetic ethanol (2)	2.74 E-06	4.41 E-08	2	8.8 E-08
Bioethanol	1.845 E-04	1.99 E-06	2	4.0 E-06

Acknowledgements

The authors warmly thank B. Trinchera (INRiM), for his availability and his help in the development of the measurement system.

References

[1] European Co-operation for Accreditation, EA 4/02, Expression of the Uncertainty of Measurement in Calibration. Dec. 1999.

[2] JCGM 100:2008, GUM 1995 with minor corrections. Evaluation of measurement data - Guide to the expression of uncertainty in measurement, First edition 2008.

Appendix B

Publications

Accred Qual Assur (2014) 19:11–16
DOI 10.1007/s00769-013-1023-6

GENERAL PAPER

Development of an in-line calibration system for flow-through cells for low electrolytic conductivity values

Elena Orrù · Francesca Durbiano · Massimo Ortolano

Received: 17 September 2013 / Accepted: 22 November 2013 / Published online: 6 December 2013

Abstract This paper describes a comparison calibration system applicable to meters for low electrolytic conductivity values. In this system, measurements are performed in a closed circuit with a flowing solution. This circuit contains a flow-through reference cell and a flow-through cell under calibration. Results of calibrations by substitution and by comparison at 3 mS/m (KCl aqueous solution) are compared. The result of a calibration by comparison at 0.3 mS/m is also reported.

Keywords Electrolytic conductivity · Flow-through conductivity cell · Calibration by comparison · Low conductivity aqueous solutions

Introduction

Electrolytic conductivity is one of the most commonly used parameters for establishing the degree of water purity, and it is becoming increasingly important in several industrial sectors such as pharmaceutics, biotechnology, semiconductor, power generation, and food safety. To provide reliable conductivity measurements [1], it is necessary to develop a calibration method for conductivity cells designed to characterize pure water, i.e., aqueous solutions with conductivity values below 1 mS/m. In the following, it is described the comparison calibration method developed at the Istituto Nazionale di Ricerca Metrologica (INRIM), Italy.

For a generic conductivity cell filled with a solution of conductivity κ, the relation between κ and the resistance R measured at the cell terminals is given by

$$\kappa = \frac{K_{\text{cell}}}{R}, \tag{1}$$

where K_{cell} is the *cell constant*. Calibration is the process of determining this cell constant under specified conditions, that is, with a working solution having a specified conductivity value and with the cell at a specified temperature [2], typically 25 °C. At high conductivity values, calibration is commonly performed by means of a substitution method [3, 311-02-04]: First, the conductivity of the working solution is determined with a reference cell; then, this solution is used as a transfer standard to calibrate the unknown cell constant. However, at low conductivity values, this method is no longer accurate because air carbon dioxide CO_2 causes a drift of the solution conductivity which is unpredictable and different among the two cells. For this reason, according to [4, 5], it was decided to investigate a calibration system with a flowing solution in closed circuit. In this system, the cell constant of a flow-through cell under calibration is determined by comparison against that of a flow-through reference cell. Since the two cells contain shares (at approximately equal temperatures) of the same solution, the drift is homogeneous throughout the two communicating cells and the effects of CO_2 cancel out because they are in common mode.

A similar system, which is used for the calibration of commercial coaxial conductivity cells, is described in

E. Orrù · F. Durbiano (✉)
Divisione Elettromagnetismo, Istituto Nazionale di Ricerca Metrologica (INRiM), Turin, Italy
e-mail: f.durbiano@inrim.it

E. Orrù
e-mail: e.orru@inrim.it

M. Ortolano
Dipartimento di Elettronica e Telecomunicazioni, Politecnico di Torino, Turin, Italy

[6, 7]. The differences between the system presented in [6, 7] and the one of this work are outlined in "Conclusions" section.

Measurement system

The calibration system is composed of the two flow-through cells—the one under calibration and the reference one—connected in closed circuit with an expansion chamber and a peristaltic pump by means of a Pyrex® glass pipeline (Fig. 1). This pipeline, which has a length of 183 cm and an inner diameter of 6 mm, is connected to the cells and to the expansion chamber by means of 6 Teflon® stopcocks. Each stopcock has a length of 12 mm and an inner diameter of 4.2 mm. In each of the cells used in this work, the solution inlet has a length of about 15 mm and an inner diameter of about 2 mm. Examples of flow-through cell designs can be found in [8, 9]. All the components but the peristaltic pump are placed inside a thermostatic air chamber at a nominal temperature of 25 °C. The pump is placed outside of the thermostatic chamber because, as a source of heat, it might worsen the system temperature stability.

The impedance measurement system consists of an Agilent E4980A LCR meter alternatively connected to the two cells by means of a HP 3235 switch control unit. For each cell, the LCR meter measures the impedance by making a frequency sweep over a narrow bandwidth. This bandwidth is centered around the characteristic frequency, dependent on the cell geometry and the solution conductivity, where the modulus of the reactance, i.e., the imaginary part of the impedance, has a minimum value. On the one hand, the two measurement bandwidths should be kept as narrow as possible to minimize the measurement time and, therefore, the effect of temperature instabilities. On the other hand, they should be wide enough to detect changes in the characteristic frequencies caused by solution drift. Typically, an impedance measurement cycle consisting of two successive sweeps takes <2 min, and a calibration run consists of a number of measurement cycles depending on the target uncertainty. The applied excitation is a sine wave with an rms value of 0.5 V to avoid ion discharge at the electrodes.

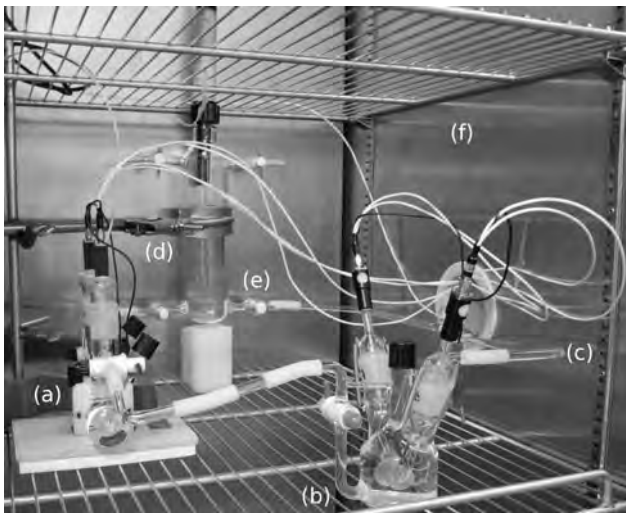

Fig. 1 Picture of the flow-through calibration system: *a* reference cell, *b* cell under calibration, *c* pipeline, *d* expansion chamber, *e* stopcock, *f* thermal chamber. The peristaltic pump is located outside of the chamber and is not shown in the picture

The temperature of the reference cell is measured with a Pt100 platinum resistance thermometer. This thermometer is in contact with the outer surface of the reference cell, and its resistance is measured by an Agilent 3458A multimeter. The temperature of the cell under calibration is inferred from that of the reference cell by considering the chamber temperature inhomogeneity.

The above-described measurement system and procedure were also employed for the calibration by substitution by removing the pipeline connecting the cells.

Calibration procedure

In the following, subscript 1 refers to the quantities related to the reference cell, while subscript 2 refers to those related to the cell under calibration. Measuring the resistance of the two cells yields, according to Eq. 1, two resistance values $R_1 = K_{\text{cell},1}/\kappa_1$ and $R_2 = K_{\text{cell},2}/\kappa_2$, where $K_{\text{cell},1}$ and $K_{\text{cell},2}$ are the two cell constants, and κ_1 and κ_2 are the conductivities of the solutions contained in the cells. Ideally, a calibration should be carried out with $\kappa_1 = \kappa_2$ and with the cells at the specified temperature. When this condition is met,

$$\frac{K_{\text{cell},2}}{K_{\text{cell},1}} = \frac{R_2}{R_1} \tag{2}$$

and $K_{\text{cell},2}$ can be directly determined in terms of $K_{\text{cell},1}$.

If contamination and temperature affect the conductivity (the temperature coefficient can range from 0.02 K^{-1} to 0.07 K^{-1} for ultra-pure water [4]), then $\kappa_1 \neq \kappa_2$. These effects can be modeled by the following equation:

$$\kappa_2(T_2) = \kappa_1(T_1)[1 + \alpha_T(T_2 - T_1)](1 + \eta_2 - \eta_1), \tag{3}$$

where T_1 and T_2 are the cell temperatures; α_T is the temperature coefficient of the solution conductivity at the specified temperature; and η_1 and η_2 represent the relative change in the conductivity due to contamination in each cell.

Taking into account Eq. 3, $K_{\text{cell},2}/K_{\text{cell},1}$ becomes

Table 1 Uncertainty budget for the calibration of $K_{cell,2}/K_{cell,1}$ with the substitution method (3 mS/m working solution)

Uncertainty source X_i	Estimate x_i	Standard uncertainty $u(x_i)$	Unit	Assumed distribution/Type	Sensitivity coefficient c_i	Unit	Contribution to the absolute standard uncertainty of $K_{cell,2}/K_{cell,1}$ $u_i(y)$
$K_{cell,2}/K_{cell,1}$	4.479906×10^{-2}	1.2×10^{-7}		Norm./A	1.0		1.2×10^{-7}
R_1	1.12×10^{5}	5.6	Ω	Rect./B	-4.0×10^{-7}	Ω^{-1}	2.2×10^{-6}
R_2	5.01×10^{-3}	0.25	Ω	Rect./B	8.9×10^{-6}	Ω^{-1}	2.2×10^{-6}
α_T	2.00×10^{-2}	1.2×10^{-3}	K^{-1}	Rect./B	4.9×10^{-3}	K	5.9×10^{-6}
ΔT	0.110	3.0×10^{-2}	K	Rect./B	-1.3×10^{-3}	K^{-1}	3.9×10^{-5}
$\Delta\eta$	0	1.0×10^{-3}	S/m	Rect./B	4.5×10^{-2}	m/S	4.5×10^{-5}

Combined uncertainty $u_c(K_{cell,2}/K_{cell,1}) = 6.0\times10^{-5}$

Expanded uncertainty ($k = 2$) $U(K_{cell,2}/K_{cell,1}) = 1.2\times10^{-4}$

Relative expanded uncertainty $U(K_{cell,2}/K_{cell,1})/(K_{cell,2}/K_{cell,1}) = 2.7\times10^{-3}$

$$\frac{K_{cell,2}}{K_{cell,1}} = \frac{R_2}{R_1}\frac{\kappa_2(T_2)}{\kappa_1(T_1)} \approx \frac{R_2}{R_1}(1 + \alpha_T\Delta T + \Delta\eta), \quad (4)$$

where $\Delta T = T_2 - T_1$ and $\Delta\eta = \eta_2 - \eta_1$. In the above equation, the expression within parentheses constitutes an error term.

With the substitution method, this error is not negligible because, even though the two cells are filled with shares of the same transfer solution, temperature and contamination drifts can be different. While the term $\alpha_T\Delta T$ can be corrected by measuring ΔT, $\Delta\eta$ is unpredictable and cannot be corrected. Therefore, $\Delta\eta$ is a nonnegligible source of uncertainty.

Instead, with the comparison method, the solution flows in both cells, so that both the temperature and the solution (though contaminated) are homogeneous throughout the circuit, $T_2 \approx T_1$ and $\eta_2 \approx \eta_1$, and the error term is negligible.

Results

A KCl aqueous working solution with a nominal conductivity of 3 mS/m (molality: 1.9×10^{-4} mol/kg solvent) was used to compare the two methods of calibration. In addition, a calibration by comparison only was performed with a KCl aqueous working solution with a nominal conductivity of 0.3 mS/m (molality: 1.1×10^{-5} mol/kg solvent). In this case, calibration by substitution would be infeasible because of the high contamination drift.

Substitution method

Table 1 reports the uncertainty budget of $K_{cell,2}/K_{cell,1}$ in the case of calibration by substitution with the 3 mS/m working solution. The uncertainty components related to Eq. 4 were evaluated on the basis of the following considerations:

1. R_1 and R_2 were measured by employing the sequence described in "Measurement system" section. Figure 2 shows the behavior of repeated measurements of $K_{cell,2}/K_{cell,1}$ estimated according to model Eq. 4. The origin of the time axis corresponds to the time when the cells are laid in the chamber after being filled. Since their initial temperature differs from that of the chamber, there is an initial transient to reach thermal equilibrium. This transient has a duration of about 3×10^4 s and has to be skipped. Data analysis starts at time $t_0 \approx 3\times10^4$ s, as highlighted in Fig. 2. Starting from t_0, the behavior of $K_{cell,2}/K_{cell,1}$ clearly shows a drift which is actually due to the different contamination of the two solutions. From t_0 to t_1, the drift is linear and can be easily modeled. The least-square estimate of $K_{cell,2}/K_{cell,1}$ at t_0 is 4.479906×10^{-2} with a type A uncertainty $u(K_{cell,2}/K_{cell,1}) = 1.2\times10^{-7}$.
2. The Type-B uncertainties of R_1 and R_2 depend on the LCR bridge calibration. This was carried out against standard resistors in the range from 1 kΩ to 1 MΩ. The following contributions were taken into account: uncertainty of the standards, AC errors, and LCR bridge linearity [10].
3. According to [5], $\alpha_T \approx 0.02\ K^{-1}$; for this quantity, it has been assumed a rectangular distribution with a relative half-width of 10 %, considering the wide spread of the measurements described in this work.
4. As described in "Measurement system" section, the temperature is measured on the reference cell, only; thus, the temperature difference $\Delta T = T_2 - T_1$ in Eq. 4 can be written as $\Delta T = \Delta T_m + \Delta T_b$, where ΔT_m is the temperature difference measured by the thermometer between two successive sweeps and ΔT_b is the temperature bias which takes into account the chamber temperature inhomogeneity. ΔT_b was independently estimated to be 0.11 K; for this quantity, it has been assumed a rectangular distribution with a half-width of

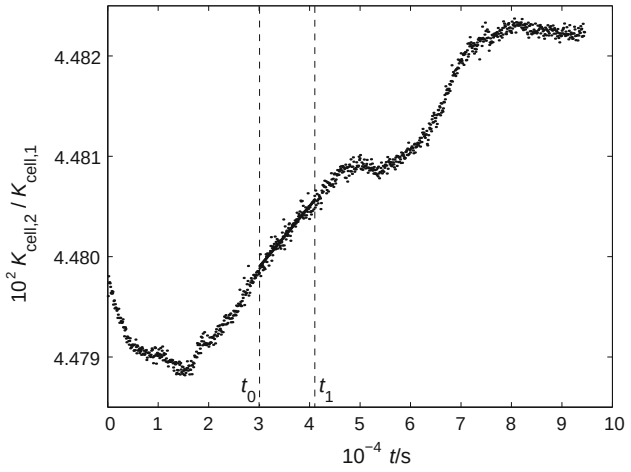

Fig. 2 Example measurement with the substitution method: $K_{cell,2}/K_{cell,1}$ versus time. The data employed in the estimation of $K_{cell,2}/K_{cell,1}$ are taken in the interval from t_0 to t_1. During the transient from time 0 to t_0, thermal equilibrium is not yet established; after t_1 drift cannot be modeled easily

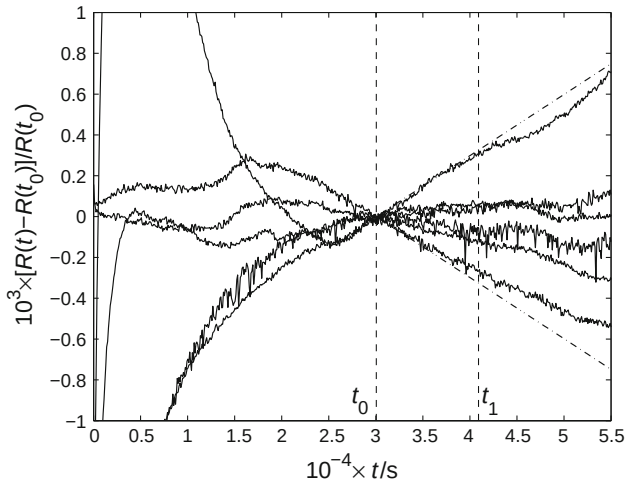

Fig. 3 Relative change of cell resistance with respect to the value at t_0 for several solution samples at 3 mS/m. Before t_0, the thermostatic chamber and the cells are not yet in thermal equilibrium and the resistance change is unpredictable. After t_0 resistance shows a substantially linear drift, bounded by the two *dash-dot lines*

0.05 K. ΔT_m, instead, has zero average value along the measurement cycles, with negligible uncertainty.

5. As pointed out in point 1, before t_0, the thermal equilibrium is not yet established among the solution, the cells, and the chamber. During this transient, solution conductivity changes in an unpredictable way because both of contamination drift and temperature variations. This behavior is shown in Fig. 3 for several solution samples at 3 mS/m. Between time 0 and t_0, the drift due to contamination is masked by the effect of the wide temperature changes. After t_0, contamination becomes the main source of drift and conductivity shows a substantially linear drift. The two dash-dot lines visible in Fig. 3 bound to the spread of the drifts of different solution samples between $d_{min} = -3\times10^{-8}\ s^{-1}$ and $d_{max} = 3\times10^{-8}\ s^{-1}$. Assuming that between time 0 and t_0 contamination drift is bounded by the same limits, a rectangular distribution with zero mean and half-width $(d_{max} - d_{min})t_0 = 1.8\times10^{-3}$ was assigned to the differential change $\Delta\eta$.

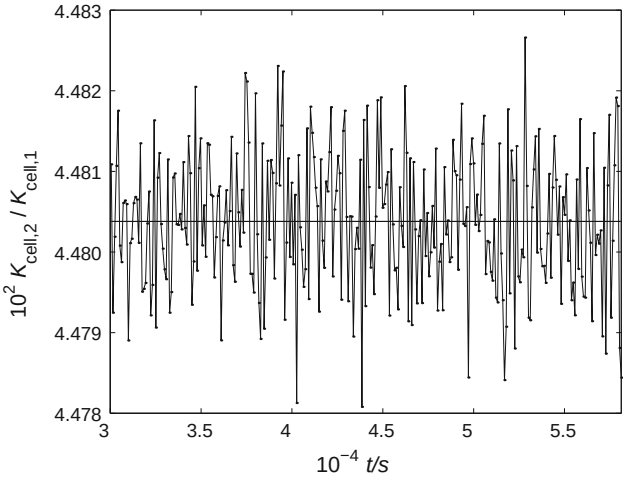

Fig. 4 Ratio of resistances measured with the reference cell and with the flow-through cell at the same time for a 3 mS/m solution. The *thick solid line* marks the mean value of $K_{cell,2}/K_{cell,1}$

Table 2 Uncertainty budget for the calibration of $K_{cell,2}/K_{cell,1}$ with the comparison method. 3 mS/m working solution

Uncertainty source X_i	Estimate x_i	Standard uncertainty $u(x_i)$	Unit	Assumed distribution/Type	Sensitivity coefficient c_i	Unit	Contribution to the absolute standard uncertainty of $K_{cell,2}/K_{cell,1}$ $u_i(y)$
$K_{cell,2}/K_{cell,1}$	4.480380×10^{-2}	4.9×10^{-7}		Norm./A	1.0		4.9×10^{-7}
R_1	1.09×10^{5}	5.5	Ω	Rect./B	-4.1×10^{-7}	Ω^{-1}	2.2×10^{-6}
R_2	4.89×10^{3}	0.24	Ω	Rect./B	9.2×10^{-6}	Ω^{-1}	2.2×10^{-6}

Combined uncertainty $u_c(K_{cell,2}/K_{cell,1}) = 3.1\times10^{-6}$

Expanded uncertainty ($k = 2$) $U(K_{cell,2}/K_{cell,1}) = 6.2\times10^{-6}$

Relative expanded uncertainty $U(K_{cell,2}/K_{cell,1})/(K_{cell,2}/K_{cell,1}) = 1.4\times10^{-4}$

Table 3 Uncertainty budget for the calibration of $K_{cell,2}/K_{cell,1}$ with the comparison method (0.3 mS/m working solution)

Uncertainty source X_i	Estimate x_i	Standard uncertainty $u(x_i)$	Unit	Assumed distribution/Type	Sensitivity coefficient c_i	Unit	Contribution to the absolute standard uncertainty of K_{cell}, $2/K_{cell}$, 1 $u_i(y)$
$K_{cell,2}/K_{cell,1}$	4.480605×10^{-2}	8.1×10^{-7}		Norm./A	1.0		8.1×10^{-7}
R_1	1.10×10^{6}	55	Ω	Rect./B	-4.1×10^{-8}	Ω^{-1}	2.2×10^{-6}
R_2	4.93×10^{4}	2.5	Ω	Rect./B	9.1×10^{-7}	Ω^{-1}	2.2×10^{-6}
Combined uncertainty $u_c(K_{cell,2}/K_{cell,1}) = 3.2\times10^{-6}$							
Expanded uncertainty ($k = 2$) $U(K_{cell,2}/K_{cell,1}) = 6.4\times10^{-6}$							
Relative expanded uncertainty $U(K_{cell,2}/K_{cell,1})/(K_{cell,2}/K_{cell,1}) = 1.4\times10^{-4}$							

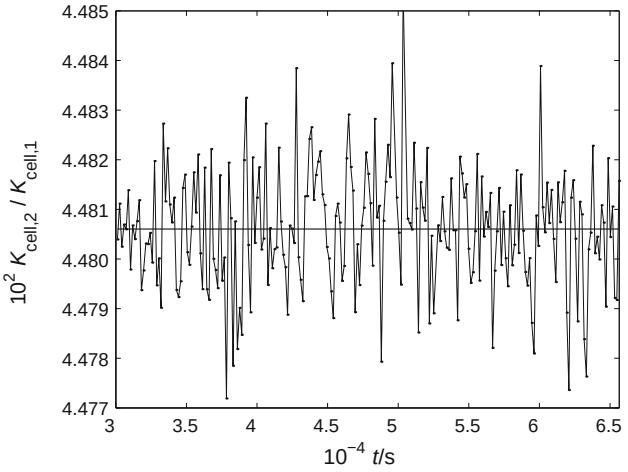

Fig. 5 Ratio of resistances measured with the reference cell and the flow-through cell at the same time for a 0.3 mS/m solution. The *thick solid line* marks the mean value of $K_{cell,2}/K_{cell,1}$

Comparison method

Table 2 reports the uncertainty budget of $K_{cell,2}/K_{cell,1}$ in the case of calibration by comparison with the 3 mS/m working solution. The uncertainty components related to Eq. 2 were evaluated on the basis of the following considerations:

1. Figure 4 shows the behavior over time, after the initial transient, of $K_{cell,2}/K_{cell,1}$ with a 3 mS/m flowing solution. Analysis of the corresponding time series shows a negligible drift over more than 7 h of measurement time. This implies that the solution is homogeneous among the two cells; that the error term due to ΔT and $\Delta\eta$ can be neglected and that Eq. 2 is a suitable measurement model.
2. The Type-B uncertainties of R_1 and R_2 that come from LCR bridge calibration were evaluated as in point 2 of "Substitution method" section.
3. In the calibration by comparison, there can be an additional source of error associated with resistance measurement, not present when the two cells are separated. In fact, when the LCR meter is connected to one of the cells, the measured impedance is actually affected by the rest of the circuit. This causes a systematic error which is of difficult estimation because it depends in a somewhat complicated way on the circuit impedance and on its distributed capacitance toward the ground. When the LCR meter is measuring the impedance between the terminals of one of the cells, the terminals of the other cell should then be grounded. In this way, no current is injected through the circuit to the low side of the LCR meter, and the above-described error becomes negligible.

,

Thus, calibration by comparison shows an uncertainty which is one order of magnitude better than that obtained with the substitution method.

Table 3 reports the uncertainty budget of $K_{cell,2}/K_{cell,1}$ in the case of calibration by comparison with the 0.3 mS/m working solution. In this case, the uncertainty components are the same described in the above for the 3 mS/m solution. Figure 5 shows the behavior over time, after the initial transient, of $K_{cell,2}/K_{cell,1}$: Also, in this case, the ratio is stable and the effects of temperature and contamination are negligible. The uncertainty obtained with the 0.3 mS/m is comparable to that achieved in the case of the 3 mS/m.

Conclusions

This work describes a comparison calibration system for conductivity cells working at low conductivity values. This system allows the rejection of drifts caused by solution contamination and the homogenization of the temperature in the reference cell and in the cell under calibration. A comparison between two calibration methods, substitution and comparison, was carried out with a 3 mS/m working solution. This showed that the uncertainty achieved with the comparison method is one order of magnitude better than that obtained by the substitution one. The result of a

calibration by comparison with a 0.3 mS/m working solution is also reported. All the calibration results are compatible within the uncertainties.

With respect to the system described in [6, 7], the following differences can be outlined. The present system was tested with solutions with different conductivities, and it is not specific for ultra-pure water; it allows the calibration of cells with different geometries, and although it was tested only with one cell under calibration, it could be extended, with little technical modifications, to the simultaneous calibration of several commercial conductivity probes. Contrary to the commercial system, the one here presented does not have an in-line temperature control, but the temperature was verified to be sufficiently homogeneous between the two cells and, where necessary, a compensation procedure was presented.

References

1. Gingerella M, Jacanin JA (2000) Cal Lab 29–36
2. OIML International Recommandation No. 68. (1985) Calibration method for conductivity cells
3. IEC. International Electrotechnical V ocabulary. http://www.electropedia.org/
4. ASTM International (2009) D5391-99. Standard test method for electrical conductivity and resistivity of flowing high purity water sample
5. ASTM International (2009) D1125-95. Standard test methods for electrical conductivity and resistivity of water
6. Bevilacqua AC (1998) Semiconductor pure water and chemicals conference. Santa Clara
7. Light TS, Licht S, Bevilacqua AC, Morash KR (2005) Electrochem Solid-State Lett 8:E16
8. Boveri C, Durbiano F, Serazio D (2009) In: Proceedings of the XIX IMEKO World congress on fundamental and applied metrology
9. Orrù E, Durbiano F, Ortolano M (2013) Meas Sci Tech 24:035903
10. Callegaro L (2012) Electrical impedance. Principles, measurement, and applications. Taylor & Francis

Meas. Sci. Technol. **24** (2013) 035903 (6pp) doi:10.1088/0957-0233/24/3/035903

Reference measurement system for low electrolytic conductivity values with a flowing solution

E Orrù[1], F Durbiano[1] and M Ortolano[1,2]

[1] Divisione Elettromagnetismo, Istituto Nazionale di Ricerca Metrologica (INRIM), Strada delle Cacce 91, I-10135 Torino, Italy
[2] Dipartimento di Elettronica e Telecomunicazioni, Politecnico di Torino, Corso Duca degli Abruzzi 24, I-10129 Torino, Italy

E-mail: e.orru@inrim.it

Received 21 November 2012, in final form 7 January 2013
Published 7 February 2013
Online at stacks.iop.org/MST/24/035903

Abstract
In order to answer the needs of the industrial and the clinical sectors, INRiM has undertaken activities to extend the traceability of electrolytic conductivity measurements to pure water values. In this progress report, the new cell and the measurement system with flowing solution are described. Since international documents prescribe the use of a system with flowing solution to reduce CO_2 contamination for solutions with conductivity lower than 50 μS cm^{-1}, preliminary measurements were carried out on three solutions with conductivity values of 50, 30 and 10 μS cm^{-1}. Moreover, a comparison between a system with static solution and one with flowing solution was executed.

Keywords: electrolytic conductivity, impedance measurements, traceability, aqueous solution

(Some figures may appear in colour only in the online journal)

1. Introduction

Water constitutes the main component of many reagents, buffers and diluents used in clinical laboratory testing. It is used for washing and sanitizing instruments and laboratory glassware, generating autoclave steam etc. Inadequate control of water contamination is an important potential cause of laboratory errors [1]. In quality control, electrolytic conductivity is commonly employed as a measure of water's overall ionic purity. This parameter can be easily determined without expensive equipment and, for this reason, it is of widespread use in pharmaceutical, environmental and microelectronic sectors. However, just like any other measurement, conductivity values can be trusted only if they are traceable to the International System of Units (SI) [2].

The Istituto Nazionale di Ricerca Metrologica (INRiM) has developed and is maintaining a metrological reference for electrolytic conductivity measurements in the range from 50 μS cm^{-1} to 2 S m^{-1} with an associated relative uncertainty better than 0.7% at a temperature of 25 °C. The measurement system has also been verified in several international comparisons [3–5]. The conductivity values obtained with the Jones-type primary cell [6, 7] developed at INRiM are traceable to the SI units because conductivity measurements are based on length and resistance measurements carried out with calibrated instruments.

Recently INRiM, in order to answer the needs of the industrial and the clinical sectors, has undertaken activities to extend the traceability of electrolytic conductivity measurements to pure water values ($\leqslant$10 μS cm^{-1}). The measurement system under development allows traceable measurements of low conductivity values and, at the same time, secondary cell calibrations. In this case, significant difficulties arise from (i) solution contamination by air CO_2 and other contaminants from the glass walls, (ii) temperature variations and (iii) parasitic phenomena which affect resistance measurements.

On the basis of the conductivity values of hydrogen and hydroxide ions and the dissociation constant of water, the theoretical value for the electrolytic conductivity of pure water

(*a*) (*b*) (*c*)

Figure 1. Photograph of the new primary cell developed at INRiM (*a*); details of the centre section (*b*) and of the closure system (*c*).

at 25 °C is 0.055 μS cm^{-1}. Absorption of air CO_2 by water can increase the electrolytic conductivity depending on its level [8, 9]. Typically, CO_2 can reach an equilibrium concentration in water of about 1 mg l^{-1} and add approximately 1 μS cm^{-1} to the conductivity, due to the formation of carbonic acid [10].

In addition, electrolytic conductivity is strongly influenced by temperature. For example, a solution with conductivity greater than 50 μS cm^{-1} has a temperature coefficient of approximately 2%/°C at 25 °C. For pure water, the conductivity temperature coefficient increases to approximately 5%/°C [11].

To deal with the above issues, after the development of a suitable secondary cell [12], a new primary cell was designed and built. In particular, to minimize solution contamination, both from air CO_2 and other contaminants, a glass system with flowing solution and argon buffer gas is under development [10, sections 7.2.1, 10.4].

In this progress report, the new cell design, the circuit set-up for the measurements with flowing solution, the experimental procedure and the uncertainty evaluation for solutions with low conductivity values are described. Moreover, this paper reports the results of a comparison between a system with a static solution and one with a flowing solution, both equipped with the new primary cell.

2. Experimental set-up

2.1. The primary cell

The new primary cell (figure 1(*a*)) for pure-water electrolytic conductivity measurements was designed at INRiM and created by the glass blowers *Disa Raffaele e F.lli*. It is composed of two Pyrex® glass half-cells and a removable hollow cylindrical central section.

Each half-cell contains a smooth round planar platinum electrode (thickness 0.5 mm, diameter 20 mm) [13], which guarantees chemical inertness and minimizes the permeability to impurities [11]. These electrodes, embedded into a glass bar, are removable to allow thorough cleaning. Two platinum wires, spot-welded to the back of the electrodes, connect the electrodes to two coaxial connectors. Each half-cell is equipped with two pipes: a filling pipe with an SVL® cap to avoid solution contamination and a valve pipe to allow solution flow.

The removable central section is made of Pyrex® glass. It has a length $l \approx 10$ mm and an inner hole with a nominal diameter $d \approx 15$ mm (figure 1(*b*)).

This kind of primary cell can be assembled in two different configurations—with or without the removable central section—to allow differential resistance measurements.

The cell constant, C_{cell}, which is a measure of the length to effective area ratio of the central section, depends on l and d. To take into account the inhomogeneity of d along the hole, the central section is considered to be a series of $N = 6$ slices with diameter d_i and the cell constant is estimated with the following equation:

$$C_{\text{cell}} = \frac{4l}{\pi N} \sum_{i=1}^{N} \left(\frac{1}{d_i} \right)^2. \quad (1)$$

The estimated cell constant is

$$C_{\text{cell}} = 55.8703 \text{ m}^{-1} \text{ with } U(C_{\text{cell}})_{(k=2)} = 0.0305 \text{ m}^{-1}. \quad (2)$$

A special quick closure system in Delrin® (polyoxymethylene) homogeneously distributes mechanical stresses around the glass flanges. Moreover, it tightens the glass flanges preventing lateral and rotational movements of the two half-cells (figure 1(*c*)).

The cell was designed with a volume of about 160 ml in order to have a good thermal capacity.

2.2. Experimental apparatus

For the measurement of low electrolytic conductivity values, the new primary cell is included in a Pyrex® glass closed circuit in order to have a flowing solution, as shown in figure 2. The solution flow (50 ml min^{-1}) is ensured by a peristaltic pump (Watson-Marlow Bredel Sci-Q 323).[3] The circuit also contains a secondary cell and an expansion chamber.

The secondary cell developed at INRiM has a fixed geometry. It is made of a single Pyrex® glass chamber, holding two platinum parallel and facing electrodes. In addition, it has two pipelines that allow the solution flow [12]. The geometric constant of this secondary cell was estimated by calibrating it against the primary cell.

The expansion chamber is a Pyrex® glass cylindrical flask equipped with two bottom pipelines, to allow the solution flow,

[3] Brand names are used for the purpose of identification. Such use does not imply endorsement by INRiM or assume that the materials and equipment are the best available.

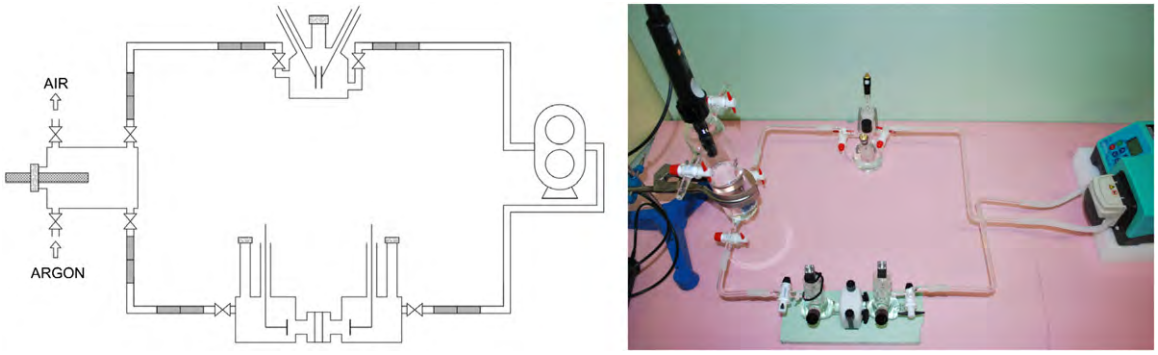

(*a*) (*b*)

Figure 2. Diagram (*a*) and photograph (*b*) of the INRiM circuit.

and two top ones to inject an inert gas. This device is partially filled with the solution to be measured and partially with argon gas to avoid solution contamination with air CO_2 and to damp possible fast rises of the flow pressure. A commercial CO_2 probe (Testo 535) is inserted into the input pipeline of the expansion chamber to monitor the CO_2 concentration in the argon gas during the measurement period.

Silicone joints (Masterflex Biopharm Plus) with a length of about 6 cm are used to connect pipelines and other glass components. All the materials employed were chosen because of their high inertness, so that solution contamination could be kept to a minimum.

To obtain conductivity values at a reference temperature of 25 °C, the circuit is placed into a thermostatic air bath (Branca Ideal Air). A calibrated Pt100 platinum resistance thermometer is placed in contact with the cell wall and connected to a digital multimeter (Agilent Technologies 3458A) to monitor the solution temperature.

An LCR meter (Agilent Technologies E4980A) is employed to perform accurate impedance measurements of the electrolytic solutions. The meter is connected to the electrolytic cell by means of Teflon®-insulated, BNC-terminated coaxial cables (Axon' cable), using a four-terminal configuration with reference planes located at the cell top.

An open/short procedure is periodically applied to the LCR meter to compensate for cable effects. The applied excitation is a sine wave with an rms value of 0.5 V: the use of low voltage values avoids phenomena of ion discharge at the electrode surfaces.

The electrolytic conductivity of sample solutions is investigated in the 20 Hz–2 MHz frequency range.

A switch unit (HP3235) is employed to switch the LCR meter from the primary to the secondary cells. Data acquisition is managed by software developed at INRiM in LabWindows/CVI. Three aqueous solutions with different concentrations of KCl and with nominal conductivity values of 50, 30 and 10 μS cm^{-1} were investigated.

3. Measurement method

Conductivity is determined by a differential resistance measurement. Thus, the measurement is divided into two distinct phases: in the first phase the primary cell is assembled with the central section, while in the second phase it is assembled without the central section.

In each phase, each circuit component is washed several times with ultra-pure water. To check leakage and to clean residual impurities from glass surfaces and interstices, the cell is filled with ultra-pure water and left to rest for at least 1 h. When water conductivity is lower than 1 μS cm^{-1} (estimated with a commercial conductivity meter, WTW InoLab TetraCon 325), the cell is considered clean and ready to be primed. The same washing procedure is applied to other circuit components. The whole circuit is assembled within the thermostatic air bath and, finally, it is filled with the solution sample and the expansion chamber is loaded with argon gas.

Impedance measurements are carried out overnight to achieve the best temperature stability and the total measurement time is about 15 h.

The impedance of a generic electrolytic cell is characterized by a medium-frequency region where the resistance, i.e. the real part of the impedance, is approximately constant. At low frequencies, the resistance increases because of the double layer, while at high frequencies the resistance decreases because of capacitive effects. The centre of the constant-resistance region is located at a frequency f^*, where the modulus of the reactance, i.e. the imaginary part of the impedance, has a minimum (figure 4).

The conductivity k of the aqueous solution contained in the primary cell is estimated by the following equation:

$$k = \frac{C_{\mathrm{cell}}}{\overline{R}_{\mathrm{W}} - \overline{R}_{\mathrm{N}}} + \delta k_{\mathrm{W}} + \delta k_{\mathrm{IN}}, \tag{3}$$

where:

(1) $\overline{R}_{\mathrm{W}}$ is the average of n resistance measurements $R^{\mathrm{C}}_{\mathrm{W},j}$ ($j = 1, \ldots, n$) carried out on the cell with the central section and corrected for the temperature difference $T_{\mathrm{W},j} - T_{\mathrm{ref}}$, where $T_{\mathrm{W},j}$ is the air bath temperature during the jth measurement. The correction is given by

$$R^{\mathrm{C}}_{\mathrm{W},j} = R_{\mathrm{W},j}[1 + \alpha_T (T_{\mathrm{W},j} - T_{\mathrm{ref}})], \tag{4}$$

where α_T is the temperature coefficient of the solution conductivity [11].

(2) $\overline{R}_{\mathrm{N}}$ is the average of n resistance measurements $R^{\mathrm{C}}_{\mathrm{N},j}$ ($j = 1, \ldots, n$) carried out on the cell without the central section and corrected for the temperature difference $T_{\mathrm{N},j} - T_{\mathrm{ref}}$,

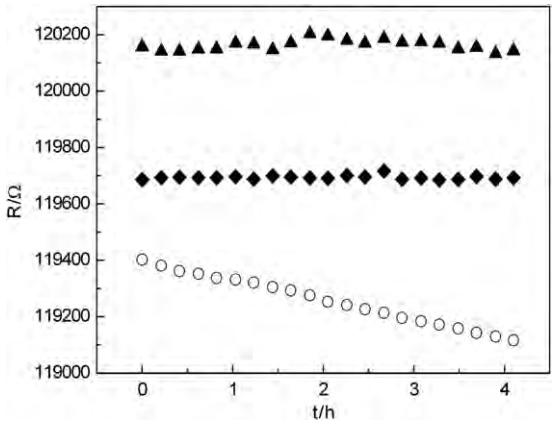

Figure 3. 30 μS cm^{-1} solution, primary cell without central section, drift of resistance measurements with (i) static solution (circles); (ii) flowing solution without argon buffer gas (diamonds) and (iii) flowing solution with argon buffer gas (triangles).

where $T_{\mathrm{N},j}$ is the air bath temperature during the jth measurement. The correction is given by

$$R^{\mathrm{C}}_{\mathrm{N},j} = R_{\mathrm{N},j}[1 + \alpha_T (T_{\mathrm{N},j} - T_{\mathrm{ref}})]. \quad (5)$$

(3) δk_{W} and δk_{N} are additional terms taking into account the resistance drift due to solution contamination (see section 4).

In this work, for each solution, $n = 3$.

4. Results

4.1. Stability measurements with a 30 μS cm^{-1} solution

Preliminary measurements on a 30 μS cm^{-1} solution were carried out to compare the stability of a system with flowing solution against that of one with static solution. The results are in agreement with the indication reported in [10, 11], which prescribe, for solutions with conductivity lower than 50 μS cm^{-1}, the use of a system with flowing solution to reduce CO_2 contamination. Figure 3 shows the results of (i) a measurement with the system containing a static solution (circles); (ii) a measurement with flowing solution without argon buffer gas (diamonds) and (iii) a measurement with flowing solution and argon buffer gas injected into the expansion chamber (triangles). Each curve represents a time-series of resistance values measured at f^*.

From figure 3, it is clear that without flowing solution the resistivity drifts significantly (drift coefficient $\approx -1.4\times10^{-4}$), whereas with flowing solution the stability of the resistivity is much higher (drift coefficient $\approx -2.0 \times 10^{-7}$). Argon gas was also used with flowing solution to try to further reduce contamination from air CO_2: in this case, however, figure 3 does not show any significant improvement with respect to the measurement carried out without argon gas. Probably, at lower conductivity values, where CO_2 contamination is relatively higher, argon gas might help to reduce such contamination. A more complete stability analysis will be the object of a future work oriented towards ultra-pure water conductivity measurements.

According to these preliminary stability results, the measurements described below were taken with flowing solution and argon gas.

4.2. Conductivity measurement of a 50 μS cm^{-1} solution

Figure 4 shows an example of three impedance measurements on a 50 μS cm^{-1} solution carried out on the cell without the central section. The minimum value of the reactance can be identified at a frequency $f^* = 424$ Hz.

In the treatment of the measurement uncertainty, the relevant international documents [14, 15] were followed. In the measurement model (3), all quantities were considered uncorrelated. The uncertainty budget for the solution with a nominal conductivity of 50 μS cm^{-1} is reported in table 1. Remarks are as follows.

(1) The uncertainties $u(\overline{R}_W)$ and $u(\overline{R}_N)$ are obtained by considering the following contributions: (i) LCR meter calibration against a 100 kΩ Tinsley standard ac resistor, (ii) LCR meter resolution, (iii) temperature correction and (iv) the type A uncertainty resulting from repeatability.
(2) $u(\delta k_{\mathrm{W}})$ and $u(\delta k_{\mathrm{N}})$ are estimated from the conductivity drift of representative measurements taken respectively

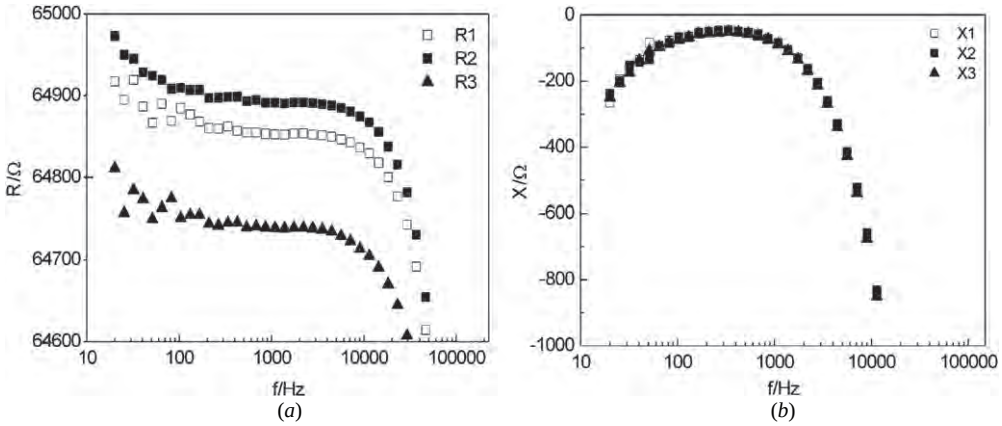

Figure 4. Example of raw impedance measurements carried out on the cell without the central section: (*a*) real component (resistance) and (*b*) imaginary component (reactance).

Table 1. Uncertainty budget for nominal conductivity of 50 μS cm^{-1} solution at 25 °C.

Uncertainty source X_i	Estimate x_i	Assumed distribution/ type A, B	Standard uncertainty $u(x_i)$	Sensitivity coefficient c_i	Contribution to standard uncertainty (S m^{-1}) $u_i(y)$
C_{cell}	55.870 m^{-1}	Norm./B	1.53×10^{-2} m^{-1}	9.58×10^{-5} S	1.46×10^{-6}
$\overline{R}_W$	75144.40 Ω	Norm./A	13.96 Ω	-5.13×10^{-7} S^2 m^{-1}	7.16×10^{-6}
$\overline{R}_N$	647 05.60 Ω	Norm./A	11.09 Ω	5.13×10^{-7} S^2 m^{-1}	5.69×10^{-6}
δk_{W}	0 S m^{-1}	Rect./B	5.20×10^{-7} S m^{-1}	1	5.20×10^{-7}
δk_{N}	0 S m^{-1}	Rect./B	4.04×10^{-7} S m^{-1}	1	4.04×10^{-7}

with and without the cell central section over a period of 10 h at f^*.

The estimated conductivity value is 53.50 μS cm^{-1}; the combined standard uncertainty is 9.3×10^{-2} μS cm^{-1} and the expanded uncertainty with $k = 2$ is 0.19 μS cm^{-1}.

The repeatability of the set-up with flowing solution and inert gas was compared with that under static conditions without inert gas. The new set-up achieved a repeatability of about 20 Ω which compares favourably with the 52 Ω achieved by the static set-up.

4.3. Conductivity measurement of a 10 μS cm^{-1} solution

With the 10 μS cm^{-1} solution the resistance values at $f^* =$ 81.9Hz were identified as corresponding to the minimum of the impedance imaginary component. The estimated α_T is 3%/°C with an uncertainty of 10% [10].

Uncertainty contributions and calculation procedure for this solution were the same as in the 50 μS cm^{-1} case. The obtained conductivity value is 12.15 μS cm^{-1}; the combined standard uncertainty is 1.1×10^{-1} μS cm^{-1} the expanded uncertainty with $k = 2$ is 0.22 μS cm^{-1}.

5. Conclusion

The new primary cell for very low electrolytic conductivity measurements was designed and tested at INRiM. Compared to the previous one, this new cell has the following characteristics: (i) a central section with lower cell constant suitable for measuring diluted solutions; (ii) pipelines added laterally to half-cells to allow the solution flow; (iii) removable electrodes for thorough cleaning and (iv) a quick closure system to shorten assembly time and to obtain a repeatable cell alignment.

Moreover, a measurement system with flowing solution was developed to reduce CO_2 contamination at low conductivity values. In this system, a secondary cell can be inserted in series with the primary one for in-line calibration. This system could be considered for the measurement of other types of low-conductivity solutions with some caution: for instance, the compatibility between the solution and the silicone joints should be verified.

The old system with static solution and the new one were compared with solutions with conductivity values of 30 and 50 μS cm^{-1}. The new system showed reduced drift and better repeatability.

The characterization of a 50 μS cm^{-1} solution yielded an expanded uncertainty of 0.19 μS cm^{-1}. This uncertainty is better than that obtained with a static solution, because the flowing solution improved the measurement repeatability. The characterization of a 10 μS cm^{-1} solution yielded an expanded uncertainty of 0.21 μS cm^{-1} (2.1%).

Future work will be mainly devoted to (i) build a new central section with a more accurate cylindrical hole, with the aim of improving the corresponding uncertainty contribution; (ii) substitute the peristaltic pump with a magnetic one, with the aim of improving flow stability; (iii) reduce the number of silicone joints used to connect the glass pipes and the cells, with the aim of reducing solution contamination and (iv) improve argon monitoring to prevent gas leakage in the system.

The final aim is to obtain a system for conductivity measurements of ultra-pure water with a target uncertainty lower than 1%.

Acknowledgments

The authors are grateful to the INRiM Mechanics Division for the dimensional characterization of the cell central section.

References

[1] Miller W G, Gibbs E L, Jay D W, Pratt K W, Vojt C M and Whitehead P 2006 *Preparation and Testing of Reagent Water in the Clinical Laboratory (CLSI Approved Guideline* vol 26*)* 4th edn (Wayne, PA: Clinical and Laboratory Standards Institute) C3-A4

[2] Spitzer P, Rossi B, Gaignet Y, Mabic S and Sudmeier U 2005 New approach to calibrating conductivity meters in the low conductivity range *Accredit. Qual. Assur.* **10** 78–81

[3] Durbiano F and Orrù E 2011 Key comparison CCQM-K92: electrolytic conductivity at 0.05 S/m *INRiM Measurement Report RT22/2011* (Turin: INRiM)

[4] Jensen H D 2010 *Final report on CCQM-K36* (Bureau International des Poids et Measures) http://kcdb.bipm.org/AppendixB/appbresults/ccqm-k36/ccqm-k36_final_report.pdf
Durbiano F, Callegaro L, Capra P P and D'Elia V 2005 Key comparison CCQM-K36: electrolytic conductivity at 0.5 and 0.005 S/m, IEN Measurement Report *IEN Technical Report* (Turin: INRiM) n 694

[5] Durbiano F, Ferrara E, Marullo Reedtz G and Capra P P 2001 Pilot study CCQM-P22 on electrolytic conductivity IEN Measurement Report *Rapporto Tecnico IEN* (Turin: INRiM) no. 629

[6] Wu Y C, Pratt K W and Koch W F 1989 Determination of the absolute specific conductance of primary standard KCl solutions *J. Solut. Chem.* **18** 515–28

[7] Wu Y C and Koch W F 1991 Absolute determination of electrolytic conductivity for primary standard KCl solutions from 0 to 50 °C *J. Solut. Chem.* **20** 391–401

[8] Wu Y C and Berezansky P A 1995 Low electrolytic conductivity standards *J. Res. Natl Inst. Stand. Technol.* **100** 521–7
[9] Light T S 1984 Temperature dependence and measurement of resistivity of pure water *Anal. Chem.* **56** 1138–42
[10] ASTM Designation 2009 Standard test method for electrical conductivity and resistivity of a flowing high purity water sample *ASTM D* pp 5391–9
[11] ASTM Designation 2009 Standard test method for electrical conductivity and resistivity of water *ASTM D* pp 1125–95
[12] Boveri C, Durbiano F and Serazio D 2009 Development of a flow-through cell for accurate measurements of low electrolytic conductivity *Proc. 19th IMEKO World Congress Fundamental and Applied Metrology (Portugal, 6–11 Sept.)* 2619–23
[13] Becchi S M, Callegaro L, Durbiano F, D'Elia V and Strigazzi A 2007 Novel impedance cell for low conductive liquids: determination of bulk- and interface contributions *Rev. Sci. Instrum.* **78** 113902
[14] European Co-operation for Accreditation 1999 Expression of the uncertainty of measurement in calibration *Publication EA 4/02*
[15] JCGM 2008 *Evaluation of Measurement Data—Guide to the Expression of Uncertainty in Measurement* JCGM 100:2008 1st edn

An Impedance Spectrometer for the Metrology of Electrolytic Conductivity

Luca Callegaro, Francesca Durbiano, Elena Orrù, and Bruno Trinchera

***Abstract*—Conductivity measurements of liquids ask for measurements of impedance spectra in a wide frequency range to identify stray parameters caused by electrode-surface effects. On low-conductivity liquids, such as ultrapure water, frequencies of interest range below those available on precision LCR meter (usually in the 10-Hz range). A new impedance spectrometer based on multifrequency excitation and discrete Fourier transform analysis is presented here. The spectrometer defines the impedance under measurement as a two-port standard and measures impedance spectra covering 5 dec, reaching frequencies in the millihertz range. The instrument accuracy is verified by measurements on calibrated resistance standards. As an example of application, measurement results on pure-water samples and a comparison with measurements performed with an LCR meter are reported.**

***Index Terms*—Analog–digital conversion (ADC), conductivity measurement, electrochemical impedance spectroscopy, impedance measurement, measurement techniques, precision measurements.**

I. Introduction

THE measurement of electrolytic conductivity is applicable for such purpose as impurity or trace detection and the quantitative measurement of ionic constituents dissolved in water. It is the primary means of monitoring the performance of demineralization and other high-purity water treatment operations. It is also used to detect ionic contamination in boiler water, microelectronics rinse waters, pharmaceutical process waters, etc. [1], [2]. Metrology-grade experiments are typically performed in two-electrode cells. Conductivity $\chi(\omega)$ is related with resistance R_b and reactance X_b of the solution bulk by the following relation:

$$\chi = C\frac{R_b}{R_b^2 + X_b^2} \tag{1}$$

where C is the *cell constant*, known by calibration or by calculations from geometrical measurements [3]. For liquids and ionic solutions having low molecular weight, $\chi(\omega)$ can be considered constant up to gigahertz frequency.

Neglecting radiative effects, the measured impedance, i.e.,

$$Z(\omega) = R(\omega) + jX(\omega) = Z_b + Z_e \tag{2}$$

is the sum of the bulk impedance $Z_b(\omega) = R_b(\omega) + jX_b(\omega)$ and the electrode–solution interface $Z_e(\omega)$. It is therefore necessary to identify Z_b.

The behavior of $Z_e(\omega)$ is dependent on the liquid under study and on the electrode composition and surface structure. In particular, the double layer occurring at the electrode–liquid interface gives impedance increasing for lower frequencies. With proper modeling of Z_e [4]–[8], it can be shown that $R_b = R(\omega^*)$ at the particular frequency ω^* for which $X(\omega^*) = 0$ (or, more precisely, a minimum of $|X(\omega)|$) occurs.

The particular ω^* value is dependent on the sample and on the measurement cell, and has to be experimentally identified. Hence, measurements of $Z(\omega)$ over a wide frequency bandwidth are needed. Typically, commercial LCR bridges are the impedance meters employed for the measurement, programmed to perform repeated frequency sweeps. A useful graphical representation to find ω^* is the Cole–Cole (or Nyquist) $R(\omega) - X(\omega)$ graph.

The challenge of low-conductive liquid measurements is that ω^* can lie much below the working frequency range of LCR meters (typically in the 10-Hz range). A dedicated impedance meter capable of extending the measurement bandwidth below hertz is necessary. Commercial instruments (impedance analyzers and dynamic potentiostats) devoted to electrochemical impedance spectroscopy, capable of reaching the millihertz or even microhertz range, are available on the market; however, they usually have a relative uncertainty in the 10^{-3} range. Moreover, being "closed" instruments, the metrological traceability of their measurements can be difficult to assess.

The impedance spectrometer proposed here is based on a commercial analog–digital conversion (ADC)/digital–analog conversion (DAC) board,[1] a simple custom-made analog frontend amplifier, and acquisition and processing software. An earlier version of the spectrometer has been presented in [9]; this paper gives a detailed description of the new instrument version (where excitation capabilities and corresponding data processing have been extended) and includes new measurements.

II. Measurement Setup

A block schematic of the spectrometer is shown in Fig. 1.

The measurement cell [10] is shown in Fig. 2. The cell has constant $C \approx 15\ \mathrm{m}^{-1}$, calibrated by comparison with a primary system [11]. Electrically, the cell is a two-terminal impedance, connected with coaxial leads, as shown in Fig. 1.

Manuscript received June 20, 2012; revised September 10, 2012; accepted September 18, 2012. Date of publication January 15, 2013; date of current version May 8, 2013. The Associate Editor coordinating the review process for this paper was Dr. Lucas Di Lillo.

L. Callegaro, F. Durbiano, and B. Trinchera are with the Electromagnetism Division of the Istituto Nazionale di Ricerca Metrologica (INRIM), 10135 Torino, Italy (e-mail: l.callegaro@inrim.it).

E. Orrù is with the Istituto Nazionale di Ricerca Metrologica (INRIM), 10135 Torino, Italy, and also with the Politecnico di Torino, 10129 Torino, Italy.

Digital Object Identifier 10.1109/TIM.2012.2230731

[1]National Instruments mod. PXI-4461, including two simultaneously sampled ADCs and two DACs; 24-bit resolution and 204.8-kS/s maximum sampling rate.

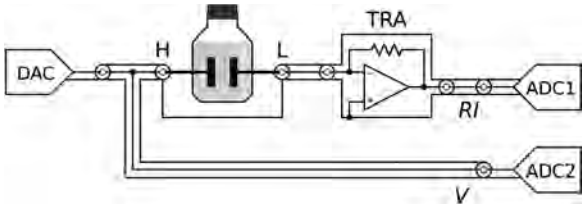

Fig. 1. Simplified schematics of the spectrometer. ADC1, ADC2, and DAC are the ADCs and the DAC belonging to the acquisition board. DAC energizes the conductivity cell with voltage V at port H; V is measured by ADC2. Current I at port L is converted to voltage RI by TRA, a transresistance amplifier having gain R. RI is measured by ADC1.

Fig. 2. Secondary cell employed for the measurements. The enclosure is in Pyrex glass, with a capacity of 150 ml; two circular parallel-plate Pt electrodes are supported by Pt wires that go through glass seals and permit electrical connection. The cell is provided with pipes for flowthrough measurements.

To measure ultrapure water by avoiding contamination by air CO_2 and other contaminants, an in-flow setup becomes necessary. The setup is shown in Fig. 3.

III. Data Acquisition and Processing

The DAC is energized with a sampled frequency comb of sine waves, i.e.,

$$s[j] = A \sum_{h \in \mathcal{H}} \cos\left(2\pi\, h \frac{j}{n} + \phi_h\right) \qquad j = 0, \ldots, 2^n. \quad (3)$$

Each sine wave of the comb is an harmonic of index h, belonging to the harmonic set $\mathcal{H} \subset \{1 \ldots 2^{n-2}\}$ of a fundamental having a period of 2^n samples. At sampling frequency f_S, harmonic h has frequency $f_h = (h/2^n) f_S$. All harmonics have the same peak amplitude A and a random phase ϕ_h; if

Fig. 3. In-flow setup for the measurement of ultrapure water. The production unit employed (Millipore mod. RiOs-Di and Milli-Q academic) is connected with Pyrex pipelines to the measurement cell in Fig. 2. Water outlet is collected in a beaker for temperature measurement.

$\mathcal{H}$ is sufficiently large, set $s[k]$ approximately has a normal distribution [12]. A is chosen to achieve the desired root-mean-square value of s, i.e.,

$$s_{\mathrm{RMS}} = \left(2^{-n} \sum_j s^2[j]\right)^{\frac{1}{2}}. \quad (4)$$

The signal described has been first proposed by Creason *et al.* (see [13] and references therein). Other energizing functions, such as the linear or log chirp [13]–[16], can be made available by software extensions.

Samples $v_1[j]$ and $v_2[j]$, $j = 1 \ldots 2^n$, are acquired at the sampling frequency f_S and processed with discrete Fourier transform (DFT) to obtain amplitude spectra $V_1[k]$ and $V_2[k]$, where $k = 0 \ldots 2^{n-2}$ and $f_k = k(f_S/2^n)$. Impedance $Z(f)$ can be estimated [17], [18] at all frequencies f_h with the DFT ratio, i.e.,

$$Z(f_h) = R(f_h) \frac{V_2[h]}{V_1[h]} \quad (5)$$

where $R(f_h)$ is the gain of the transresistance amplifier (see Fig. 1) at frequency f_h. Equation (5) can be rewritten in terms of the auto and cross power spectral densities P_1 and C_{12} (of v_1 and between v_1 and v_2, respectively) for which functions that

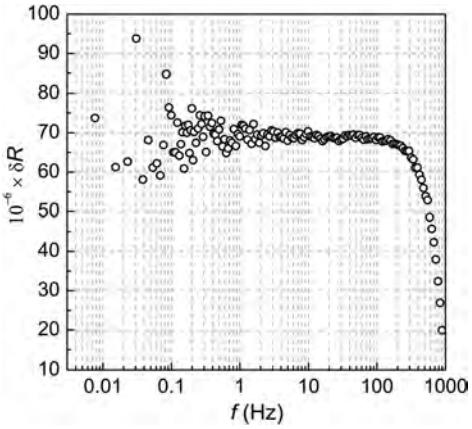

Fig. 4. Deviation of the spectrometer resistance readings from the calibrated impedance value of a 100-kΩ resistor (ESI mod. SR1-100 kΩ, with adapters for two-port measurements).

are more convenient than the bare fast Fourier transform may be available in the programming environment,[2] i.e.,

$$Z(f_h) = R(f_h)\frac{C_{12}[h]}{P_1[h]}. \tag{6}$$

The choice of set $\mathcal{H}$ is arbitrary; for a given s_{RMS} value, its numerosity $n_{\mathcal{H}}$ influences the signal-to-noise ratio (SNR) of readings $Z(f_h)$. As a rule of thumb, the SNR is proportional to $(n_{\mathcal{H}})^{-1}$. A method for the optimal choice of set $\mathcal{H}$ has been published [19]. Presently, the software allows selecting between two possible combs:

1) Linear comb: $\mathcal{H} = 1 \ldots 2^{n-2}$; all possible harmonics [20] are present in s.
2) Log comb: $\mathcal{H}$ includes approximately the same number of harmonics per frequency octave.

Typical sampling parameters are $n = 18$, $f_S = 2$ kHz. The resulting minimum frequency (and frequency spacing between harmonics) is ≈7.63 mHz; for a linear comb $n_{\mathcal{H}} = 2^{16} \approx 6 \times 10^4$ frequencies, a log comb with ten frequencies per octave results in $n_{\mathcal{H}} = 153$.

IV. Measurements

A. Resistance standard

A first test of the spectrometer has been conducted on a calibrated resistor having nominal value of 100 kΩ. Fig. 4 shows the deviation of the spectrometer readings with respect to the calibrated resistor value, when a nominal gain value of $R(f) = 100$ kΩ is employed in (5). The measurement outcome can be employed as an input of adjustment procedures of the spectrometer [22] (see also Section VI).

B. Pure Water Contaminated With CO_2

The investigated sample is ultrapure water contaminated by exposure to atmospheric CO_2, whose dissociation increases conductivity (to a maximum of about 1 μS · cm^{-1}). The measurements are performed at 25 °C in a thermostated environment.

[2]As occurs with our choice of programming language, National Instruments LabWindows/CVI, where `autopowerspectrum()` and `crosspowerspectrum()` are native functions.

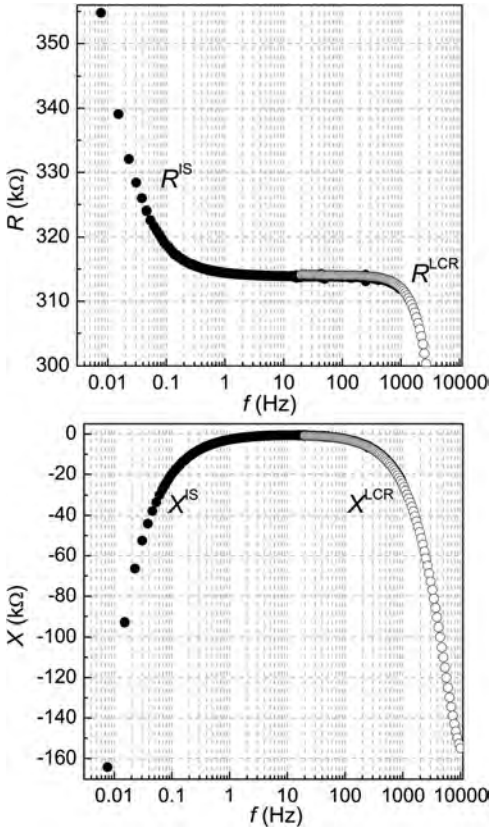

Fig. 5. Comparison of impedance measurements performed with the impedance spectrometer (IS) and the LCR meter (LCR). Top: Series resistance $(R^{\mathrm{IS}}, R^{LCR})$ measurement versus frequency f. Bottom: Series reactance $(X^{\mathrm{IS}}, X^{LCR})$.

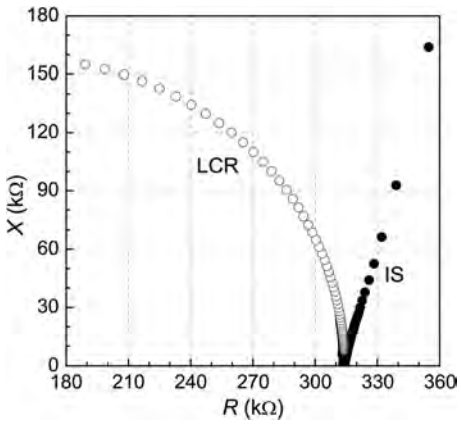

Fig. 6. Same data in Fig. 5, here shown as an $R, -X$ Nyquist diagram. Only the measurements conducted with the impedance spectrometer (IS), at variance with those of the LCR meter, allow the observation of data at frequency ω^* (corresponding to $X(\omega^*) = 0$) and the effect of the electrode impedance Z_e, which gives the straight line on the right-hand side of the graph.

Results of impedance measurements with spectrometer $Z^{\mathrm{IS}} = R^{\mathrm{IS}} + jX^{\mathrm{IS}}$ and with a commercial LCR meter[3] $Z^{LCR} = R^{LCR} + jX^{LCR}$ are reported in Figs. 5 and 6. For this sample, $\omega^* \approx 10$ Hz cannot be reached by the particular meter employed.

The maximum relative difference $\delta = |Z^{\mathrm{IS}} - Z^{LCR}|/|Z^{LCR}|$ in the superposition frequency range (20 Hz–1 kHz) is 0.2%.

[3]Agilent Tech. mod. 4284A; frequency range: 20 Hz–1 MHz.

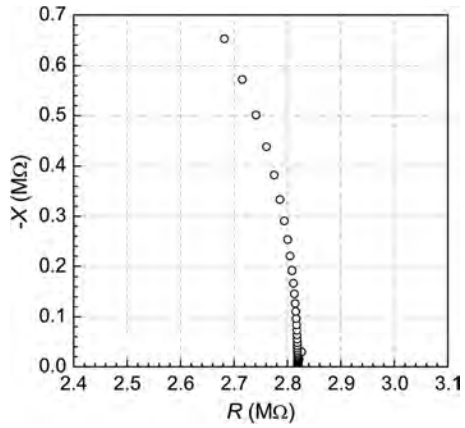

Fig. 7. $R, -X$ Nyquist diagram of measurement performed on in-flow pure water.

TABLE I
PRELIMINARY UNCERTAINTY BUDGET FOR THE MEASUREMENT OF RESISTIVE $Z = 100\,\mathrm{k\Omega}$ IMPEDANCE. $s_{\mathrm{RMS}} = 0.5$ V, SAMPLING PARAMETERS AS IN SECTION III, LOG COMB, AND ONE SINGLE ACQUISITION

Uncertainty source	$f = 10\,\mathrm{mHz}$ $u_{\mathrm{R}} \times 10^6$	$f = 100\,\mathrm{Hz}$ $u_{\mathrm{R}} \times 10^6$
TRA gain error[a]	60	70
TRA & ADC intermod. distortion[b]	30	30
ADC channel mismatch[c]	100	100
ADC channel separation[d]	1	1
Noise	50	5
Combined uncertainty	130	126

a Deviation from nominal due to feedback resistor tolerance and open-loop finite gain.
b Evaluated from specifications for large signals.
c From direct measurement.
d From specifications.

C. Pure Water, in-Flow

First measurements on ultrapure water not contaminated by exposure to air have been conducted with the system shown in Fig. 3. A theoretical conductivity of 0.055 $\mu\mathrm{S} \cdot \mathrm{cm}^{-1}$ at 25 °C is expected [23], [24]. Results of the measurements are shown in Fig. 7.

The estimated conductivity value is 0.053 $\mu\mathrm{S} \cdot \mathrm{cm}^{-1}$ at 21 °C, compatible with the absence of contamination. For this sample, $\omega^* \approx 1$ Hz, which is well beyond the inferior frequency limit of the LCR meter.

V. UNCERTAINTY

A detailed expression of measurement uncertainty will be a matter of future work; it will involve an analysis under *GUM Supplement 2* [25] and will be cumbersome because of the presence of DFT calculations in the measurement model. An estimate for $Z = 100\,\mathrm{k\Omega}$ resistive is shown in Table I.

The measurement accuracy can be substantially improved by the calibration of the spectrometer components, particularly the transresistance amplifier gain $R(f)$ and the ADC mismatch, and by adjusting the corresponding numerical constants in the software. An alternative route for accuracy improvement is to implement adjustment methods (improperly called *calibrations*) typical of LCR meters and network analyzers, such as short–open–load calibration [22]. Effects of intermodulation distortion in the measurement components or due to the electrochemical cell behavior can be substantially mitigated with careful choices of set H (see, e.g., [26]).

Measurement model (5) assumes the steady state under the periodic excitation $s[j]$. The condition can be violated by reactive devices under test with long time constants (as actually occurs in measurements in Sections IV-B and IV-C), and measurement errors can result from the effect of slow transients in the measurement current. Such errors can be mitigated by activating the excitation signal in advance respect to the actual measurement time, as soon as the experiment permits it (e.g., for the measurements in Section IV-B, during the thermostatization settling time).

VI. CONCLUSION

This paper has described a new impedance spectrometer, based on multifrequency excitation and DFT analysis. The spectrometer allows performing measurements of impedance spectra in a bandwidth extending down to the millihertz range. Tests of the impedance spectrometer have been performed with measurements on a calibrated resistance standard, on a sample of pure water contaminated by atmospheric CO_2, and on in-flow pure water.

The accuracy of the spectrometer has been confirmed by comparison with the resistance standard calibrated value and with LCR meter measurements for pure water equilibrated with air.

REFERENCES

[1] *Standard Test Method for Electrical Conductivity and Resistivity of a Flowing High Purity Water Sample*, ASTM Std. D5391-99, 2009.
[2] S. Xiaoping, P. Spitzer, and U. Sudmeier, "Novel method for bulk resistance evaluation in conductivity measurement for high-purity water," *Accredit. Qual. Assur.*, vol. 12, no. 7, pp. 351–355, Jul. 2007.
[3] *Calibration Method for Conductivity Cells*, OIML Std. R 68, 1985.
[4] E. Warburg, "Über das verhalten sogenannter unpolarisirbarer elektroden gegen wechselstrom," *Ann. Phys.*, vol. 303, no. 3, pp. 493–499, 1899.
[5] K. S. Cole and R. H. Cole, "Dispersion and absorption in dielectrics. I. Alternating current characteristics," *J. Chem. Phys.*, vol. 9, no. 4, pp. 341–351, Apr. 1941.
[6] K. S. Cole and R. H. Cole, "Dispersion and absorption in dielectrics. II. Direct current characteristics," *J. Chem. Phys.*, vol. 10, no. 2, pp. 98–105, Feb. 1942.
[7] J. E. Randles, "Kinetics of rapid electrode reactions," *Discuss. Faraday Soc.*, vol. 1, pp. 11–19, 1947.
[8] T. Pajkossy and D. M. Kolb, "Double layer capacitance of the platinum group metals in the double layer region," *Electrochem. Commun.*, vol. 9, no. 5, pp. 1171–1174, May 2007.
[9] L. Callegaro, F. Durbiano, E. Orrù, and B. Trinchera, "An impedance spectrometer for the metrology of electrolytic conductivity," in *Proc. CPEM*, Washington, DC, Jul. 1–6, 2012, pp. 714–715.
[10] C. Boveri, F. Durbiano, and D. Serazio, "Development of a flow-through cell for accurate measurements of low electrolytic conductivity," in *Proc. 19th IMEKO World Congr.*, Lisbon, Portugal, Sep. 6–11, 2009.
[11] F. Durbiano, "Taratura di conduttivimetri per confronto," IEN, Torino, Italy, Tech. Rep. 671, Jan 2004.
[12] D. R. White and S. P. Benz, "Constraints on a synthetic noise source for Johnson noise thermometry," *Metrologia*, vol. 45, no. 1, pp. 93–101, Feb. 2008.
[13] B. Sanchez, G. Vandersteen, R. Bragos, and J. Schoukens, "Basics of broadband impedance spectroscopy measurements using periodic excitations," *Meas. Sci. Technol.*, vol. 23, no. 10, p. 105 501, Oct. 2012.
[14] G. S. Popkirov and R. N. Schindler, "A new impedance spectrometer for the investigation of electrochemical systems," *Rev. Sci. Instrum.*, vol. 63, no. 11, pp. 5366–5372, Nov. 1992.

[15] K. Darowicki and P. Slepski, "Determination of electrode impedance by means of exponential chirp signal," *Electrochem. Commun.*, vol. 6, no. 9, pp. 898–902, Sep. 2004.
[16] M. Min, R. Land, T. Paavle, T. Parve, P. Annus, and D. Trebbels, "Broadband spectroscopy of dynamic impedances with short chirp pulses," *Physiol. Meas.*, vol. 32, no. 7, pp. 945–958, Jul. 2011.
[17] C. L. Heizman, "Signal analysis with digital time-series analyzers," *Gen. Radio Exp.*, vol. 44, no. 7–9, pp. 3–7, Jul.–Sep. 1970.
[18] E. A. Sloane, "Measurement of transfer function and impedance," *Gen. Radio Exp.*, vol. 44, no. 7–9, pp. 8–13, Jul.–Sep. 1970.
[19] B. Sanchez, C. R. Rojas, G. Vandersteen, R. Bragos, and J. Schoukens, "On the calculation of the D-optimal multisine excitation power spectrum for broadband impedance spectroscopy measurements," *Meas. Sci. Technol.*, vol. 23, no. 8, p. 085702, 2012.
[20] H. Herlufsen, "Dual-channel FFT analysis (Part I)," *Brüel Kjær Tech. Rev.*, no. 1/2, pp. 3–56, 1984.
[21] H. Herlufsen, "Dual-channel FFT analysis (Part II)," *Brüel Kjær Tech. Rev.*, no. 1/2, pp. 3–45, 1984.
[22] *Effective Impedance Measurement Using OPEN/SHORT/LOAD Correction*, Agilent Technol., Santa Clara, CA, 1998, Appl. Note 346-3.
[23] T. S. Light and S. L. Licht, "Conductivity and resistivity of water from the melting to critical point," *Anal. Chem.*, vol. 59, no. 19, pp. 2327–2330, Oct. 1987.
[24] T. S. Light, S. Licht, A. C. Bevilacqua, and K. R. Morash, "The fundamental conductivity and resistivity of water," *Electrochem. Solid State Lett.*, vol. 8, no. 1, pp. E16–E19, 2005.
[25] *Evaluation of measurement data—Supplement 2 to the "Guide to the expression of uncertainty in measurement"—Extension to any number of output quantities*, BIPM, Sèvres, France, 2011, JCGM 102:2011.
[26] J. Házì, D. M. Elton, W. A. Czerwinski, J. G. Schiewe, V. A. Vicente-Beckett, and A. M. Bond, "Microcomputer-based instrumentation for multi-frequency Fourier transform alternating current (admittance and impedance) voltammetry," *J. Electroanal. Chem.*, vol. 437, no. 1/2, pp. 1–15, Nov. 1997.

Luca Callegaro (1967) received the M.S. degree in electronic engineering and the Ph.D. degree in physics from the Politecnico di Milano, Milano, Italy, in 1992 and 1996, respectively.

Since 1996, he has been with the Istituto Nazionale di Ricerca Metrologica (INRIM: formerly Istituto Elettrotecnico Nazionale, IEN), Torino, Italy. From 1998 to 2005, he was a member of the Scientific Council of IEN. He was an Adjunct Professor of electronic measurements with the Politecnico di Torino, Torino. He is responsible of research activity on electrical impedance with the INRIM and of the Italian National standards of electrical capacitance, inductance, ac resistance, and ac voltage ratio. He is the Italian contact person of the European Association of National Metrology Institutes Technical Committee for Electricity and Magnetism and is a Member of its Working Group on Strategic Planning. He is the Italian Deputy Officer for the Commission A of Union Radio Scientifique Internationale. He has authored about 70 papers on international reviews and of the book *Electrical impedance: principles, measurement and applications*, Taylor & Francis, 2012.

Francesca Durbiano was born in Torino, Italy, in 1969. She received the M.S. degree in chemistry from the University of Torino, Torino, in 1996 and the Ph.D. degree in metrology from the Politecnico di Torino, Torino, in 2004.

She was with the Istituto di Metrologia "G. Colonnetti." Since 1996, she has been with the Istituto Nazionale di Ricerca Metrologica (INRIM), Torino, working on gas dynamic mixtures. She is engaged in electrochemical measurements and responsible for the national standard of electrolytic conductivity of aqueous solutions. She is a convenor of the Electrochemistry Subcommittee of the Technical Committee Metrology in Chemistry of the European Association of National Metrology Institutes and the contact person for the INRIM of the Electrochemical Analysis Working Group of the Consultative Committee for Amount of Substance.

Elena Orrù was born in Torino, Italy, in 1981. She received the M.S. degree in industrial chemistry from the University of Torino, Torino, in 2008. She is currently working toward the Ph.D. degree in metrology at the Istituto Nazionale di Ricerca Metrologica (INRIM), Torino, with the research program "Traceability of the electrolytic conductivity measurements for ultrapure water."

Ms. Orrù was a recipient of a scholarship for training in research financed by Fondazione Cassa di Risparmio di Torino in 2008.

Bruno Trinchera was born in 1973. He received the M.S. degree in physics from the University of Torino, Torino, Italy, in 2001 and the Ph.D. degree in metrology from the Politecnico di Torino, Torino, in 2007. The research toward the Ph.D. degree was conducted in the Istituto di Metrologia "Gustavo Colonnetti" [now merged with the Istituto Nazionale di Ricerca Metrologica (INRIM)] on precision radiation thermometry at low temperatures.

Since 2005, he has been with the Electromagnetic Department, INRIM, where he currently works on high-accuracy impedance comparison systems based on digital signal synthesis and on the modeling, characterization, and design of specific wideband mixed-signal embedded systems for electric power metrology and precise alternating-current–direct-current transfer measurements.

Bibliography

[1] C. H. Hamann, A. Hamnett, and W. Vielstich. *Electrochemistry Second, Completely Revised and Updated Edition*. Wiley - VCH Verlag GmbH & Co. KGaA, Weinheim, 2007.

[2] E. Bava, M. Kühne, and A. M. Rossi. Metrology and Physical Constants. In *Proceedings of International School of Physics Enrico Fermi - Corso 185*, 2012.

[3] M. J. T. Milton and T. J. Quinn. Primary methods for the measurement of the amount of substance. *Metrologia*, 38:289–296, 2001.

[4] P. Taylor, H. Kipphardt, and P. De Bièvre Accred Qual Assur (2001). The definition of primary method of measurement (PMM) of the "highest metrological quality" : a challenge in understanding and communication. *Accreditation and Quality Assurance*, 6 (3):103–106, 2001.

[5] P. Spitzer and B. Werner. Improved reliability of pH measurements. *Analytical and Bioanalytical Chemistry*, 374 (5):787–795, 2002.

[6] R. P. Buck, S. Rondinini, A. K. Covington, F. G. K. Baucke, C. M. A. Brett, M. F. Camoes, M. J. T. Milton, T. Mussini, R. Naumann, K. W. Pratt, P. Spitzer, and G. S. Wilson. Measurement of pH. Definition, standards, and procedures (IUPAC Recommendations 2002). *Pure and Applied Chemistry*, 74 (11):2169–2200, 2002.

[7] H. S. Harned and B. B. Owen. *The Physical Chemistry of Electrolyte Solutions*. New York: Reinhold Scientific, 1958.

[8] D. I. Hitchcock. A measure of acidity obtained from the electromotive force of a cell without liquid junction. *Journal of the American Chemical Society*, 58 (5):855–856, 1936.

[9] IUPAC. Status of the Faraday constant as an analytical standard. *Pure and Applied Chemistry*, 45 (2):125–130, 1976.

[10] J. E. Harrar. Analytical controlled-potential coulometry. *TrAC, Trends in Analytical Chemistry*, 6 (9):152–157, 1987.

[11] H. Felber, M. Weber, and C. Rivier. Final report on key comparison CCQM-K8 of monoelemental calibration solutions. *Metrologia*, 39 - Technical Supplement: 08002, 2002.

[12] Y. Le Duigou, W. Leidert, and M. Bickel. A controlled potential coulometer for high precision uranium and plutonium analysis. *Fresenius Journal of Analytical Chemistry*, 351 (6):499–506, 1995.

[13] ASTM International. Standard test method for electrical conductivity and resistivity of flowing high purity water sample. ASTM Designation D5391-99, 2009.

[14] S. Xiaoping, P. Spitzer, and U. Sudmeier. Novel method for bulk resistance evaluation in conductivity measurement for high-purity water. *Accreditation and Quality Assurance*, 12 (7):351–355, 2007.

[15] R. A. Robinson and R. H. Stokes. *Electrolyte Solutions - The Measurement and Interpretation of Conductance, Chemical Potential and Diffusion in Solution of Simple Electrolytes - 2nd edition (revised)*. Butterworths Scientific Publications, London, 1965.

[16] D. A. Skoog and J. J . Leary. *Principles of Instrumental Analysis - Fourth Edition*. Saunders College Publishing, USA, 1992.

[17] A. J. Bard and L. R. Faulkner. *Electrochemical Methods: Fundamentals and Applications*. John Wiley & Sons, New York, 1980.

[18] G. Bianchi and T. Mussini. *Fondamenti di elettrochimica*. Masson, Milano, 1993.

[19] J. Koryta, J. Dvořák, and L. Kavan. *Principles of Electrochemistry*. John Wiley & Sons Inc., Chichester, UK, 1993.

[20] C. M. A. Brett and A. M. Oliveira Brett. *Electrochemistry Principles, Methods and Applications*. Oxford Science Pubblications, 2005.

[21] E. Warburg. Ueber das verhalten sogenannter unpolarisirbarer elektroden gegen wechselstrom. *Annalen der Physik*, 303 (3):493–499, 1899.

[22] K. S. Cole and R. H. Cole. Dispersion and absorption in dielectrics. I. Alternating current characteristics. *Journal of Chemical Physics*, 9 (4):341–351, 1941.

[23] K. S. Cole and R. H. Cole. Dispension and absorption in dielectrics. II. Dicrect current characteristics. *Journal of Chemical Physics*, 10 (2):98–105, 1942.

[24] J. E. Randles. Kinetics of rapid electrode reactions. *Discussions of the Faraday Society*, 1:11–19, 1947.

[25] T. Pajkossy and D. M. Kolb. Double layer capacitance of the platinum group metals in the double layer region. *Electrochemistry Communications*, 9 (5): 1171–1174, 2007.

[26] *Agilent E4980A Precision LCR Meter Userś Guide.*

[27] L. Callegaro and F. Durbiano. Four-terminal-pair impedances and scattering parameters. *Measurement Science and Technology*, 14 (4):523–529, 2003.

[28] L. Callegaro. Misura e metrologia dell impedenza elettrica in bassa frequenza. Lectures of Ph.D. in Metrology - Polytecnic of Turin, 2010.

[29] *Branca Idealair Measure Box Model 3715 Instruction Manual.*

[30] *Agilent Technologies 3458A Multimeter Userś Guide.*

[31] *WTW inoLab Conductivity Meter Level 3 Instruction Manual.*

[32] F. Brinkmann, N. E. Dam, E. Deák, F. Durbiano, E. Ferrara, J. Fükö, H. D. Jensen, M. Máriássy, R. Shreiner, P. Spitzer, U. Sudmeier, M. Surdu, and L. Vyskočil. Primary methods for the measurement of electrolytic conductivity. *Accreditation and Quality Assurance*, 8 (7):346–353, 2003.

[33] G. Jones and S. M. Christian. The mesurement of the conductance of electrolytes. VI. Galvanic polarization by alternating current. *Journal of the American Chemical Society*, 57 (2):272–284, 1935.

[34] Y. C. Wu, K. W. Pratt, and W. F. Koch. Determination of the absolute specific conductance of primary standard KCl solutions. *Journal of Solution Chemistry*, 18 (6):515–528, 1989.

[35] Y.C. Wu, W. F. Koch, and K. W. Pratt. Proposed new electrolytic conductivity primary standards for KCl solutions. *Journal of Research of the National Institute of Standards and Technology*, 96 (2):191–201, 1991.

[36] CENELEC. Expression of performance of electrochemical analyzers - Part 1 - General. European Committee for Electrotechnical Standardization, 2003.

[37] ASTM International. Standard test methods for electrical conductivity and resistivity of water. ASTM Designation D1125-95, 2009.

[38] OIML. International Recommandation No. 68: Calibration method for conductivity cells. Organisation International de la Métrologie Légale, 1985.

[39] IEC. International Electrotechnical Vocabulary. Online. URL `http://www.electropedia.org/`.

[40] A. Bevilacqua. Ultrapure water the standard for resistivity measurements of ultrapure water. In *Semiconductor Pure Water and Chemicals Conference (Santa Clara)*, 1998.

[41] T.S. Light, S. Licht, A.C. Bevilacqua, and K.R. Morash. The fundamental conductivity and resistivity of water. *Electrochemical and Solid-State Letters*, 8 (1):E16–E19, 2005.

[42] *Watson-Marlow peristaltic pump Bredel Sci-Q 323 Instruction Manual.*

[43] *Termics02 Resistance Thermometer, INRiM Calibration Certificate, 2013.*

[44] C. Boveri, F. Durbiano, and D. Serazio. Development of a flow-through cell for accurate measurements of low electrolytic conductivity. In *Proceedings of the XIX IMEKO World Congress on Fundamental and Applied Metrology*, 2009.

[45] L. Callegaro, F. Durbiano, E. Orrú, and B. Trinchera. An impedance spectrometer for the metrology of electrolytic conductivity. In *CPEM, Washington DC*, pages 714–715, 1-6 July 2012.

[46] D. R. White and S. P. Benz. Constraints on a synthetic noise source for johnson noise thermometry. *Metrologia*, 45:93–101, 2008.

[47] C. L. Heizman. Signal analysis with digital time-seriesanalyzers. *Gen. Radio Exp.*, 44:3–7, 1970.

[48] E. A. Sloane. Measurement of transfer function and impedance. *Gen. Radio Exp.*, 44:8–13, 10970.

[49] B. Sanchez, C. R. Rojas, G. Vandersteen, R. Bragos, and J. Schoukens. On the calculation of D-optimal multisine excitation power spectrum for broadband impedance spectroscopy measurements. *Measurement Science and Technology*, 23 (8):085702, 2012.

[50] H. Herlufsen. Dual-channel FFT analysis (part I). *Bruel & Kjaer Technical Reviews*, 1/2:3–45, 1984.

[51] S.M. Becchi, L. Callegaro, F. Durbiano, V. D Elia, and A. Strigazzi. Novel impedance cell for low conductive liquids: determination of bulk- and interface contributions. *Rev. Sci. Instrum.*, 78 (11):113902, 2007.

[52] EA. Expression of the Uncertainty of Measurement in Calibration EA4/02. European Co-operation for Accreditation, 1999.

[53] JCGM. 100:2008 GUM 1995 with minor modifications - Evaluation of measurement data - Guide to the expression of uncertainty in measurement. BIPM, Sèvres, France, 2008.

[54] H. P. Thomas. The International Temperature Scale of 1990 (ITS-90). *Metrologia*, 27:3–10, 1990.

[55] F. Durbiano and E. Orrú. CCQM-K92 Key Comparison: Electrolytic Conductivity at 0.05 S/m. Technical report, INRIM Measurement Report, 2011.

[56] F. Durbiano and E. Orrú. EURAMET Study 1202: Electrolytic Conductivity of Bioethanol. Technical report, INRIM Measurement Report, 2012.

[57] P. Spitzer, P. Fisicaro, S. Seitz, and R. Champion. pH and electrolytic conductivity as parameters to characterize bioethanol. *Accreditation and Quality Assurance*, 14 (12):671–676, 2009.

[58] L. Callegaro. *Electrical Impedance. Principles, Measurement, and Applications.* Taylor & Francis, 2012.

[59] Agilent Technologies. Effective Impedance Measurement Using OPEN/SHORT/LOAD Correction. Technical report, Appl. Note 346–3, 1998.

[60] T. S. Light and S. L. Licht. Conductivity and resistivity of water from the melting to critical point. *Analytical Chemistry*, 59 (19):2327–2330, 1987.

[61] JCGM. 102:2011 Evaluation of measurement data - Supplement 2 to the Guide to the expression of uncertainty in measurement - Extension to any number of output quantities. BIPM, Sèvres, France, 2011.

[62] *Millipore RiOs-DI 3 UV/Reservoir/Milli-Q Academic Instruction Manual.*

[63] BIPM. Mutual recognition of national measurement standards and of calibration and measurement ccertificate iissue by nnationa metrology institutes. Bureau International des Poids et Mesures, Pavillon de Breteuil, Sèvres Cedex, France, 1999.

[64] M. G. Cox. The evaluation of key comparison data. *Metrologia*, 39:589–595, 2001.

[65] L. Nielsen. Identification and handling of discrepant measurements in key comparisons. Technical Report Tech. Rep. DFM-02-R28, Danish Institute of Fundamental Metrology (DFM), Denmark, 2002.

[66] M. G. Cox. The evaluation of key comparison data: determining the largest consistent subset. *Metrologia*, 44:187–200, 2007.

[67] Unesco/ICES/SCOR/IAPSO. Background papers and supporting data on the Pratical Salinity Scale 1978. *Uncesco Technical Papers in marine science*, 37, 1981.

[68] T. M. Dauphinee. Introduction to the special issue on the Pratical Salinity Scale 1978. *IEEE Journal of Oceanic Engineering*, OE-5 (1):11–12, 1980.

[69] E. L. Lewis. The Pratical Salinity Scale 1978 and its antecedents. *IEEE Journal of Oceanic Engineering*, OE-5 (1):13–18, 1980.